SUBSTRATE DEPENDENT HETEROTROPHIC CO_2-FIXATION AS INDICATOR FOR METABOLIC PHENOTYPES

Dissertation

der Mathematisch-Naturwissenschaftlichen Fakultät
der Eberhard Karls Universität Tübingen
zur Erlangung des Grades eines
Doktors der Naturwissenschaften
(Dr. rer. nat.)

vorgelegt von
M.Sc. Marina Spona-Friedl, geb. Spona
aus München

Tübingen
2020

Gedruckt mit Genehmigung der Mathematisch-Naturwissenschaftlichen Fakultät der Eberhard Karls Universität Tübingen.

Tag der mündlichen Qualifikation:	16.09.2020
Stellvertretender Dekan:	Prof. Dr. József Fortágh
1. Berichterstatter:	Prof. Dr. Martin Elsner
2. Berichterstatter:	Prof. Dr. Andreas Kappler

Für meine Familie

Even those who are gone are with us as we go on,
your journey has only begun. Tears of pain, tears of joy
one thing nothing can destroy: Is our pride, deep inside
We are one.

(Lion King)

Danksagung

Unglaubliche Erleichterung gepaart mit großer Freude, Dankbarkeit und Stolz sind die Gefühle, die am besten beschreiben, was in diesem Moment in mir vorgeht, da die Arbeit endlich vollendet ist. Die letzten Jahre waren geprägt von Entbehrungen und Verlusten sowie von schönen Erfolgen und lustigen Begebenheiten. Neben den Menschen die mir in dieser Zeit stets zur Seite standen, war die Musik eine wichtige Wegbegleiterin und daher möchte ich auch mit Ihrer Hilfe Danke sagen.

Ich bedanke mich herzlich bei meinem Doktorvater Prof. Dr. Martin Elsner für seine kompetente, fachliche Betreuung und Hilfe, die interessante Themenstellung sowie für die kreativen Denkanstöße. Sein Engagement sowie die vielen hilfreichen Diskussionen haben sehr zum Gelingen der Arbeit beigetragen.

Ich bedanke mich bei Prof. Dr. Andreas Kappler für die Zweitbetreuung dieser Arbeit, die konstruktiven Kommentare sowie für seine große Hilfsbereitschaft.

Von Herzen bedanke ich mich bei meinem externen Betreuer Prof. Dr. Wolfgang Eisenreich für seine große Unterstützung in den letzten Jahren. Vor allem in schwierigen Zeiten hatte er stets ein offenes Ohr, großes Verständnis und aufmunternde Worte für mich. Die vielen interessanten Diskussionen und kreativen Anregungen waren mir stets eine große Hilfe. (Lifesaver - Sunrise Avenue)

Meinem Bürokollegen Dr. Alexander Braun danke ich für die gute und freundschaftliche zweijährige Zusammenarbeit. Meinen IGÖ-Kollegen, im Besonderen Anne, Corinna, Günter, Gabi, Judith, Niklas, Petra, Ramona und Tina, danke ich für die gute Zusammenarbeit und ihre Hilfe bei den Herausforderungen des Laboralltags sowie technischen Problemen. Ein Highlight waren unsere lustigen Tischkicker-Matches, die uns aus dem Mittagstief holten und für neue Motivation und großen Teamgeist gesorgt haben.

I cordially thank my labmates Kankana and Aileen for their technical and emotional support and help whenever there was a problem. In- and outside the lab we had such a great time and so much fun together! I could always count on you - Thank you! (Never let go - Sunrise Avenue)

Ich bedanke mich herzlich bei Frau Andrea Heider-Rieth, die mich in der schwersten Zeit meiner Doktorarbeit wieder aufgebaut hat. (Wenn der Himmel weint - Peter Maffay)

Der größte Dank gebührt meiner gesamten Familie; ohne sie wäre ich nicht da wo ich jetzt bin! (Welcome - Phil Collins)
Ich danke meinen Eltern, die immer hinter mir stehen, an mich glauben und mich in allem was ich tue unterstützen. Ohne sie hätte ich diesen Weg nicht beschreiten können und ich bin unendlich dankbar, dass ihr mir all das ermöglicht habt. (Bridge Over Troubled Water - Simon & Garfunkel)

Meiner Schwester Teresa danke ich dafür, dass sie immer für mich da ist und stets zu mir hält. Sie ist die beste Schwester der Welt und versteht mich wie sonst niemand. (I'll Always Be Right There - Bryan Adams)

Meinem Mann Christoph Danke ich von Herzen für seine Liebe, seine unschätzbare Hilfe, all den gespendete Trost und die aufbauenden Worte. Ohne ihn hätte ich es nicht geschafft. (You Raise Me Up - Josh Groban)

Ich bedanke mich bei meiner Tochter Isabella für ihre zunächst aufmunternden Tritte und ihr strahlendes Lachen womit sie mich stets motiviert hat. (I've Been Waiting For You - ABBA/ Mamma Mia II version)

Table of contents

Summary

Virtually all heterotrophic organisms incorporate carbon dioxide (CO_2) into their biomass *via* anaplerosis. Despite the fact that the activity of anaplerotic enzymes, such as pyruvate carboxylase, depends on the utilised organic substrate(s), this relation has hardly been explored so far.

To study whether CO_2-incorporation can reveal which substrates out of a pool of dissolved organic carbon (DOC) are utilised by environmental microorganisms, the model organism *Bacillus subtilis* W23 (*B. subtilis* W23) was grown in a minimal medium with different types of organic substrates: glucose, lactate, or malate, respectively, each together with 1 g/L $NaH^{13}CO_3$. Incorporation of $H^{13}CO_3^-$ was traced by elemental analysis-isotope ratio mass spectrometry (EA-IRMS) of bulk biomass and gas chromatography-mass spectrometry (GC-MS) of protein-derived amino acids after derivatisation. Until the late logarithmic phase, ^{13}C-incorporation into the tricarboxylic acid (TCA) cycle increased over time and occurred *via* [4-^{13}C]oxaloacetate formed by carboxylation of pyruvate. Levels of ^{13}C-incorporation were highest for growth on glucose and lowest on malate. ^{13}C-Incorporation into gluconeogenesis products was mainly detected in the lactate and malate experiment, whereas glucose down-regulated this path. Ratios of ^{13}C-excess calculated from the ^{13}C-excess values of the M+1 isotopomers of specific sets of amino acids served as a diagnostic tool to identify (i) substrates that initiate active anaplerosis and (ii) substrates that require active gluconeogenesis at high statistical significance. During growth of *B. subtilis* W23 on glucose or lactate the ratios of ^{13}C-excess in anaplerosis-relevant amino acids *vs.* “baseline” amino acids (i.e. Asp/Val, Asp/Ala, Glu/Val and Glu/Ala) yielded values above 20 displaying an active anaplerosis. In contrast, values below 10 were obtained for the same sets of amino acids, when *B. subtilis* W23 grew on malate. To identify active gluconeogenesis, the ^{13}C-excess in a second set of amino acids was considered: gluconeogenesis-derived *vs.* “baseline” amino acids, i.e. Tyr/Val, Tyr/Ala, Phe/Val and Phe/Ala. When growing on lactate, values clearly above 1 evidenced the presence of active gluconeogenesis, whereas growth on glucose resulted in values below 1.

A proof-of-principle study with a natural groundwater community confirmed that incorporation of $H^{13}CO_3^-$ by natural communities could be traced and led to specific labelling patterns in the amino acids. Ratios of ^{13}C-excess showed on the one hand no need for active anaplerosis (Asp/Val,… < 10) and on the other hand an active gluconeogenesis (Tyr/Val,… > 1). Remarkably, these ratios and labelling patterns exhibited a striking similarity to those ratios and patterns obtained from growth experiments with *B. subtilis* W23 and malate (Asp/Val,… < 10 and Tyr/Val,… > 1.5) as carbon source. This similarity suggests that groundwater microbes mainly fed on humic substances (i.e. a mixture of many molecules, with an aromatic centre and phenolic and carboxylic substituents) that are decomposed into short organic acids, such as succinate, entering the central carbon metabolism at the stage of the TCA cycle. This exemplifies that our approach may elucidate the type of the main organic carbon substrate metabolised by the majority of the heterotrophic bacterial community in an environmental sample.

We explored whether this simple approach – using heterotrophic fixation of $^{13}CO_2/H^{13}CO_3^-$ under *in vivo* conditions – could also answer questions concerning metabolic deficiencies and bacterial physiology. To investigate this capability, the metabolism of leucine was addressed, because this amino acid is an unfavourable substrate for *B. subtilis* W23. Again, ^{13}C-incorporation of $H^{13}CO_3^-$ was traced by EA-IRMS of bulk biomass and GC-MS of protein- and cell wall-derived amino acids. Remarkably, no ^{13}C-incorporaton into gluconeogenetic products was detected when leucine was offered as growth substrate. The amino acids' ^{13}C-labelling patterns were very similar to the patterns obtained from our experiments with *B. subtilis* W23 growing on glucose. The ratios (Asp/Val,… > 20 and Tyr/Val,… < 1) calculated from the ^{13}C-excess values of the M+1 isotopomers of our chosen indicator amino acids proved this observation. This implies that, rather than leucine, the bacteria must have used organic matter leftovers from the inoculum, which mainly consisted of carbohydrates. Leucine metabolism presumably stopped at the level of 3-methylbutanoyl-CoA, if metabolised at all. Further, we tested whether our approach could be used to study the effect of carbon catabolite repression: we were able to confirm the strict repression of other carbon sources by malate in a co-substrate experiment conducted with malate and leucine.

Hence, the combined results from controlled experiments with model organisms/ model substrates, a proof-of-principle study with a natural groundwater community and a physiological case study on metabolic bacterial deficiency underline the potential of the labelling approach to (i) characterise carbon sources of heterotrophic microorganisms in their natural environments, (ii) elucidate bottlenecks in metabolism of heterotrophic organisms and (iii) study co-substrate metabolism with regard to carbon catabolite repression.

Zusammenfassung

Nahezu alle heterotrophen Organismen bauen über anaplerotische Enzyme, wie z.B. Pyruvatcarboxylase, Kohlenstoffdioxid (CO_2) in ihre Biomasse ein. Obwohl bekannt ist, dass das Ausmaß des anaplerotischen Einbaus von der Art des verwendeten organischen Substrats abhängt, ist die Anwendbarkeit dieses Zusammenhangs bisher kaum näher erforscht worden.

In dieser Arbeit wurde daher untersucht, ob die Art des Substrats, welches von Mikroorganismen aus einem Pool von gelöstem organischen Kohlenstoff (DOC) tatsächlich verstoffwechselt wird, anhand des CO_2-Einbaus identifiziert werden kann. Hierzu wurde der Modelorganismus *Bacillus subtilis* W23 (*B. subtilis* W23) in einem Minimalmedium gezüchtet, das mit 1 g/L $NaH^{13}CO_3$ und außerdem entweder Glukose, Laktat oder Malat versetzt war. Der Anteil von ^{13}C (aus $H^{13}CO_3^-$) an der resultierenden Biomasse wurde mittels Elementaranalyse-Isotopenverhältnis-Massenspektrometrie (EA-IRMS) bestimmt. Gleichzeitig wurde der Einbau von $H^{13}CO_3^-$ in die aus Proteinen gewonnenen Aminosäuren (nach Derivatisierung) mittels Gaschromatographie-Massenspektrometrie (GC-MS) verfolgt. Der ^{13}C-Eintrag nahm bis in die späte logarithmische Wachstumsphase der Bakterien stetig zu. Der Einbau erfolgte in den Tricarbonsäurezyklus (TCA Zyklus) über [4-^{13}C]Oxalacetat, welches durch Carboxylierung von Pyruvat gebildet wurde. Die ^{13}C-Aufnahme war während des Wachstums auf Glukose am höchsten und während des Wachstums auf Malat am geringsten. Der ^{13}C-Einbau in Glukoneogenese-Produkte wurde hauptsächlich im Laktat- und Malat-Experiment nachgewiesen, wohingegen Glukose diesen Stoffwechselweg hemmte. ^{13}C-Überschussverhältnisse wurden aus den ^{13}C-Überschusswerten der M+1-Isotopomere spezifischer Indikatoraminosäuren berechnet und dienten mit hoher statistischer Signifikanz als diagnostisches Instrument zur Identifizierung der Art des Substrats, das von den Organismen verwendet wurde. Die ^{13}C-Überschussverhältnisse von Anaplerose-beeinflussten versus „Baseline“ Aminosäuren (d.h. Asp/Val, Asp/Ala, Glu/Val und Glu/Ala) ergaben Werte über 20, wenn *B. subtilis* W23 auf Glukose oder Laktat gewachsen war und zeigten damit die Verwendung von Substraten an, die eine aktive Anaplerose

erforderten. Die Berechnung der gleichen Verhältnisse ergab Werte unter 10, wenn *B. subtilis* W23 auf Malat gewachsen ist. Ein zweites Indikatoraminosäureset wurde benutzt, um Substrate zu identifizieren, die eine aktive Glukoneogenese erfordern: hierfür werden die ^{13}C-Überschussverhältnisse zwischen Glukoneogenese-beeinflussten versus „Baseline“-Aminosäuren (Tyr/Val, Tyr/Ala, Phe/Val und Phe/Ala) betrachtet.

Eine Proof-of-Principle-Studie mit einer natürlichen mikrobiellen Grundwassergemeinschaft zeigte, dass auch in Umweltproben die Verstoffwechselung von ^{13}C-markietem Bikarbonat nachgewiesen werden konnte und zu charakteristischen Markierungsmustern in den Aminosäuren führte. Die ^{13}C-Überschussverhältnisse der gewählten Indikatoraminosäuren zeigten, dass unter den gewählten Bedingungen keine Notwendigkeit für eine aktive Anaplerose bestand (Asp/Val,... < 10), die Bakterien allerdings aktiv Glukoneogenese betrieben (Tyr/Val,... > 1). Bemerkenswerterweise wiesen diese Verhältnisse und Markierungsmuster eine auffallende Ähnlichkeit mit den Verhältnissen und Mustern auf, die aus Wachstumsexperimenten mit *B. subtilis* W23 und Malat als Kohlenstoffquelle (Asp/Val,... < 10 und Tyr/Val,... > 1,5) gewonnen wurden. Die Ähnlichkeit legt nahe, dass sich die Mikroorganismen der Grundwasserprobe hauptsächlich von Huminstoffen ernährten. Huminstoffe sind Stoffgemische aus vielen Molekülen welche ein aromatisches Zentrum mit beispielsweise phenolischen und carboxylischen Substituenten aufweisen. Huminstoffe werden zu kurzen organischen Säuren, wie z.B. Succinat, zersetzt und über den TCA Zyklus in den zentralen Kohlenstoffmetabolismus aufgenommen. Somit erklärt sich die Ähnlichkeit zwischen den erhaltenen ^{13}C-Verhältnissen und Markierungsmustern der Umweltprobe und des Malat-Versuchs. Diese Ergebnisse veranschaulichen, dass unsere Methode in der Lage ist, die Art des organischen Kohlenstoffsubstrats zu identifizieren, welche von der Mehrheit der heterotrophen Organismen (in einer Umweltprobe) verstoffwechselt wird.

Des Weiteren untersuchten wir, ob mittels heterotropher $^{13}CO_2/H^{13}CO_3^-$-Fixierung (unter *in vivo* Bedingungen) Fragen zu Stoffwechseldefiziten sowie zur bakteriellen Physiologie adressiert werden können. Wir entschieden uns, zu diesem Zweck die Nutzung von Leucin als Kohlenstoffquelle zu untersuchen, da diese Aminosäure ein unvorteilhaftes Substrat für *B. subtilis* W23 ist. Der Einbau von ^{13}C-Kohlenstoff wurde wieder mittels EA-IRMS Analyse der gesamten Biomasse und mittels GC-MS

Analyse der Aminosäuren verfolgt. Interessanterweise wurde kein ^{13}C-Einbau in glukoneogenetische Produkte nachgewiesen, wenn Leucin als Wachstumssubstrat angeboten wurde. Darüber hinaus glichen die ^{13}C-Markierungsmuster der Aminosäuren jenen Mustern, die wir von den Experimenten mit *B. subtilis* W23 und Glukose erhalten haben. Die ^{13}C-Überschussverhältnisse (Asp/Val,... > 20 und Tyr/Val,... < 1), berechnet aus den ^{13}C-Überschußwerten der M+1-Isotopomere der Indikatoraminosäuren, bestätigten diese Beobachtung. Dies impliziert, dass die Bakterien an Stelle des Leucins vorhandene Reste an organischem Material aus dem Inokulum (hauptsächlich Kohlenhydrate) für ihr Wachstum verwendet haben müssen. Der Leucin-Stoffwechsel, falls Leucin überhaupt verstoffwechselt wurde, stoppte vermutlich bei 3-Methylbutanoyl-CoA. In einem weiteren Experiment testeten wir, ob sich heterotrophe $^{13}CO_2/H^{13}CO_3^-$-Fixierung zur Untersuchung des Phänomens der Katabolitrepression nutzen ließe: In einem Co-Substrat-Experiment mit Malat und Leucin konnten wir die strikte Unterdrückung anderer Kohlenstoffquellen durch Malat bestätigen.

Zusammenfassend unterstreichen die kombinierten Ergebnisse aus klar definierten Experimenten mit Modellorganismen und -substraten, einer Proof-of-Principle-Studie mit einer natürlichen mikrobiellen Grundwassergemeinschaft und einer physiologischen Fallstudie bezüglich Mangelerscheinungen im bakteriellen Stoffwechsel das Potential der $^{13}CO_2/H^{13}CO_3^-$-Markierung (i) Kohlenstoffquellen heterotropher Mikroorganismen in ihrer natürlichen Umgebung zu charakterisieren, (ii) Engpässe im Stoffwechsel heterotropher Organismen aufzuklären und (iii) den Co-Substrat-Stoffwechsel mit Hinblick auf die Katabolitrepression zu charakterisieren.

I

GENERAL INTRODUCTION

Dissolved Organic Matter

Dissolved organic matter (DOM) in groundwater ecosystems represents a source of nutrients for the organisms that inhabit these systems. Its origin can be manifold and is influenced by factors like surface vegetation or soil characteristics. Figure 1.1 shows an example for dissolved organic matter formation. Organic material released by plants (i.e. leaf, twig and root litter as well as organic acids (e.g. malate), sugars and other low molecular weight compounds) is metabolised by soil dwelling microorganisms. The microorganisms use the organic material to build up their biomass, thereby decomposing the plant material and synthesising new organic compounds, which are secreted to the soil. Thus, the microorganisms alter and shape the soil organic matter (SOM) composition. Precipitation as well as surface waters transport the organic molecules through the soil column towards the groundwater zone. Along the flow path, sorption and desorption to and from soil minerals due to polarity, charge or size of the molecules lead to different retention times of the organic molecules: hydrophobic molecules are stronger retained by the soil particles than hydrophilic molecules. Consequently, organic matter constantly changes with regard to its composition and concentration. Organic matter that enters the groundwater reservoir is summarised as dissolved organic matter (Fig. 1.1) [1-5].

Methods to characterise dissolved organic matter are well established: amongst others, multidimensional nuclear magnetic resonance spectroscopy (NMR), negative- and positive-ion electrospray ionisation Fourier-transform ion cyclotron resonance mass spectrometry, optical spectroscopy, liquid chromatography organic carbon detection (LC-OCD) and elemental analysis-isotope ratio mass spectrometry (EA-IRMS) are used to analyse dissolved organic matter with regard to its chemical and isotopic composition [5-11]. Using this techniques and analytical tools structural motifs of dissolved organic matter are identified, for example humic substances, low molecular weight acids, lignin-like compounds, aromatic compounds, aliphatic compounds, carbohydrates and amino acids [5, 6, 9, 11, 12].

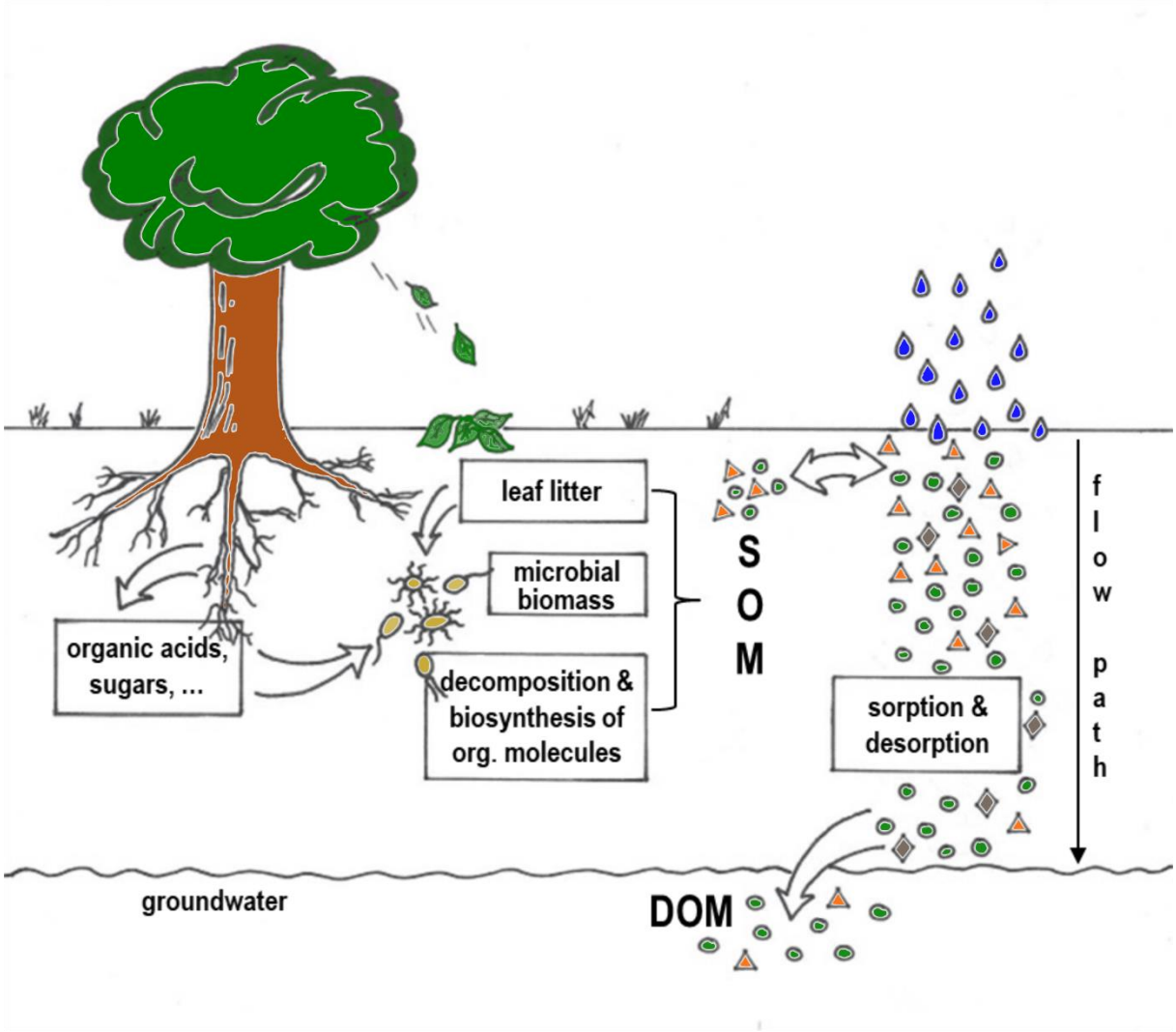

Figure 1.1: Soil organic matter and dissolved organic matter formation. Generally soil organic matter (SOM) consists of plant litter, microbial biomass and microbial metabolites. The hydrophilic organic matter is symbolised by full green circles and the hydrophobic organic matter is symbolised by full orange triangles. Along the flow path, sorption and desorption to and from soil minerals (symbolised as full grey diamonds) alter the organic matter composition and concentration. The retention of hydrophilic molecules by the soil particles/minerals is less strict compared to the hydrophobic molecules. Organic matter that enters the groundwater zone is summarised as dissolved organic matter (DOM) [1-5].

Although sophisticated analytical methods and techniques exist to characterise dissolved organic matter, it remains difficult to identify the part of dissolved organic matter that is truly bioavailable to microorganisms. Researchers use, for example, total organic carbon (TOC) analyser to determine the time variable concentrations of dissolved organic carbon in their (groundwater) samples. Based on such results the bioavailable proportion of dissolved organic matter is estimated [5]. Bioassay experiments represent another possibility to determine the bioavailable proportion of

dissolved organic matter. The focus lies again on the analysis of changing dissolved organic matter/carbon concentrations. Here, compounds like amino acids or carbohydrates are used as indicators for bioavailable dissolved organic matter [13]. However, the bioavailable part of dissolved organic matter is generally small, highly variable and subject to physicochemical and biological processes. Consequently, precise determination of truly bioavailable dissolved organic matter remains difficult, when relying on concentration measurements and structural analysis of dissolved organic matter alone.

It is possible to visualise the turnover of (organic) compounds by applying their stable isotope-labelled counterparts and trace their metabolic fate. The method behind this approach is called metabolic flux analysis (MFA) [14]. However, this method necessitates the feeding of organic carbon substrates which alters and thus disturbs the natural organic matter composition. Consequently, this need makes it impossible to study the bioavailability of the naturally present organic matter. Finding a link between the utilisation of organic matter and an inorganic carbon source and thus using an inorganic stable isotope-labelled carbon source, however, would evade the problem of disturbing the natural organic matter composition.

The microorganisms living in soil and groundwater systems are the ones that actually metabolise the bioavailable organic matter, which is why making them “tell” what they feed on would be direct evidence for the truly bioavailable part of organic matter. For this reason it could be worthwhile to study the metabolism of microorganisms and microbial communities that inhabit the ecosystem under study.

Isotopologue profiling presents a technique that combines the two ideas stated above: it enables the study of microbial metabolism *in vivo* using stable isotope-labelled (in)organic substrates.

Isotopologue Profiling

Among the various methods of MFA [15], isotopologue profiling emerged as powerful technique to study biosynthetic pathways in prokaryotic and eukaryotic cells. Isotopologue profiling is based on incorporation experiments using stable isotope-labelled compounds (e.g. ^{13}C-glucose, ^{13}C-/ ^{15}N-amino acids, ^{13}C-fatty acids) as growth substrates for prokaryotic or eukaryotic cells. Both, ^{13}C-carbon and ^{15}N-nitrogen are very rare in nature (1.1 % and 0.4 %) and their distribution in organic

matter is close to random [16]. Consequently, by feeding ^{13}C- or ^{15}N-labelled compounds the natural quasi-random distribution of these isotopes is disturbed and it is possible to achieve an accumulation of these isotopes in *de novo* synthesised biomass. A disturbance of that kind is rapidly spread over the entire metabolic network of cells and organisms, resulting in characteristic ^{13}C-/ ^{15}N-labelling patterns – i.e. isotopologue profiles – for each cellular compound, e.g. protein-derived amino acids. The label incorporation can be analysed by gas chromatography-mass spectrometry (GC-MS) or NMR spectroscopy. The analysis of the resulting mass and NMR spectra visualises the characteristic isotopologue profiles of each detected compound. These characteristic profiles reflect the biosynthetic routes that lead from the fed labelled substrate (i.e. precursor) to the product, displaying fingerprints of all reactions that contributed to the biosynthesis of the respective compound [16-20]. Thus, the results provide qualitative as well as quantitative information about metabolic processes (such as glycolysis, gluconeogenesis, pentose phosphate pathway or tricarboxylic acid (TCA) cycle) in the experimental system under study.

Next to organic growth substrates, $^{13}CO_2$ (or $H^{13}CO_3^-$ as its soluble form) is also used in stable isotope labelling experiments. This simple and inexpensive inorganic carbon source is readily available and used as a building block in the metabolism of both autotrophic and heterotrophic organisms.

Heterotrophic CO_2-Fixation

Talking about CO_2-fixation, everybody automatically thinks about photosynthesis and green plants, in the first place. Indeed, CO_2-fixation by autotrophic organisms (including plants) is one of the most important biosynthetic processes in the biosphere [21-24]. Nevertheless, the presence and diversity of carboxylating enzymes in nature could not be covered by autotrophs alone.

In 1935 Wood and Werkman reported, for the first time, fixation of CO_2 into microbial biomass during growth of heterotrophic bacteria producing propionic acid (*Propionibacteria*) [25]. Up until now, at least 18 carboxylases (i.e. CO_2-fixing enzymes) were found in the central and peripheral metabolism of heterotrophic organisms. Hence, it is well recognised that virtually all heterotrophic organisms – from microorganisms to humans – incorporate CO_2 *via* a variety of pathways [26-29]. In his review, T. J. Erb summarises and functionally defines four different types of

carboxylases that could serve in the metabolism of heterotrophic organisms [29]: (i) “assimilatory carboxylases” transform organic substrates into central precursor molecules (e.g. TCA cycle intermediates) *via* an essential carboxylation step in order to make the substrate available for the organism; (ii) “anaplerotic carboxylases” serve in TCA cycle refilling reactions; (iii) “biosynthetic carboxylases” operate in the biosynthesis of cellular building blocks starting from central carbon metabolites; (iv) “redox-balancing carboxylases” are enzymes catalysing reactions in which CO_2 is used as electron acceptor in order to remove excess reducing equivalents, such as NADPH. Some carboxylases exhibit a pure catalytic function while others efficiently incorporate CO_2 into an organisms’ biomass. If the carboxylation of a molecule, e.g. during its assimilation process, is preceded or followed by a decarboxylation step, no CO_2 is incorporated into the respective molecule and thus carboxylation is of purely catalytic nature [29].

The TCA cycle functions also in biosynthetic processes, next to its task of oxidising acetyl coenzyme A (Ac-CoA) to CO_2 to generate energy (in form of GTP or the redox equivalents $NADH/H^+$). Consequently, the intermediates of the cycle are constantly withdrawn for the biosynthesis of, for example, amino acids or carbohydrates like glucose. Anaplerotic carboxylases replenish the intermediates of the TCA cycle to ensure its continued function. Reactions catalysed by these enzymes often employ a carboxylation step. Therefore, it is not surprising that carbon from anaplerotic CO_2-fixation accounts for a significant amount (i.e. 2-8 %) of a cell’s biomass carbon abundance [29-35].

Among the anaplerotic carboxylases, pyruvate carboxylase takes an outstanding role being the archetypical anaplerotic enzyme [35]. Pyruvate carboxylase catalyses the bicarbonate-dependent conversion of pyruvate into oxaloacetate. Interestingly, the activity of pyruvate carboxylase depends on the organic carbon substrate that is utilised for cell growth. The enzyme is widely distributed across the three kingdoms of life and highly conserved in many organisms [29, 35-37]. As a component of a putative ancestral reverse TCA cycle, the enzyme is also present in chemolitho-autotrophic bacteria [38], which are considered as one of the most ancient forms of life. The reaction of pyruvate carboxylase could therefore represent a metabolic feature that goes back to the early evolution of life [39].

Incorporation of CO_2 by heterotrophic organisms was already successfully traced using isotopically labelled CO_2 (i.e. $^{13}CO_2$, $^{14}CO_2$) and applied to study microbial activity. As an example, Alonso-Sáez et al. found that heterotrophic CO_2-incorporation was important in marine microbes under resource depleted conditions [40]. Miltner et al. concluded from their experiments that CO_2-fixation is an important process and represents a significant factor of microbial activity in soils [41]. It is further possible to distinguish rates of CO_2-fixation from autotrophic and heterotrophic organisms in natural microbial communities by analysing the membrane lipids with regard to the dissolved inorganic carbon incorporation [42, 43]. Common to these studies is the observation and analysis of microbial growth in environmental samples, which point at the crucial role of CO_2-fixation in heterotrophs [44-48]. However, none of these studies have exploited the potential of heterotrophic CO_2-fixation to reveal information about the physiology or the metabolism of microbes, without altering the (dissolved) organic carbon pool. The need to refill the TCA cycle by anaplerotic CO_2-fixation is common to almost all heterotrophic organisms. In combination with the substrate-dependent activity of anaplerotic carboxylases, experiments using $^{13}CO_2/H^{13}CO_3^-$ as isotopic tracer bear the potential to reveal the type of the main organic carbon substrate or at least the substrate family that is used by the heterotrophic organisms or the microbial community under study.

Objectives

This thesis aims to use the incorporation of CO_2 into microbial biomass to reveal the type of the metabolised organic carbon substrate, both in batch experiments and in an environmental sample. Additionally, CO_2-fixation is used to enable superior insight into the metabolism of *Bacillus subtilis* W23. Furthermore, the thesis aims to show that heterotrophic $^{13}CO_2$-fixation, used as technique to study microbial metabolism, yields comparable results to similar studies conducted with labelled organic substrates.

The work presented in **Chapter 2** focused on the interdependency of pathways and rates of CO_2-fixation on the concurrent usage of organic substrate(s). *Bacillus subtilis* W23 was grown in the presence of glucose, lactate and malate, respectively. CO_2-Fixation was monitored by applying ^{13}C-labelled bicarbonate as tracer and analysing the ^{13}C-incorporation into bulk biomass and individual amino acids. It was further tested whether this approach could reveal which substrate(s), out of a pool of dissolved organic carbon, was utilised by microorganisms.

The focus of **Chapter 3** was on a proof-of-principle experiment conducted in order to elucidate the possibility to trace ^{13}C-lable incorporation by natural communities. Label incorporation into individual amino acids was analysed by GC-MS and the results were compared to the results obtained from the experiments with *Bacillus subtilis* W23 growing on glucose, lactate and malate, respectively.

Chapter 4 showed the possibility to use heterotrophic CO_2-fixation to study the physiology of an organism and to gain superior insight into its carbon metabolism. ^{13}C-Lable incorporation into bulk biomass and individual amino acids from heterotrophic $H^{13}CO_3^-$-fixation was again analysed and revealed the reason behind the inability of *Bacillus subtilis* W23 to grow on leucine as sole source of carbon.

II

SUBSTRATE-DEPENDENT CO_2-FIXATION IN HETEROTROPHIC BACTERIA REVEALED BY STABLE ISOTOPE LABELLING

Author	Author position	Scientific ideas [%]	Data generation [%]	Analysis & Interpretation [%]	Paper writing [%]
M. Spona-Friedl	1	50	90	70	50
A. Braun	2	20	0	5	0
C. Huber	3	0	10	5	10
W. Eisenreich	4	10	0	10	15
C. Griebler	5	5	0	0	5
A. Kappler	6	0	0	0	5
M. Elsner	7	15	0	10	15
Title of paper:		Substrate-dependent CO_2 fixation in heterotrophic bacteria revealed by stable isotope labelling			
Status in publication process:		Accepted; Spona-Friedl M, Braun A, Huber C, Eisenreich W, Griebler C, Kappler A, Elsner, M. Substrate-dependent CO_2 fixation in heterotrophic bacteria revealed by stable isotope labelling. FEMS Microbiology Ecology. 2020. 96 (6). DOI: 10.1093/femsec/fiaa080			

Abstract

Virtually all heterotrophs incorporate carbon dioxide (CO_2) by anaplerotic fixation. Little explored, however, is the interdependency of pathways and rates of CO_2-fixation on the concurrent usage of organic substrate(s). Potentially, this could reveal which substrates out of a pool of dissolved organic carbon (DOC) are utilised by environmental microorganisms. To explore this possibility, *Bacillus subtilis* W23 was grown in a minimal medium with normalised amounts of either glucose, lactate or malate as only organic substrate, each together with 1 g/L $NaH^{13}CO_3$. Incorporation of $H^{13}CO_3^-$ was traced by elemental analysis-isotope ratio mass spectrometry (EA-IRMS) of biomass and gas chromatography-mass spectrometry (GC-MS) of protein-derived amino acids. Until the late logarithmic phase, ^{13}C-incorporation into the tricarboxylic acid (TCA) cycle increased with time and occurred *via* [4-^{13}C]oxaloacetate formed by carboxylation of pyruvate. The levels of ^{13}C-incorporation were highest for growth on glucose and lowest on malate. Incorporation of ^{13}C-carbon into gluconeogenesis products was mainly detected in the lactate and malate experiment, whereas glucose down-regulated this path. The characteristic labelling patterns of the amino acids in combination with the marker ratios of ^{13}C-excess between selected amino acids could identify the type of the main organic carbon substrate used by the heterotrophic organism under study. Thus, this labelling approach bears high potential to characterise carbon sources of heterotrophic microorganisms in their natural environments.

Introduction

Reductive carbon fixation under volcanic conditions played a key role in a potential chemoautotrophic origin of life [49] and CO_2-fixation by autotrophic organisms including plants is among the most important biosynthetic processes in the biosphere [21-23, 50]. However, the presence and diversity of carboxylating (CO_2-fixing) enzymes in nature are not restricted to autotrophs alone. Already 80 years ago, utilisation of CO_2 was reported for heterotrophic bacteria producing propionic acid (Propionibacteria) [51]. Today, it is recognised that virtually all heterotrophic organisms – from microorganisms to humans – incorporate CO_2 *via* a variety of pathways involving at least 18 different carboxylases in the central and peripheral metabolism [27-29, 52]. Among these enzymes, anaplerotic carboxylases incorporate CO_2 into biomass and replenish intermediates of the tricarboxylic acid (TCA) cycle, which are constantly withdrawn for the biosynthesis of amino acids and other metabolic products [29]. It is therefore not surprising that carbon from anaplerotic CO_2-incorporation accounts for a significant amount (i.e. 2-8 %) of the cell's biomass carbon abundance [30-34, 45].

Among the protein family of carboxylases, pyruvate carboxylase, an anaplerotic carboxylase, catalyses the bicarbonate (HCO_3^-)-dependent conversion of pyruvate into oxaloacetate. As a component of a putative ancestral reverse TCA cycle, the enzyme is also present in chemolitho-autotrophic bacteria [38], which are considered as one of the most ancient forms of life. The reaction of pyruvate carboxylase could therefore represent a metabolic feature that goes back to the early evolution of life [39].

The enzyme is widely distributed across the three kingdoms of life and has also been retained in many heterotrophic organisms including the Gram-positive bacterium *Bacillus subtilis* (*B. subtilis*) W23. Generally, pyruvate carboxylase occupies a vital position in the central carbon metabolism, since it is located at the "phosphoenolpyruvate-pyruvate-oxaloacetate node" [35, 37, 53]. This metabolic hub unites structurally entangled reactions that interconnect the major pathways of carbon metabolism, i.e. glycolysis (catabolism), gluconeogenesis (anabolism) and

the TCA cycle (energy supply of the cell) [54]. However, the direction of the carbon fluxes at this metabolic hub (towards catabolism, anabolism or energy supply) primarily depends on the type of the available dissolved organic carbon (DOC) and it can be expected that the amount of incorporated CO_2 (or $^{13}CO_2/H^{13}CO_3^-$ in tracer experiments, respectively) varies even within the same organism depending on the assimilated organic carbon source [31-34, 45]. Given a typical metabolic network of a heterotrophic organism capable of carrying out the reaction of pyruvate carboxylase using $H^{13}CO_3^-$ as a substrate, the following simplified scenarios A – C may be distinguished (Fig. 2.1):

Scenario A: During growth on carbohydrates like glucose (Glc), the glycolytic flux constantly produces pyruvate (Pyr), which is further oxidised to acetyl coenzyme A (Ac-CoA). Ac-CoA requires oxaloacetate (Oxa) to form citric acid (Cit) in the first reaction of the TCA cycle. The TCA cycle serves, on the one hand, to catabolise substrates to CO_2. On the other hand, intermediates of the TCA cycle are used as building blocks for biosynthesis. Hence, equivalents of Oxa are constantly withdrawn from the TCA cycle for the formation of Asp and related amino acids. Therefore, the pool of Oxa must be replenished to keep the cycle running. To this end, in *B. subtilis* W23, pyruvate carboxylase directly converts Pyr to Oxa *via* the addition of $H^{13}CO_3^-$. Consequently, TCA cycle metabolites and any products derived thereof, e.g. amino acids like Asp, Lys, Thr, Glu or Pro, are expected to carry this label from $H^{13}CO_3^-$.

Scenario B: Oxa must be replenished *via* the reaction catalysed by pyruvate carboxylase, in the same way as in the first scenario, when substrates such as lactate (Lac) enter the metabolic network somewhere between glycolysis and the TCA cycle. In this case, however, also gluconeogenesis *via* Oxa and phosphoenol pyruvate (PEP) would be expected to become active in order to satisfy the need of the organism for glucose and its derivatives (e.g. for building up membranes and the cell wall of the Gram-positive bacterium). As a result, the ^{13}C-label from $H^{13}CO_3^-$ is not only expected in the metabolites and the products of the TCA cycle (like in the first scenario), but also in those derived from gluconeogenesis or the pentose phosphate pathway, such as Ser, Gly, His, Phe or Tyr.

Scenario C: The substrate directly replenishes the TCA cycle when cells grow on TCA cycle intermediates like malate (Mal). Hence, Pyr carboxylation seems not to be necessary *per se* and central carbon metabolites are not expected to show ^{13}C-incorporation in labelling experiments with $H^{13}CO_3^-$.

However, the assumption that heterotrophic fixation of CO_2/HCO_3^- depends on the organic substrate has not been fully exploited yet. This is surprising since this dependency also has the potential to assign the main carbon source which is utilised by heterotrophic microorganisms. Our study aims to close this gap of knowledge by investigating $H^{13}CO_3^-$ incorporation into *B. subtilis* W23, a well-known model for a heterotrophic bacterium, during growth on glucose, lactate and malate, respectively. These carbon substrates are indicative of the three different entry points to the central carbon metabolism as depicted in the simplified scenarios in Fig. 2.1. Additionally, these substrates also represent naturally occurring components in soil and dissolved organic matter [1, 2, 48, 55].

To assess and to quantify ^{13}C-incorporation from $H^{13}CO_3^-$ in our experiments, we used ^{13}C-based metabolic pathway/flux analysis as a key method [56, 57]. Using this technology, carbon from $^{13}CO_2/H^{13}CO_3^-$ can be traced back through the metabolic network of the organism under study. On this basis, mechanisms of CO_2-fixation, but also downstream fluxes *via* the TCA cycle or gluconeogenesis into metabolic products can be reconstructed on a functional and quantitative basis as shown earlier for plants [58-62] or microorganisms [31, 40-42, 44, 45, 63]. Indeed, the latter experiments also pointed at the crucial role of CO_2-fixation in heterotrophic environmental microbes [40, 46-48].

In the present study with *B. subtilis* W23 $H^{13}CO_3^-$-labelling experiments were monitored by elemental analysis-isotope ratio mass spectrometry (EA-IRMS) of total biomass and by GC-MS of amino acids to show an example of how to assign main (unlabelled) organic substrates on this basis. Subsequently, $H^{13}CO_3^-$-labelling experiments with a natural microbial community from groundwater were conducted to provide a proof-of-principle that this approach indeed opens a new avenue to elucidate substrate usages in complex environmental samples.

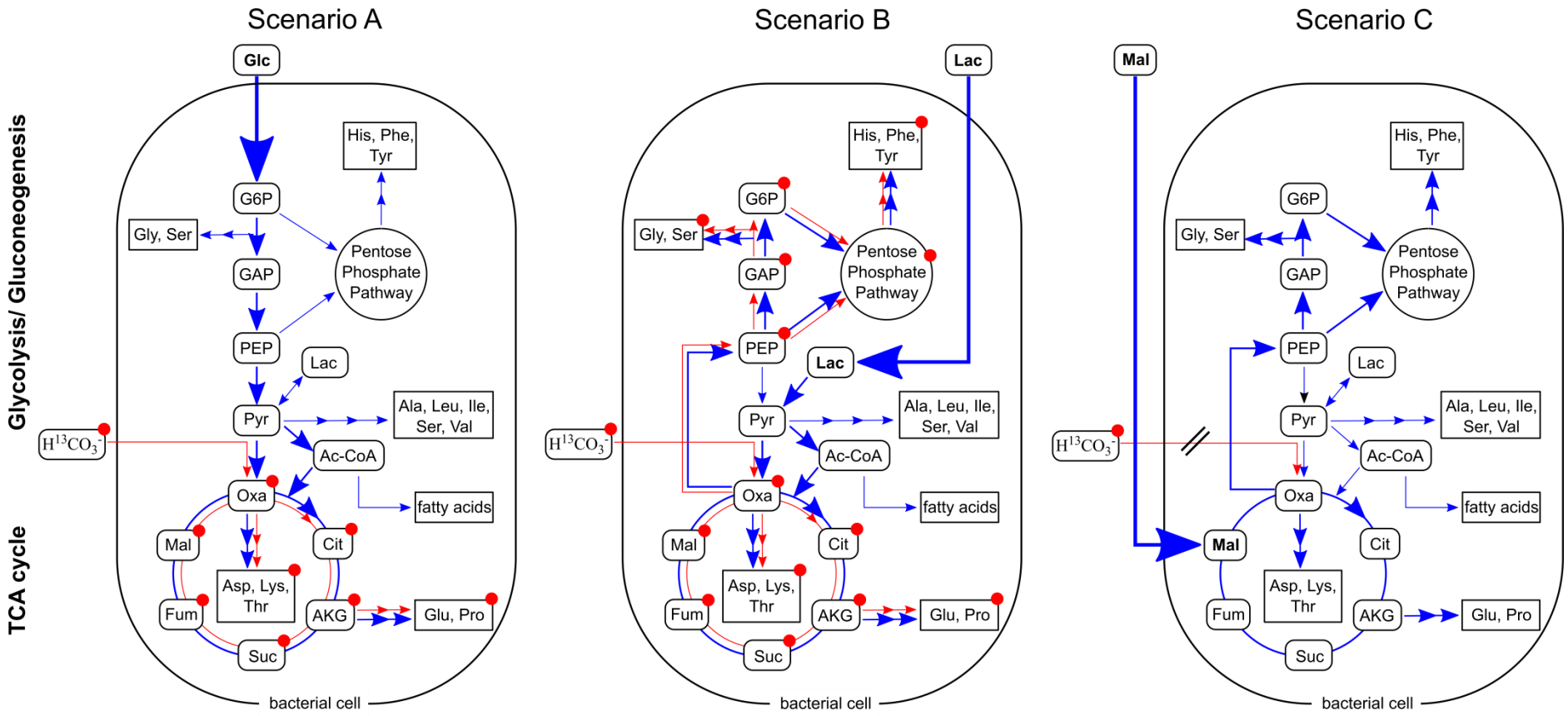

Figure 2.1: Simplified scenarios of ^{13}C-distribution after anaplerotic fixation of $H^{13}CO_3^-$ when different organic growth substrates are utilised. Scenarios A, B, and C show the expected labelling patterns from $H^{13}CO_3^-$ when using unlabelled glucose (Glc), lactate (Lac), or malate (Mal) as main organic carbon substrates. The bold arrows indicate main carbon fluxes. Red arrows show the respective fluxes from the supplied $H^{13}CO_3^-$ tracer through the metabolic network; blue arrows depict the carbon fluxes from the unlabelled organic substrates, respectively. Metabolites and products marked with a red circle are expected to receive ^{13}C-label originating from $H^{13}CO_3^-$.

Materials and Methods

Strain and growth conditions

All experiments were performed with *B. subtilis* subsp. *spizizenii* W23 (DSM No.: 6395), a prototrophic derivative of the wild type, obtained from DSMZ (Leibnitz Institute DSMZ – German Collection of Microorganisms and Cell Cultures, Braunschweig, Germany). For pre-cultivation, 5 mL of M9 minimal growth medium, supplemented with 1 g/L glucose, 1 g/L lactate or 1.1 g/L malate, respectively, and preheated to 30 °C, were inoculated with 300 µL of a glycerol stock solution of the bacterium. The amounts of organic substrates were chosen in order to ensure that the amount of carbon available to the bacteria (0.4 g/L) was the same in all three setups. The pre-cultures were incubated for 20 h. In order to prevent the formation of biofilms, the culture tubes were shaken vigorously at 300 rpm on an orbital incubation shaker (IKA KS 4000i control, IKA-Werke, Staufen, Germany). Each pre-culture was used to inoculate 195 mL of M9 minimal growth medium, preheated to 30 °C, in 500 mL Schott bottles. The M9 minimal growth medium was a mixture of 165 mL of M9 minimal medium, 20 mL of a 10 g/L glucose, 10 g/L lactate or 11 g/L malate stock solution, respectively, and 10 mL of a 20 g/L sodium bicarbonate stock solution. The bicarbonate was either $NaH^{13}CO_3$ (98 atom% ^{13}C, Sigma Aldrich, Darmstadt, Germany) in the ^{13}C-labelling experiments or unlabelled $NaHCO_3$ (1.1 % natural ^{13}C-abundance, Sigma Aldrich, Darmstadt, Germany) in the control experiments. The bottles were closed gastight after inoculation to block the release of $^{13}CO_2$. To avoid depletion of O_2, an aliquot of fresh air (filter-sterilised using a 0.22 µm syringe filter) that equals the volume of a taken sample, was added at every time point of sampling. The cultivations were performed at 30 °C and 150 rpm on an orbital incubation shaker.

The M9 minimal growth medium consisted of the following components (per litre): 8.5 g of $Na_2HPO_4 \cdot 2\ H_2O$, 3 g of KH_2PO_4, 1 g of NH_4Cl and 0.5 g of NaCl (=base salts solution). The following components were autoclaved separately before being added to the base salts solution in the given order (per litre): 1 mL of 0.1 M $CaCl_2$, 10 mL trace salts stock solution, 1 mL of 1 M $MgSO_4$ and 1 mL of 50 mM $FeCl_3$ ·

6 H_2O (filter-sterilised using a 0.22 µm syringe filter). The trace salts stock solution contained (per litre): 100 mg of $MnCl_2 \cdot 4\ H_2O$, 170 mg of $ZnCl_2$, 43 mg of $CuCl_2 \cdot 2\ H_2O$, 60 mg of $CoCl_2 \cdot 6\ H_2O$ and 60 mg of $Na_2MoO_4 \cdot 2\ H_2O$. The glucose, lactate, malate and sodium bicarbonate stock solutions were filter-sterilised, using a 0.22 µm syringe filter, before being added to the medium. All solutions were prepared using sterilised MilliQ water. All chemicals were purchased from Sigma Aldrich (St. Louis, USA).

^{13}C-Labelling experiments and microbial dry weight

B. subtilis subsp. *spizizenii* W23 was grown in M9 minimal growth medium supplemented with 1 g/L glucose, 1 g/L lactate or 1.1 g/L malate, respectively, and 1 g/L sodium bicarbonate. The ^{13}C-labelling experiments were conducted in triplicates and the control experiments with unlabelled bicarbonate in duplicates. After 10 h of incubation, one control experiment was spiked with sodium ^{13}C-bicarbonate (1 g/L); the second control experiment remained untouched. Bacterial growth was monitored by determining the optical density at 600 nm (OD_{600}). Samples for biomass and amino acid analysis were taken at intervals of 2 h after inoculation. At each of these time points, 20 mL of the bacterial culture were harvested by centrifugation (4 °C, 4000 rpm, 20 min). The supernatant was carefully removed, filter-sterilised, using a 0.22 µm syringe filter, and stored at -20 °C for HPLC analysis (see below). The cell pellet was re-suspended in 2 mL of sterile MilliQ water and transferred into an Eppendorf tube. After this washing step, a second centrifugation step (4 °C, 14000 rpm, 20 min) pelleted the cells again. The supernatant was carefully discarded and the pellet was frozen at -80 °C. The frozen pellets were freeze-dried overnight using a VirTis Sentry 8L benchtop freeze dryer (SP Industries, Warminster, PA, USA). The freeze-dried bacterial pellets were weighed using a high-resolution balance (CP2P, Sartorius AG Göttingen, Germany) to determine the microbial dry weight.

Protein hydrolysis and amino acid derivatisation

For protein hydrolysis about 0.5 mg of the freeze-dried bacterial pellet was mixed with 500 µL of 6 M hydrochloric acid and heated at 105 °C for 24 h. After cooling to

70 °C, the residual hydrochloric acid was removed by a constant stream of nitrogen gas. The dried sample was then re-suspended in 50 % glacial acetic acid by sonication for 120 sec. A small column (1 mL pipet tip) of the cation exchanger Dowex 50WX8 [200-400 mesh (=37-74 µm), H^+ form] was prepared and washed with 1 mL of methanol followed by 1 mL of MilliQ water. After loading the sample onto the column, it was washed twice with 1 mL of MilliQ water. The bound amino acids were then eluted from the column by 1 mL of 4 M ammonium hydroxide. An aliquot of the eluate was dried under a constant stream of nitrogen gas at 70 °C. For derivatisation, the dry residue was dissolved in 50 µL of water-free acetonitrile and 50 µL of N-(tert-butyldimethylsilyl)-N-methyl-trifluoroacetamide containing 1 % tert-butyldimethylsilylchlorid. This mixture was kept at 70 °C for 30 min. The resulting N-tertbutyldimethylsilyl-derivatives of the amino acids (TBDMS-amino acid derivatives) were analysed by GC-MS following established protocols [18].

Gas chromatography/mass spectrometry of silylated amino acids

GC-MS analysis was performed using a 7890A GC system (Agilent Technologies, Santa Clara, CA, United States) equipped with a fused silica capillary column (Equity TM-5; 30 m x 0.25 mm, 0.25 µm film thickness; Supelco, Bellefonte, PA, United States). The mass detector worked with electron impact ionisation at 70 eV. An aliquot (1-3 µL) of the solution containing the TBDMS-amino acid derivatives was injected in a 1:10 split mode. The interface temperature was set to 260 °C. The column temperature was held at 140 °C for 3 min, heated with a temperature gradient of 4 °C/ min to 165 °C, heated with a second temperature gradient of 15 °C/ min to 200 °C and heated with a third temperature gradient of 7 °C/ min to 280 °C where the temperature was held for 3 min. Selected ion monitoring data were acquired using a 0.3-sec sampling rate and the samples were analysed three times. Data collection was carried out *via* the GC-MSD Data Analysis software (Agilent Technologies, Santa Clara, CA, United States). The retention times and the detected mass fragments of the amino acids are listed in the supplementary Table T1. ^{13}C-Incorporation into amino acids was computed according to Lee et al. [64]. The steps include the determination of the contribution of the derivatisation reagent to the observed spectrum of the silylated amino acid and the correction for contribution from ^{13}C-carbon natural abundance using multiple linear regression analysis. The mass

isotopomer distribution after this background subtraction provides fractional ^{13}C-excess values for amino acid isotopomers carrying one ^{13}C-carbon atom (M+1), two ^{13}C-carbon atoms (M+2), three ^{13}C-carbon atoms (M+3), and so on, where the sum over all isotopomers [M + (M+1) + (M+2) + (M+3) etc.] is defined as 100 %. As an example, amino acids with an M+1 excess value of 50 % are composed of 50 % unlabelled molecules (M) and 50 % molecules carrying one ^{13}C-carbon (M+1) from the ^{13}C-labelled precursor. Amino acids that carry at least one ^{13}C-carbon atom in excess are termed labelled amino acids in the following.

Carbon isotopic analysis of biomass

Carbon isotopic ratios were determined by an elemental analyser-isotope ratio mass spectrometer (EA-IRMS) consisting of a EuroEA (Euro vector, Milano, Italy) coupled to a FinniganTM MAT253 IRMS (Themo Fisher Scientific, Bremen, Germany) by a FinniganTM ConFlow III interface (Thermo Fisher Scientific, Bremen, Germany). For EA-IRMS analysis, a small amount of the freeze-dried pellet (100-400 µg) was put into tin capsules (3.3 x 5 mm, IVA Analysentechnik, Meerbusch, Germany) and subjected to elemental analysis by dropping them into a heated reactor which contained silvered cobalt oxide and chromium oxide (IVA Analysentechnik, Meerbusch, Germany and HEKA tech, Wegberg, Germany). The biomass pellets were combusted in a stream of O_2-containing He at 1000 °C to produce N_2, NO_x, H_2O and CO_2, where NO_x was directly converted to N_2 again in an online reduction reactor filled with metallic copper filings. The gases were subsequently transferred to the isotope ratio mass spectrometer *via* a ConFlow III system using a continuous helium stream of 90 mL/ min. The CO_2 reference gas was provided by CARBO (Bad Hönningen, Germany). The resulting values from EA-IRMS analysis include the natural abundance of ^{13}C-carbon.

Analysis of substrate consumption (HPLC)

The frozen, filter-sterilised supernatant was used for substrate consumption analysis by HPLC. Briefly, glucose, lactate and malate, respectively, were separated and quantified by HPLC using a ligand exchange Aminex HPX 87H column (300 x 7.8 mm) plus precolumn (30 x 4.6 mm) (Bio-Rad Laboratories GmbH, Feldkirchen,

Germany). Aliquots of 20 µL were injected per run. The column oven was set to 40 °C. The eluent was 5 mM H_2SO_4 at a flow rate of 0.6 mL/ min. Glucose was detected using a RID-10A detector; lactate and malate were detected using the RID-10A and the DAD-SPD-M10Avp detector operating at 210 nm. The retention times of glucose, malate and lactate were 9.1 min, 9.9 min and 12.8 min, respectively.

Statistical Analysis

A two-tailed unpaired Student's t-test was used for the analysis of differences between the mean values of ^{13}C-incorporation into selected pairs of amino acids from the experiments with glucose, lactate and malate. Statistical significance is depicted as *ns* = not significant, *$p < 0.05$, **$p < 0.01$, or ***$p < 0.001$.

Results

Growth of *B. subtilis* in the presence of glucose and $H^{13}CO_3^-$

The growth experiment with *B. subtilis* W23 in M9 medium containing glucose and $H^{13}CO_3^-$ displayed the usages of both substrates for building up its biomass over time. The glucose concentration in the medium constantly decreased from 5.6 mM to below the analytical detection limit (3 mM in this setup) at 8 h after inoculation (Fig. 2.2A). With declining substrate concentration, bacterial biomass increased from 0.03 g/L to 0.44 g/L during the experiment until glucose became limiting. The ^{13}C-abundance of the biomass, as determined by EA-IRMS, steadily rose from 1.1 % (natural abundance of ^{13}C-carbon) to a maximum of 6 % at 6 h after inoculation (Fig. 2.2B). Then, the ^{13}C-abundance levelled off and stayed constant at about 5 % until the end of the experiment. The control experiment with unlabelled HCO_3^- mirrored the natural abundance of ^{13}C-carbon (1.1 %) in the environment. In the labelling experiment, the maximum of ^{13}C-abundance of 6 % at 6 h and the subsequent decline to 5 % could be explained by the production of unlabelled CO_2 *via* respiration of unlabelled glucose, which led to the formation of unlabelled CO_2/bicarbonate in the medium as growth occurred. This production of unlabelled bicarbonate led over time to a dilution of the supplied $H^{13}CO_3^-$ as indicated by model calculations (see supporting data files F1-F4 for details and supporting Fig. S1). In addition, glucose became limiting so that microbial growth slowed down. Nevertheless, $H^{13}CO_3^-$ was still present in the medium and was used by *B. subtilis* W23 for anaplerosis even during the stationary phase of growth finally leading to a stable ^{13}C-abundance of the bacterial biomass till the end of the experiment (Fig. 2.2B). Specifically, when ^{13}C-bicarbonate was spiked to a non-labelled control after exponential growth in the stationary phase, i.e. after 10 h of inoculation, the ^{13}C-abundance of the biomass still increased up to approximately 2 % (Fig. 2.2C). This clearly demonstrated that CO_2-fixation took place even in the absence of cell growth indicating active metabolism during the stationary phase. In similar experiments, we added $H^{13}CO_3^-$ to *B. subtilis* W23 during the stationary phase when grown on lactate or malate, respectively (see also below). The ^{13}C-abundance of the respective biomass was again determined by EA-IRMS and accounted for 3 % in the lactate experiment (Fig. S2C) and 2 % in the

malate experiment (Fig. S3C). Thus, irrespective of the used carbon substrate and the physiological state (growth phase or stationary phase), metabolic turn-over of oxaloacetate involving the reaction of pyruvate carboxylase remained important, probably to maintain the energy balance also in non-growing *B. subtilis* W23.

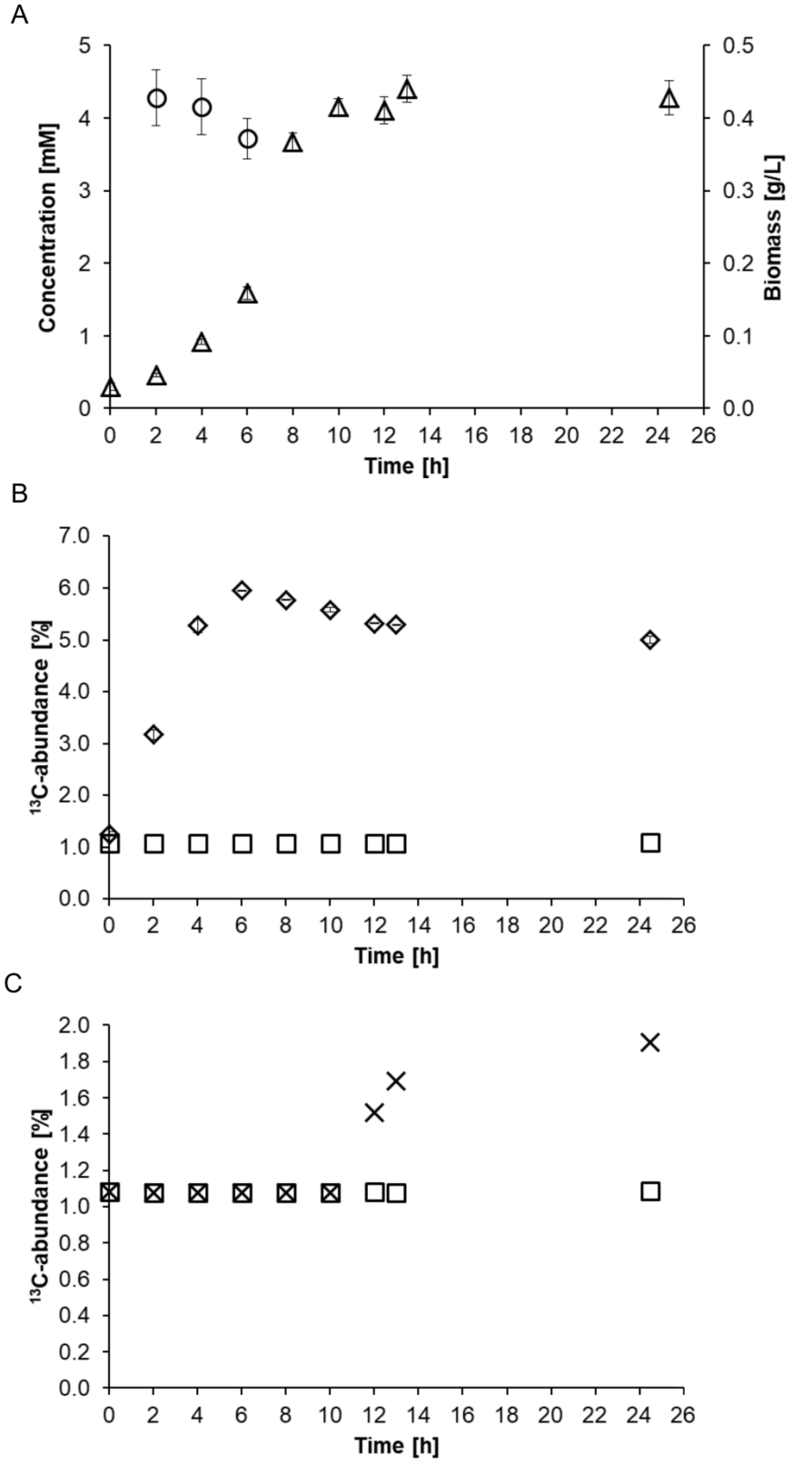

Figure 2.2: (A) Glucose consumption and biomass production by *B. subtilis* W23 growing in M9 medium containing 1 g/L glucose. The circles represent the glucose concentration and the triangles the biomass production over time. **(B) Incorporation of ^{13}C-carbon into microbial biomass by *B. subtilis* W23 growing in M9 medium containing 1 g/L glucose and 1 g/L $NaH^{13}CO_3^-$.** The diamonds represent the ^{13}C-incorporation into the biomass as determined by EA-IRMS measurements. The depicted values are mean values

of three biological replicates. The squares represent the control experiment conducted with unlabelled bicarbonate, which shows the natural abundance of ^{13}C-carbon of 1.1 % in the environment. **(C) Incorporation of ^{13}C-carbon into microbial biomass by *B. subtilis* W23 growing in M9 glucose medium containing 1 g/L $NaH^{13}CO_3^-$ during the stationary phase.** The culture was supplied with the tracer 10 h after inoculation. The ^{13}C-abundance of the biomass (depicted as crosses) increased up to 2 %. In a control experiment, no $H^{13}CO_3^-$ was added. The ^{13}C-abundance of the biomass (depicted as squares) again mirrored the natural abundance of ^{13}C-carbon in the environment.

Growth of *B. subtilis* in the presence of lactate and $H^{13}CO_3^-$

The trends for substrate consumption and biomass production for growth on lactate and $H^{13}CO_3^-$ were similar to the experiment with glucose. Briefly, the concentration of lactate decreased from 11.2 mM to 0.3 mM, while the biomass increased from 0.03 g/L to 0.43 g/L during the experiment (Fig. S2A). Again, the formation of unlabelled bicarbonate caused a dilution of the ^{13}C-label at the end of the experiment. EA-IRMS showed that under these conditions *B. subtilis* W23 incorporated 5 % of labelled inorganic carbon into its biomass, which is 1 % less compared to the glucose experiment (Fig. S2B) (see also Fig. 2.3).

Growth of *B. subtilis* in the presence of malate and $H^{13}CO_3^-$

In the third experimental setup, *B. subtilis* W23 was grown in M9 medium supplemented with malate and $H^{13}CO_3^-$. Measured substrate consumption demonstrated efficient uptake of malate [65] which was accompanied by an increase of biomass from 0.04 g/L to 0.29 g/L during the experiment. The concentration of malate in the medium decreased from 8.2 mM to below the analytical detection limit of 0.05 mM (Fig. S3A). When using ^{13}C-bicarbonate in the malate medium, the ^{13}C-abundance of the biomass of the bacteria accounted for 3 % under these conditions, as measured by EA-IRMS (Fig. S3B). Notably, this value was significantly lower compared to the glucose and lactate experiments (Fig. 2.3). Nevertheless, the detection of ^{13}C-incorporation came as a surprise, since exogenous malate could have fully refilled the TCA cycle without the need for anaplerotic replenishment, introducing the ^{13}C-label (see simplified scenario C in Fig. 2.1).

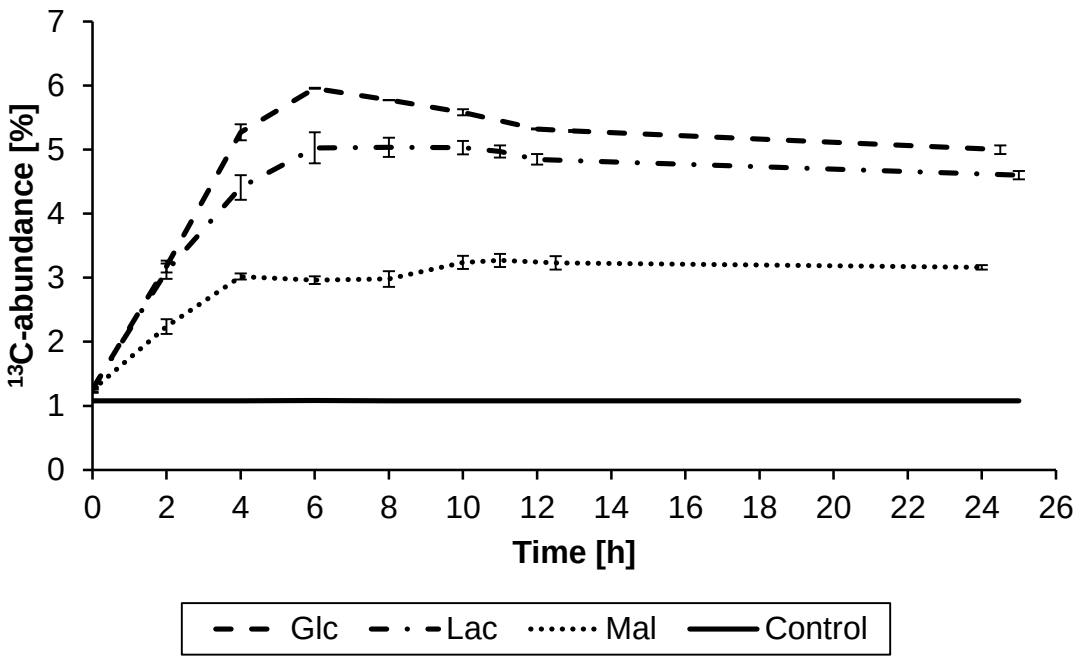

Figure 2.3: Incorporation of ^{13}C-carbon from $H^{13}CO_3^-$ into the biomass of *B. subtilis* W23 growing in M9 medium containing unlabelled glucose, lactate or malate as carbon sources, respectively. The control shows the natural abundance of ^{13}C-carbon. The depicted values are mean values of three biological replicates. The error bars represent the calculated standard deviation; in case of the control, the error bars are too small to be visible.

^{13}C-Labelling patterns of amino acids

The ^{13}C-EA-IRMS results demonstrated the general importance of heterotrophic CO_2-fixation by pyruvate carboxylase. However, the universal label incorporation under different conditions makes it difficult to achieve the primary objective of our study, namely to identify the use of different substrates. In a next step, we therefore focused on amino acid-specific incorporation of ^{13}C, which should provide more specific data concerning substrate usage. As an example, amino acids from the TCA cycle (e.g., Asp, Glu) or gluconeogenesis (e.g., Tyr, Phe) were expected to acquire a greater fraction of ^{13}C-carbon as compared to those amino acids derived from pyruvate (e.g., Val, Ala), where the incorporation of ^{13}C-carbon should be low (see Fig. 2.1). Using established protocols [18], we quantified the ^{13}C-excess (mol-%) in 14 amino acids obtained from acidic hydrolysis of the biomass. Among the labelled amino acids, ^{13}C-excess was found especially for isotopomers carrying one ^{13}C-carbon atom (M+1 isotopomers) as expected for a labelling experiment with $H^{13}CO_3^-$.

During growth on glucose, ^{13}C-excess of the M+1 isotopomers of amino acids derived from intermediates of the TCA cycle, such as Asp, Thr, Lys, Glu and Pro (see also Fig. 2.1) reached values up to 50 % (Fig. 2.4A). The ^{13}C-excess of the same isotopomers reached values up to 40 % when the bacteria were grown on lactate (Fig. 2.4B) and values up to 15 % during growth on malate (Fig. 2.4C). The ^{13}C-excess of the M+1 isotopomers of amino acids derived from gluconeogenetic intermediates was low for Ser (about 4 %) and apparently absent for His (derived from the pentose phosphate pathway intermediate, phosphoribosyl pyrophosphate, PRPP) when *B. subtilis* W23 was grown on glucose, lactate or malate, respectively. Glycine, which is also derived from gluconeogenetic intermediates, showed a moderate ^{13}C-excess of the M+1 isotopomer under all three conditions (6-8 %). Amino acids derived from pyruvate such as Ala, Val, and Leu received very low ^{13}C-label under all three conditions (< 3 %). Amino acids (Tyr and Phe) that were synthesised from the pentose phosphate pathway intermediate, erythrose-4-phosphate, showed moderate ^{13}C-excess of the respective M+1 isotopomers (about 5 %) when *B. subtilis* W23 was grown on lactate or malate (Fig. 2.4B and C), and no ^{13}C-excess of the same M+1 isotopomers when grown on glucose (Fig. 2.4A).

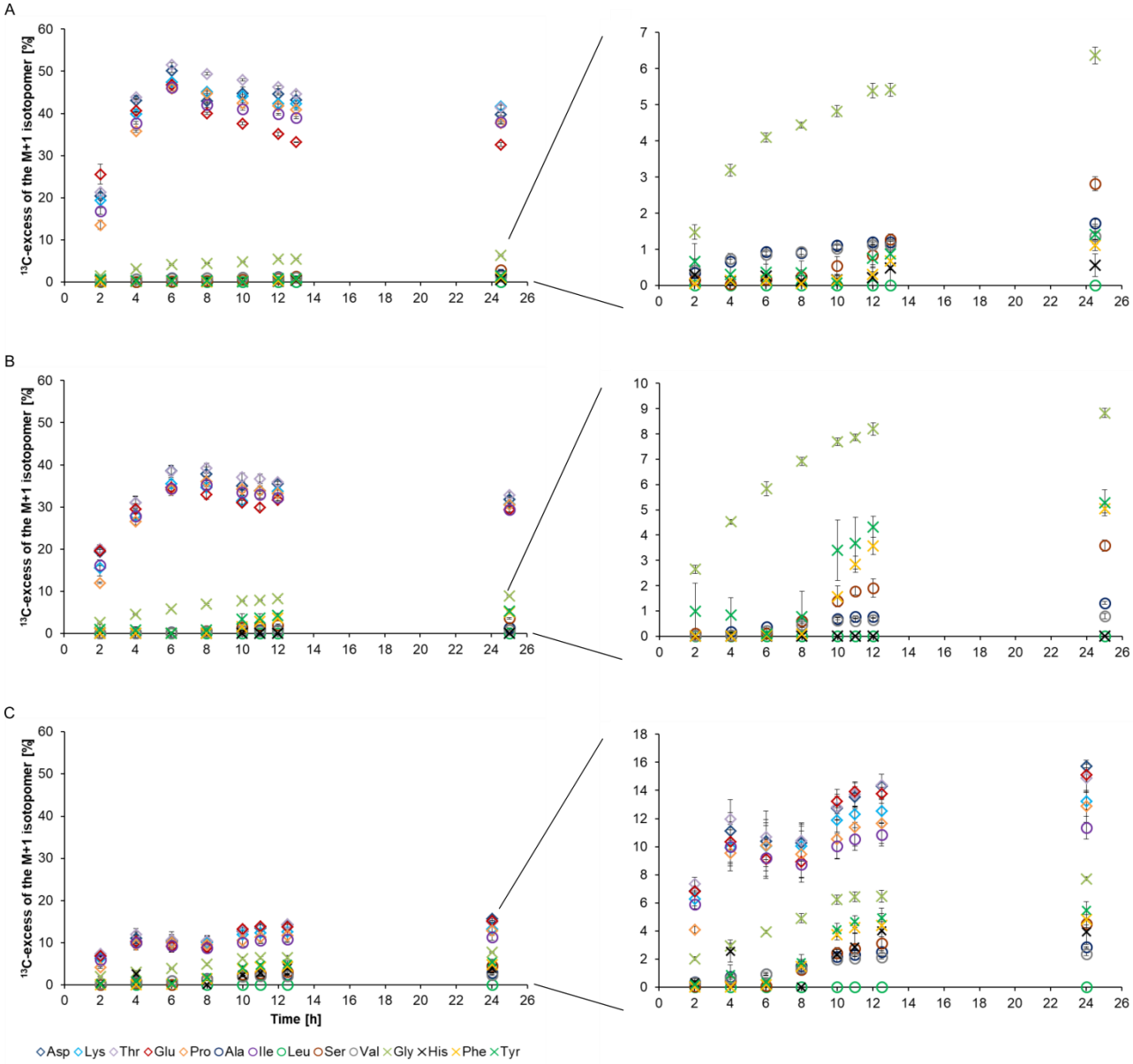

Figure 2.4: ^{13}C-excess of the M+1 isotopomers of specific amino acids produced by $H^{13}CO_3^-$-labelling experiments with glucose (A), lactate (B), and malate (C), respectively. Amino acids depicted as diamonds are derived from the TCA cycle. Amino acids depicted as circles are derived from pyruvate. Amino acids depicted as crosses are derived from the gluconeogenesis pathway. The ^{13}C-excess of the amino acids derived from pyruvate and the gluconeogenesis pathway are also displayed with a different scaling to improve visibility.

From these comparisons, it becomes already evident that the ^{13}C-patterns in amino acids specifically reflected the (unlabelled) organic carbon substrate used by *B. subtilis* W23 in our model experiments. However, to better visualise the differences in the respective substrate usages, we now compared ratios of ^{13}C-excess of the M+1 isotopomers in specific sets of amino acids (Fig. 2.5). More specifically, Ala and Val were used as representatives for ^{13}C-incorporation *via* pyruvate (i.e. displaying only very low ^{13}C-excess of the M+1 isotopomers in the experimental settings). Tyr and Phe served as representatives for ^{13}C-bicarbonate incorporation *via* gluconeogenesis and the pentose phosphate pathway, whereas Asp and Glu were used as representatives for ^{13}C-incorporation *via* the TCA cycle (see also Fig. 2.1).

The ratios of the ^{13}C-excess of the M+1 isotopomers at *quasi* steady-state conditions (from 10 h after inoculation till the end of the experiment) gave clear diagnostic trends that uniquely allowed discerning the three different scenarios shown in Fig. 2.1. When calculating the ratios between the ^{13}C-excess of the M+1 isotopomers in TCA cycle-derived amino acids and those of pyruvate-derived amino acids (i.e., Asp/Val, Asp/Ala, Glu/Val and Glu/Ala), values above 20 were obtained in the experiments with glucose or lactate, where TCA cycle metabolites must be replenished, whereas ratios below 10 were obtained for the same sets of amino acids in the experiments with malate, where anaplerosis is not needed (Fig. 2.5A). When calculating the ratios between the ^{13}C-excess of the M+1 isotopomers in gluconeogenesis-derived amino acids and those in pyruvate-derived amino acids (i.e., Tyr/Val, Tyr/Ala, Phe/Val and Phe/Ala), ratios above 4 were obtained for experiments with lactate (i.e. under apparently active gluconeogenesis), whereas ratios of 1 or lower were observed for growth on glucose where gluconeogenesis is not needed (Fig. 2.5B). Thus, ratios of ^{13}C-excess of the M+1 isotopomers between these selected groups of amino acids provided highly selective markers to distinguish the main organic carbon substrates in our model experiments.

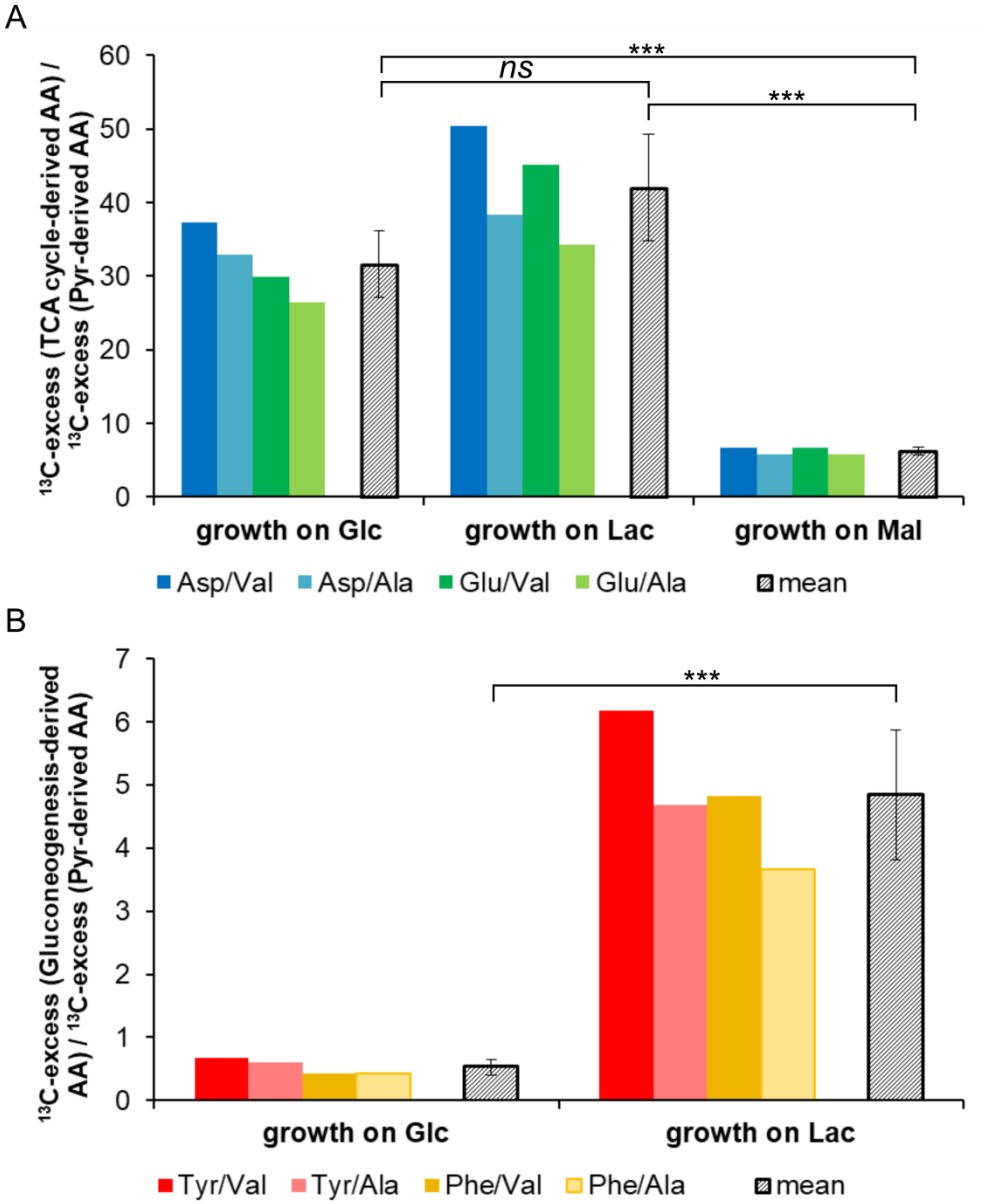

Figure 2.5: Marker ratios of ^{13}C-excess between selected amino acids. (A) ^{13}C-excess (TCA cycle-derived amino acids)/ ^{13}C-excess (pyruvate-derived amino acids). The coloured bars depict the ratios of the chosen amino acids in the labelling experiments with each of the three substrates. The grey bars show the mean values of ^{13}C-ratios for these fractions. The individual ratios as well as the mean values are significantly higher when an active CO_2-fixation is required (glucose and lactate) compared to a background or random fixation of CO_2 (malate). p-Values as calculated by Student's t-test (unpaired): p(Glc/Lac) = 0.05031, p(Glc/Mal) = 0.00003, p(Lac/Mal) = 0.00006 **(B) ^{13}C-excess (gluconeogenesis-derived amino acids)/ ^{13}C-excess (pyruvate-derived amino acids).** The coloured bars depict the ratios of the chosen amino acids when glucose or lactate were the growth substrates, respectively, and the grey bars show again the mean values of ^{13}C-ratios. These ratios are sensitive indicators to clearly differentiate lactate from glucose as the respective carbon source. p-Value as calculated by Student's t-test (unpaired): p(Glc/Lac) = 0.00017 (For detailed calculation see SI excel file F5 m+1 and ratio of label_SI Paper)

Discussion

By means of anaplerotic CO_2-fixation, *B. subtilis* W23 incorporated ^{13}C-labelled bicarbonate to a different extent into its biomass depending on the main organic carbon source being present in the minimal medium (i.e. glucose, lactate or malate, respectively). Indeed, the data from EA-IRMS analyses alone could already show significant differences between the three carbon substrates tested in this study, as illustrated in Fig. 2.3. Incorporation of $H^{13}CO_3^-/^{13}CO_2$ to an extent of 6 % and 5 % into microbial biomass during growth on glucose and lactate, respectively, reflected biomass formation involving anaplerotic carboxylation of pyruvate, which was in some agreement with our simplified scenarios A and B in Fig. 2.1. Notably, however, in comparison with the glucose experiment, the ^{13}C-abundance of the biomass was lower in the lactate experiment (6 % vs. 5 %). At first glance this came as a surprise since we expected the same or an even higher ^{13}C-abundance of the bacterial biomass, when lactate was used as the organic substrate. Under lactate conditions, ^{13}C-incorporation should also have occurred *via* ^{13}C-labelled oxaloacetate into products derived from intermediates of the TCA cycle as well as into those derived from gluconeogenesis and the pentose phosphate pathway (see scenario B in Fig. 2.1). The latter routes did not play a major role in the lactate experiment as confirmed by the low levels or the apparent absence of label in His, Ser, Tyr and Phe, respectively. Rather, lactate seemed to be directly channelled *via* pyruvate and Ser into glycerate-3-phosphate and triose phosphates [66], then serving as unlabelled precursors for glucose formation and the pentose phosphate pathway in our experimental setting [55]. Following this metabolic flux, cell wall sugars and other gluconeogenetic metabolites would not acquire label from $H^{13}CO_3^-/^{13}CO_2$ *via* ^{13}C-oxaloacetate, thus leading to the observed lower ^{13}C-incorporation. Interestingly, transcriptional, translational and post-translational down-regulation of anaplerotic reactions might be triggered by the presence of exogenous organic acids in the medium [67, 68]. Against the background of lactate, as the only organic carbon source in the medium, it seemed safe to assume that anaplerosis was restrained. Similarly, NADH in excess produced by lactate dehydrogenase in the presence of lactate would also down-regulate the TCA cycle and its anaplerotic reactions [69].

Together, less ^{13}C-carbon is incorporated into gluconeogenetic products and the overall biomass when the bacteria grow on lactate compared to growth on glucose.

The occurrence of the ^{13}C-label in amino acids also clearly assigned pyruvate carboxylase as the $H^{13}CO_3^-/^{13}CO_2$-binding enzyme in all of our settings including the experiment with malate (for details, see below). The unexpected incorporation of 3 % ^{13}C-carbon into microbial biomass during growth on malate suggests that, even under this condition, pyruvate carboxylase was still actively transforming pyruvate into oxaloacetate, even though the organism could have directly refilled the oxaloacetate pool of the TCA cycle by taking excess malate from the growth medium (see scenario C in Fig. 2.1). Thus, although being characterised as non-essential for *B. subtilis* W23 in SubtiWiki [70], the constantly expressed gene for pyruvate carboxylase implies a permanent activity for this enzyme [37, 54] – possibly to be able to quickly react when growth conditions change and anaplerosis becomes necessary for survival [71, 72]. Interestingly, metabolic activity of pyruvate carboxylase could also be detected during the stationary growth phase of *B. subtilis* W23 irrespective of the main organic substrate being used from the medium (Figs. 2.2C, S2C and S3C). This also indicates the important role of the constantly present enzyme pyruvate carboxylase in the metabolism of *B. subtilis* W23.

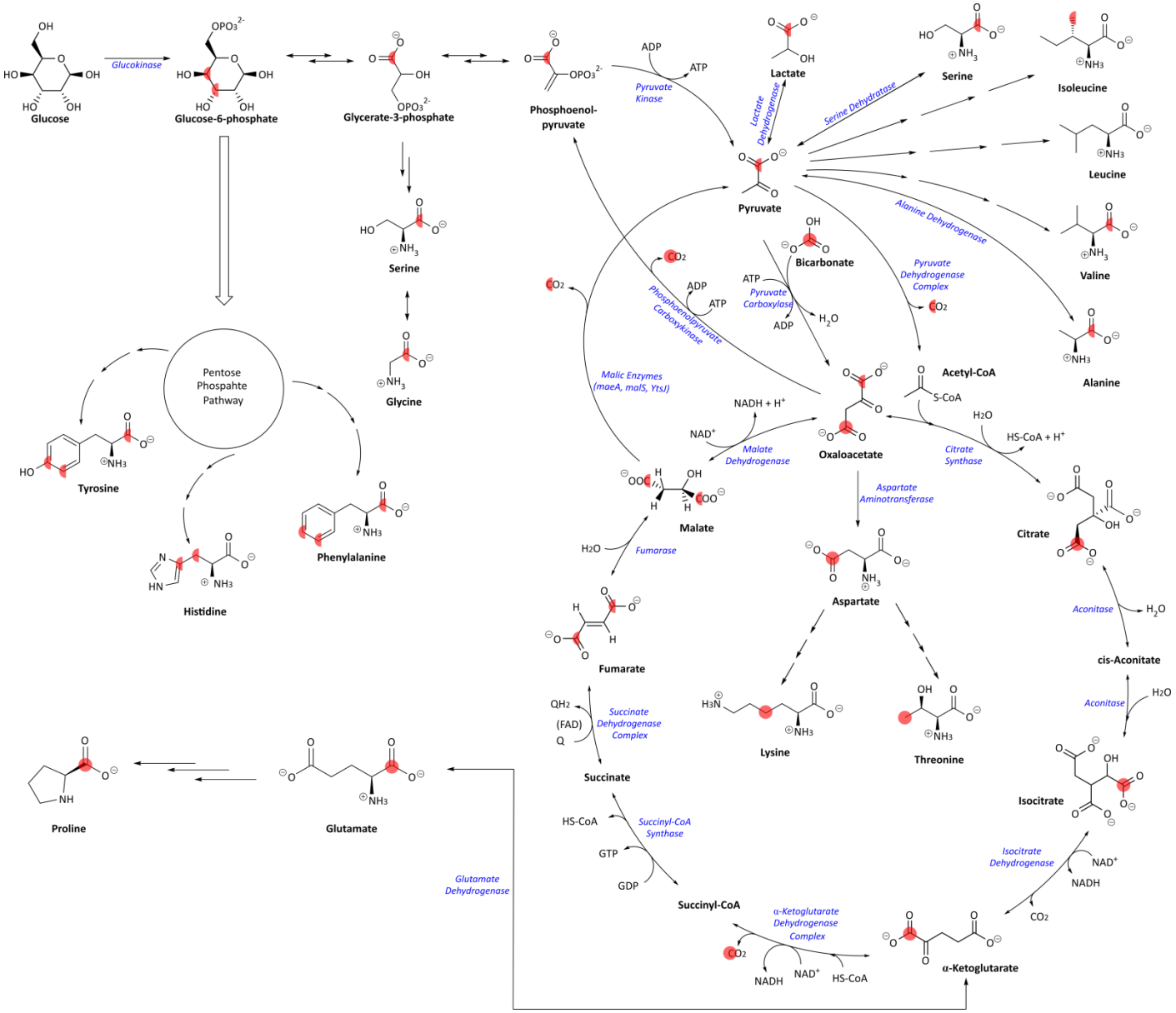

Figure 2.6: Metabolic network observed for *B. subtilis* W23 growing in M9 medium containing $H^{13}CO_3^-$ as a tracer. The full red circles mark the location of the ^{13}C-atom detected in amino acids. On this basis, the labelling profiles of their respective precursors were reconstructed. The equilibrium between the reactions of the reductive branch of the TCA cycle could transfer the ^{13}C-label from oxaloacetate to malate, fumarate and succinate. The intrinsic symmetry of fumarate leads to the formation of a 0.5:0.5 mixture of [1-^{13}C]- and [4-^{13}C]malate as well as [1-^{13}C]- and [4-^{13}C]oxaloacetate, respectively. This is indicated by the red half circles.

EA-IRMS analysis alone could not clearly pinpoint the metabolic history of the incorporated inorganic carbon under the different conditions, nor could it exclude that multiple enzymes contributed to the observed label incorporation. To further confirm that pyruvate carboxylase is responsible for ^{13}C-incorporation into microbial biomass and to follow the labelled inorganic carbon through the metabolic network of the microbial cell, we used GC-MS analysis to reveal information about the carbon positions in amino acids having acquired the label. On the basis of the detected fragmentation patterns of the silylated amino acids (for details, see Table T1), some positional assignments of the ^{13}C-label, especially those involving C-1 of the amino acids, were possible (Fig. 2.6). As an example, the fragments with m/z of 432 and 286 for Glu and Pro, respectively, contained all five carbon atoms of the original amino acids. When analysing the mass spectra we found that these fragments were accompanied by a high amount (up to 50 %) of the respective M+1 isotopomer (namely m/z 433 for Glu and m/z 287 for Pro). In contrast the fragments that had lost the C-1 carbon atom of these amino acids (i.e. m/z 404 and 330 for Glu and m/z 258 and 184 for Pro) were not accompanied by a significant excess of the respective M+1 isotopomers (< 1 %). On this basis, it can be safely concluded that Glu and Pro carried the ^{13}C-label at C-1. Similarly, the mass distribution in the fragments observed for Asp, Thr and Lys signalled high amounts of the respective M+1 isotopomers (up to 50 %). Here, the ^{13}C-labelled carbon atom was mainly present at C-4 of these amino acids, as learned from the analysis of the respective fragments. However, lower amounts of ^{13}C-label (1 – 5 %) could also be assigned to C-1 of these amino acids. As illustrated in Fig. 2.6, this label distribution can be explained because (i) C-4 of oxaloacetate acquires the ^{13}C-label from $H^{13}CO_3^-$ by the reaction of pyruvate carboxylase, (ii) [4-^{13}C]oxaloacetate is converted into [1-^{13}C]α-ketoglutarate *via* the oxidative branch of the TCA cycle (leading to the detected [1-^{13}C]-isotopomers of Glu and Pro), (iii) the biosynthesis of Asp, Thr and Lys is based on the TCA cycle intermediate oxaloacetate (leading to the detected [4-^{13}C]-isotopomers), and (iv) reversible reactions between oxaloacetate and succinate, in the reductive branch of the TCA cycle, lead to a scrambling of label between C-1 and C-4 of the symmetric intermediates fumarate and succinate. Hence, the ^{13}C-label was transferred also into C-1 of oxaloacetate and its downstream products Asp, Thr and Lys (see also Fig. 2.6, red half circles). Remarkably, the position-specific incorporation of ^{13}C-carbon at C-1 of Glu and Pro, and C-4 of Asp, Thr and Lys

reached values up to 50 % when the bacteria were grown on glucose and as high as 40 % when grown on lactate (Fig. 2.4A and B). These data demonstrated that the anaplerotic reaction catalysed by pyruvate carboxylase transferred the ^{13}C-label efficiently and quite specifically into C-4 of oxaloacetate and its related downstream products (Fig. 2.6), and, thereby, gave direct evidence of the heterotrophic CO_2-fixation. During growth on malate, the ^{13}C-label was found at the same positions, but the ^{13}C-excess of the respective M+1 isotopomers was significantly lower (< 15 %) (Fig. 2.4C). The amino acids derived from glycolytic precursors, especially Ser and Gly, were characterised by a ^{13}C-incorporation at C-1 of 2.8 %, 3.6 % or 4.5 % (Ser) and 6.4 %, 8.8 % or 7.7 % (Gly), when *B. subtilis* W23 was grown on glucose, lactate or malate, respectively. This ^{13}C-incorporation could again be explained by the equilibrium reactions of the TCA cycle: [4-^{13}C]oxaloacetate led to [4-^{13}C]-isotopomers of malate, fumarate and succinate. Since succinate and fumarate are symmetrical intermediates of the TCA cycle, they led in turn to an equal mixture of [1-^{13}C]- and [4-^{13}C]oxaloacetate (Fig. 2.6, red half circles). An active gluconeogenesis could then have transported the ^{13}C-label from the C-1-position of oxaloacetate into the C-1-position of PEP and upstream from there into [1-^{13}C]Ser and [1-^{13}C]Gly. However, *B. subtilis* W23 could also have used the reversible reaction of the Gly cleavage system [73] to synthesise Gly, as shown in the following formula:

$$\text{Glycine} + H_4\text{folate} + NAD^+ \rightleftharpoons N^5,N^{10}\text{-methylene-}H_4\text{folate} + CO_2 + NH_4^+ + NADH + H^+$$

The reverse reaction of the glycine cleavage system could have afforded [1-^{13}C]Gly which then serves as the precursor for Ser biosynthesis yielding [1-^{13}C]Ser without the requirement of an active pyruvate carboxylase [66, 73]. Alternatively, [1-^{13}C]Gly could be formed by cleavage of 2-aminoacetoacetate (obtained from Thr) whereby C-1 and C-2 of Thr are transformed into C-1 and C-2 of Gly, respectively. Thus, *via* this route the detected (low) label at C-1 of Thr is transferred to C-1 of Gly. Now, one could speculate that these alternative pathways should be active under all the experimental setups and, consequently, the same ^{13}C-excess of the respective M+1 isotopomers of Gly and Ser should have resulted in all three cases. This is not true (Fig. 2.4) and, therefore, the detected differences in ^{13}C-incorporation indicate that a significant fraction of Ser and Gly was synthesised *via* [1-^{13}C]-PEP. However, we cannot exclude that different Gly biosynthesis pathways are used by *B. subtilis* W23 when growing on different organic substrates.

The ^{13}C-excess of M+1 isotopomers in subsets of amino acids was already sufficient to give robust information about substrate usages by *B. subtilis* W23. To reveal (and better visualise) even small indicative differences in label incorporation due to substrate usage in our model experiments, a two-step procedure was used: In the first step, we calculated and compared the ratios of ^{13}C-excess for M+1 isotopomers in TCA cycle-derived amino acids to the values for pyruvate-derived amino acids. This analysis clearly assigned substrates that require TCA cycle-metabolite replenishment (Fig. 2.5A). In the second step, we calculated and compared the ratios of ^{13}C-excess for M+1 isotopomers in gluconeogenesis-derived amino acids to the values for pyruvate-derived amino acids. This value helped to identify substrates with the need for gluconeogenesis (Fig. 2.5B). Together, this procedure clearly assigned the main (unlabelled) organic substrates in our model experiments at high statistical significance.

In summary, our experiments using $H^{13}CO_3^-$ as a tracer and *B. subtilis* W23 as a model organism provide solid evidence that EA-IRMS analysis of the biomass in conjunction with GC-MS analysis of protein-derived amino acids (i) reflect the core functional metabolic networks of the organism(s) under study and (ii) can identify the type of the main organic carbon substrate or at least the substrate family being used by the heterotrophic organisms or organisms under study.

The general validity of this hypothesis is supported by the fact that almost all heterotrophs need to refill the TCA cycle by anaplerotic CO_2-fixation. For this purpose, heterotrophs either use pyruvate carboxylase which is highly conserved and found in a great variety of organisms including prokaryotes, archaea, yeasts, fungi and higher organisms (e.g. mammals) or phosphoenolpyruvate (PEP) carboxylase which is widely distributed in bacteria [36, 37, 53, 54]. PEP carboxylase serves as another anaplerotic enzyme which catalyses the reaction from phosphoenolpyruvate to oxaloacetate *via* the addition of bicarbonate. Presumably, this results in the same labelling patterns when starting from $H^{13}CO_3^-$ in comparison to organisms using the pyruvate carboxylase. Thus, labelling experiments using $H^{13}CO_3^-$ as a tracer bear high potential to generally assign the type of microbial DOC utilisation under various conditions.

III

$H^{13}CO_3^-$-INCORPORATION INTO THE BIOMASS OF A NATURAL GROUNDWATER COMMUNITY

A part of this work is published in Spona-Friedl M, Braun A, Huber C, Eisenreich W, Griebler C, Kappler A, Elsner, M. Substrate-dependent CO_2 fixation in heterotrophic bacteria revealed by stable isotope labelling. FEMS Microbiology Ecology. 2020. 96 (6). DOI: 10.1093/femsec/fiaa080

Abstract

Groundwater dissolved organic matter comprises of many different organic compounds, whereof only a small fraction is bioavailable to microorganisms. It remains very difficult to identify these truly bioavailable parts, although well-established analytical methods exist that are able to determine the structural motifs of dissolved organic matter. As shown in a recent study, incorporation of ^{13}C-labelled bicarbonate into microbial biomass, followed by gas chromatography-mass spectrometry (GC-MS) analysis of protein-derived amino acids, could reveal the type of the main (unlabelled) organic carbon substrate that has been utilised by microorganisms. To test whether this is also a feasible approach to determine which part of groundwater dissolved organic matter is bioavailable, a proof-of-principle experiment with a natural groundwater community supplemented with organic fertiliser and $H^{13}CO_3^-$ as tracer was conducted. ^{13}C-Incorporation from $H^{13}CO_3^-$ was analysed by GC-MS of protein- and cell wall-derived amino acids. ^{13}C-Carbon was mainly detected in tricarboxylic acid (TCA) cycle-derived amino acids (especially lysine) and meso-diaminopimelic acid (DAP), demonstrating label incorporation from $H^{13}CO_3^-$ by the natural groundwater community. The marker ratios of ^{13}C-excess between specific amino acids revealed that organic compounds like succinyl-CoA and succinate were used as main substrates by the microbial community. Thus, the labelling approach is capable of characterising carbon sources of heterotrophic microorganisms in their natural environments.

Introduction

Dissolved organic matter in groundwater is a colourful mixture of organic compounds ranging from macromolecules to simple organic acids. The character of the soil as well as the surface vegetation influences the dissolved organic matter in groundwater. Rain events are drivers of dissolved organic matter transport through the soil column to the groundwater zone [3, 74]. The characterisation of groundwater dissolved organic matter has been accomplished by multiple methods, e.g. multidimensional nuclear magnetic resonance spectroscopy (NMR) and Fourier-transform ion cyclotron resonance mass spectrometry [6, 7]. The (relatively small) proportion of the dissolved organic matter (in groundwater) which is bioavailable to microorganisms is often determined by bioassay experiments. The interpretation of such experiments is based on concentration measurements and uses compounds like amino acids or carbohydrates as indicators for bioavailable dissolved organic matter [13]. However, dissolved organic matter concentrations are highly variable and can be altered by multiple processes [3, 75-77]. Additionally, the bioavailability of dissolved organic matter depends more on its origin than on its mere concentration. Thus, it is rather difficult to determine which fraction out of the dissolved organic carbon pool is truly bioavailable and utilised by microorganisms, based on structural dissolved organic matter analysis alone.

In a recent study, we explored the opportunity to identify the type of the organic carbon substrate utilised by bacteria under given environmental conditions. *Bacillus subtilis* (*B. subtilis*), a well-known, soil-dwelling, Gram-positive model organism, was chosen due to its ability to metabolise many different substrates and its widespread occurrence. Isotopically labelled bicarbonate ($H^{13}CO_3^-$) was used as tracer and ^{13}C-incorporation into bulk biomass and individual amino acids was analysed in order to follow the label through the metabolic network of *B. subtilis* W23 (*see chapter II*). Briefly, if *B. subtilis* W23 was grown on glucose, the label was mainly observed in tricarboxylic acid (TCA) cycle-derived amino acids. If *B. subtilis* W23 fed on lactate, the label was additionally found in amino acids derived from gluconeogenetic intermediates. Finally, growing *B. subtilis* W23 on malate resulted in significantly

lower label incorporation into the respective amino acids. Our results also showed that the incorporation of ^{13}C-carbon into bacterial biomass could be assigned to pyruvate carboxylase, an enzyme which belongs to the family of anaplerotic carboxylases. ^{13}C-Based metabolic pathway/flux analysis was used as method of choice to quantify the ^{13}C-incorporation from $H^{13}CO_3^-$ in our tracer experiments [56, 57]. Carbon from $^{13}CO_2/H^{13}CO_3^-$ can be traced back through the metabolic network of the organism under study. Mechanisms of CO_2-fixation as well as fluxes through the pathways of the central carbon metabolism are revealed by such experiments. On this basis, it is possible to reconstruct the biosynthesis of metabolic products on a functional and quantitative level. This possibility was shown for plants or microorganisms, for example to investigate microbial activity in environmental samples consisting of diverse microbial communities [31, 40-42, 44-48, 58-63].

We could successfully reveal the main organic carbon source that was used by the heterotrophic bacterium *B. subtilis* W23 by using heterotrophic fixation of $^{13}CO_2/H^{13}CO_3^-$ (representing a simple and inexpensive label) (*see chapter II*). In this chapter of my thesis, the aim is to test whether this approach could also reveal the type of bioavailable organic carbon present in groundwater – without altering the dissolved organic carbon pool. To explore this capability, we incubated a natural groundwater community with $H^{13}CO_3^-$ for 124 days and analysed the label incorporation into individual amino acids. Importantly, the groundwater characteristics exhibit a certain contrast to the well-defined experiments with *B. subtilis* W23, namely the presence of multiple organic carbon sources at very low concentrations and, concomitantly, the absence of the carbon catabolite repression [78]. Additionally, the timeframe of such an experiment and the composition of the microbial community will inevitably lead to multiple label incorporation. Consequently, the challenge was whether it was still possible to obtain direct evidence for the utilised main organic carbon source – like we did in the experiments with *B. subtilis* W23 – even under these complex conditions.

Material and Methods

Growth conditions

Natural oligotrophic and oxic groundwater samples were collected from a shallow unconsolidated quaternary aquifer composed of fluvio-glacial carbonate gravel and sands at Neuherberg/Munich, Germany. The freshly collected groundwater contained 1.5 ± 0.2 mg/L dissolved organic carbon (DOC), 1.5 ± 0.15 mg/L nitrate (NO_3^-) and about 15 µg/L phosphate (PO_4^{3-}), whereas the concentrations of nitrite (NO_2^-) and ammonium (NH_4^+) were below the detection limit of ion chromatography (LOD of 0.1 mg/L) (Dionex ICS-1100; Thermo Fisher Scientific, USA). Aliquots of 200 µL of the filter-sterilised samples were analysed to determine the concentrations of the nutrients. A stock solution of an organic fertiliser (DOC content 300 mg/L) was prepared by dissolving the lyophilised fertiliser at a pH of 9 in ultrapure water, followed by a neutralisation and a centrifugation step. The supernatant was filter-sterilised using a 0.22 µm syringe filter. The organic fertiliser was mainly composed of humic substances of varying molecular size (PhyotoGreen®-HumusWP, PhytoSolution).

Each of two bottles with 400 mL groundwater were loaded with 30 mL and 50 mL, respectively, of the organic fertiliser, spiked with 1 g/L ^{13}C-sodium bicarbonate ($NaH^{13}CO_3$, 98 atom% ^{13}C, Sigma Aldrich, Darmstadt, Germany) and closed with a screw cap. The bottles were incubated in the dark at room temperature for 52 days (13th September 2018 – 3rd November 2018) and gently mixed once a week. Growth of the bacterial groundwater community was monitored by optical density measurements at 595 nm (OD_{595}) (Fig. 3.1A).

To enhance biomass yield, the two bottles were combined (on 3rd November 2018), filled with fresh groundwater to a volume of 1000 mL and supplemented with 25 mL of a soil extract (groundwater F+S), which was prepared from a dark conifer forest soil by solvent extraction: soil from a coniferous wood was extracted with ultra-pure water on a stirrer in darkness at 37 °C overnight. The extract was filter-sterilised using a 0.22 µm syringe filter (Millipore, USA) to remove microbes. The DOC content of the sterile soil extract stock solution was 100 mg/L. In addition, on 7th November 2018, another bottle was filled with 1000 mL groundwater, loaded with 25 mL soil

extract (groundwater S) and spiked with 1 g/L ^{13}C-sodium bicarbonate. On 20th December 2018, both bottles were again loaded with 25 mL soil extract. Bacterial growth was again monitored by OD_{595} measurements (Fig. 3.1B).

The experiment was ended on 18th January 2019 by sacrificing the whole bottles *via* centrifugation. Biomass was concentrated using centrifugal filter units (30 kDa cut-off, Amicon® Ultra-15, Sigma Aldrich) to a final volume of 2 mL. The two samples were frozen at -80 °C and freeze-dried overnight using a VirTis Sentry 8L benchtop freeze dryer (SP Industries, Warminster, PA, USA) to remove the residual water.

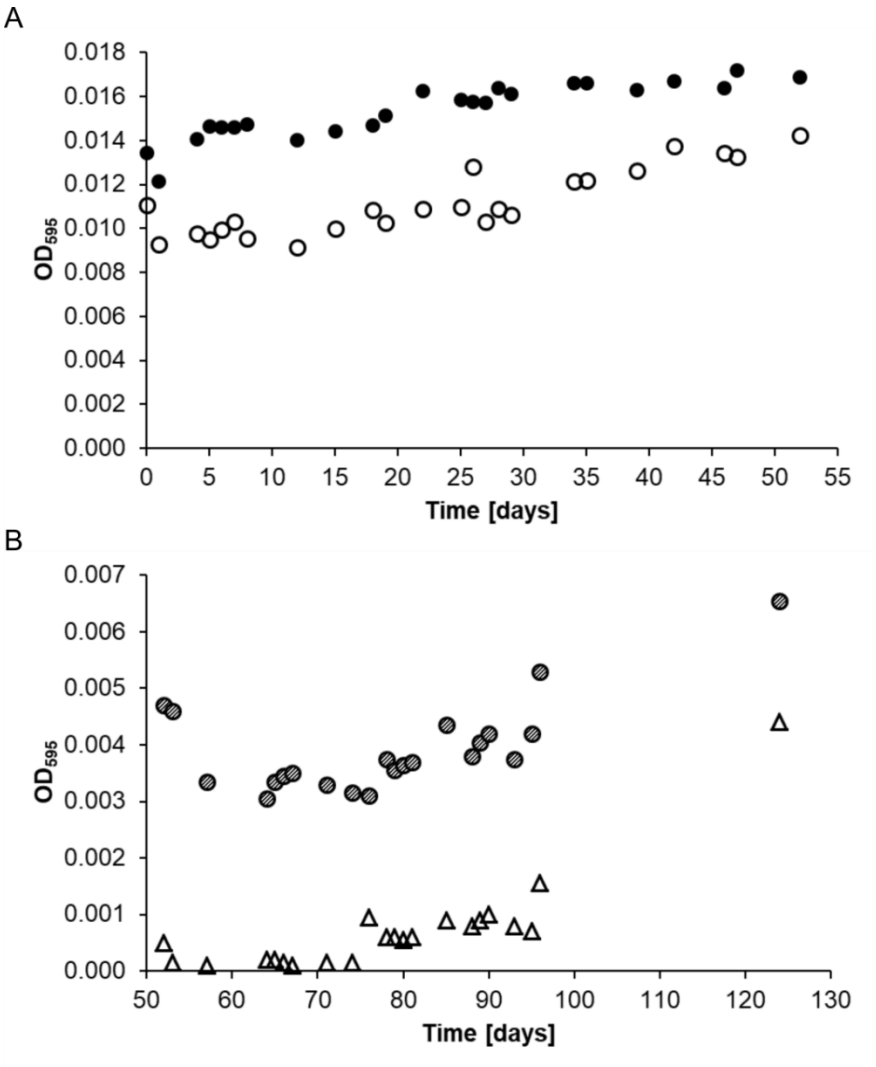

Figure 3.1: (A) Growth curves of the bacterial groundwater communities growing on different concentrations of organic fertiliser. Growth of the community supplemented with 30 mL of the organic fertiliser is depicted as open circles. Growth of the community supplemented with 50 mL of the organic fertiliser is depicted as full circles. **(B) Growth curves of the bacterial groundwater communities growing on soil extract.** The combined culture, which is now growing on organic fertiliser and soil extract, is depicted as shaded circles. Growth of the newly started groundwater community growing on soil extract is depicted as triangles.

Protein hydrolysis and amino acid derivatisation

For protein hydrolysis about 0.5 mg of the freeze-dried bacterial pellet was mixed with 500 µL of 6 M hydrochloric acid and heated at 105 °C for 24 h. After cooling to 70 °C, the residual hydrochloric acid was removed by a constant stream of nitrogen gas. The dried sample was then re-suspended in 50 % glacial acetic acid by sonication for 120 sec. A small column (1 mL pipet tip) of the cation exchanger Dowex 50WX8 [200-400 mesh (=37-74 µm), H^+ form] was prepared and washed with 1 mL of methanol followed by 1 mL of MilliQ water. After loading the sample onto the column, it was washed twice with 1 mL of MilliQ water. The bound amino acids were then eluted from the column by 1 mL of 4 M ammonium hydroxide. An aliquot of the eluate was dried under a constant stream of nitrogen gas at 70 °C. For derivatisation, the dry residue was dissolved in 50 µL of water-free acetonitrile and 50 µL of N-(tert-butyldimethylsilyl)-N-methyl-trifluoroacetamide containing 1 % tert-butyldimethylsilylchlorid. This mixture was kept at 70 °C for 30 min. The resulting N-tertbutyldimethylsilyl-derivatives of the amino acids (TBDMS-amino acid derivatives) were analysed by GC-MS following established protocols [18].

Gas chromatography/mass spectrometry of silylated amino acids

GC-MS analysis was performed using a 7890A GC system (Agilent Technologies, Santa Clara, CA, United States) equipped with a fused silica capillary column (Equity TM-5; 30 m x 0.25 mm, 0.25 µm film thickness; Supelco, Bellefonte, PA, United States). The mass detector worked with electron impact ionisation at 70 eV. An aliquot (1-3 µL) of the solution containing the TBDMS-amino acid derivatives was injected in a 1:10 split mode. The interface temperature was set to 260 °C. The column temperature was held at 140 °C for 3 min, heated with a temperature gradient of 4 °C/ min to 165 °C, heated with a second temperature gradient of 15 °C/ min to 200 °C and heated with a third temperature gradient of 7 °C/ min to 280 °C where the temperature was held for 3 min. Selected ion monitoring data were acquired using a 0.3-sec sampling rate and the samples were analysed three times. Data collection was carried out *via* the GC-MSD Data Analysis software (Agilent Technologies, Santa Clara, CA, United States). The retention times and the detected mass fragments of the amino acids are listed in the supplementary Table T1. ^{13}C-Incorporation into amino acids was computed according to Lee et al. [64]. The steps

include the determination of the contribution of the derivatisation reagent to the observed spectrum of the silylated amino acid and the correction for contribution from ^{13}C-carbon natural abundance using multiple linear regression analysis. The mass isotopomer distribution after this background subtraction provides fractional ^{13}C-excess values for amino acid isotopomers carrying one ^{13}C-carbon atom (M+1), two ^{13}C-carbon atoms (M+2), three ^{13}C-carbon atoms (M+3), and so on, where the sum over all isotopomers [M + (M+1) + (M+2) + (M+3) etc.] is defined as 100 %. As an example, amino acids with an M+1 excess value of 50 % are composed of 50 % unlabelled molecules (M) and 50 % molecules carrying one ^{13}C-carbon (M+1) from the ^{13}C-labelled precursor. Amino acids that carry at least one ^{13}C-carbon atom in excess are termed labelled amino acids in the following.

Statistical Analysis

A two-tailed unpaired Student's t-test was used for the analysis of differences between the mean values of ^{13}C-incorporation into selected pairs of amino acids from the two groundwater experiments. Statistical significance is depicted as *ns* = not significant, *$p < 0.05$, **$p < 0.01$, or ***$p < 0.001$.

Results

At the beginning of the experiment, the two groundwater communities were feeding on organic fertiliser and ^{13}C-bicarbonate as tracer. After an incubation time of 52 days, the two bottles were combined and soil extract was added to the groundwater. Thus, groundwater microbes now grew on a mixture of organic fertiliser and soil extract till the end of the experiment (i.e. for 77 days). 73 days was the incubation time for microorganisms growing only on soil extract and ^{13}C-bicarbonate as tracer (Fig. 3.1).

We could quantify the ^{13}C-incorporation in 16 amino acids obtained from acidic hydrolysis of the biomass [18]. M+1 isotopomers, i.e. amino acid isotopomers that carried one ^{13}C-carbon atom, were predominantly found. However, also isotopomers carrying more than one ^{13}C-carbon atom could be detected in both experiments.

The ^{13}C-excess of the M+1 isotopomers of meso-diaminopimelic acid (DAP) and lysine reached values up to 12 % showing the highest ^{13}C-excess (Fig. 3.2). Amino acids that are derived from TCA cycle intermediates showed a ^{13}C-excess of the respective M+1 isotopomers of 3-6 %, i.e. Asp (4 %), Thr (3 %), Met (6 %), Glu (4 %) and Pro (4 %), during growth on organic fertiliser and soil extract. The ^{13}C-excess of the respective M+1 isotopomers in the same amino acids was considerably smaller during growth on soil extract, i.e. Asp (1.5 %), Thr (1 %), Met (1 %), Lys, (4 %), DAP (7 %), Glu (1 %) and Pro (1 %) (Fig. 3.2). Amino acids derived from pyruvate (Ala, Val, Leu, Ile) or gluconeogenetic (His, Tyr, Phe) intermediates received less than 2 % of ^{13}C-carbon in both set-ups. The ^{13}C-excess of glycine and serine, which could also be derived from gluconeogenetic intermediates, reached values up to 3.5 % during growth on organic fertiliser and soil extract and values up to 2 % during growth on only soil extract.

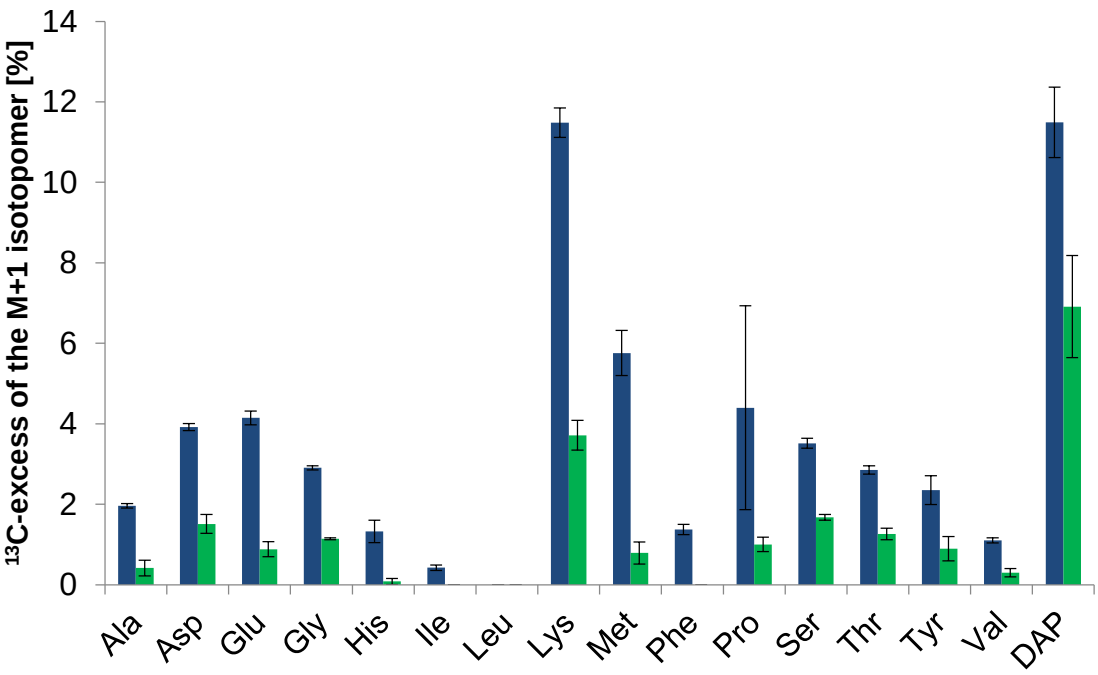

Figure 3.2: ^{13}C-excess of the M+1 isotopomers of specific amino acids produced by $H^{13}CO_3^-$-labelling experiments with a natural groundwater community. The results from microbes growing on organic fertiliser and soil extract are shown in blue bars and those from microbes growing on soil extract are shown in green bars.

In a next step, we calculated the marker ratios of ^{13}C-excess of the M+1 isotopomers in specific sets of amino acids (Fig. 3.3). To assign the ^{13}C-incorporation to key metabolites or pathways of the central carbon metabolism appropriate amino acids were chosen: Ala and Val represent ^{13}C-incorporation *via* pyruvate. Tyr and Phe represent ^{13}C-incorporation *via* gluconeogenesis and the pentose phosphate pathway. Asp and Glu represent ^{13}C-incorporation *via* the TCA cycle.

Both experiments gave rise to very similar ratios of ^{13}C-excess of the M+1 isotopomers in the selected sets of amino acids (Fig. 3.3). The calculation of the ratios from the ^{13}C-excess of the M+1 isotopomers in TCA cycle-derived amino acids and pyruvate-derived amino acids (i.e., Asp/Val, Asp/Ala, Glu/Val and Glu/Ala) resulted in values below 10 (Fig. 3.3A). The calculation of the ratios from the ^{13}C-excess of the M+1 isotopomers in gluconeogenesis-derived amino acids and pyruvate-derived amino acids (i.e., Asp/Val, Asp/Ala, Glu/Val and Glu/Ala) resulted in values below 2 (Fig. 3.3B). Thus, both the individual values and the corresponding mean values of the two groundwater experiments show a great similarity to the values obtained from our labelling experiment with *B. subtilis* W23 growing on malate (*see chapter II*).

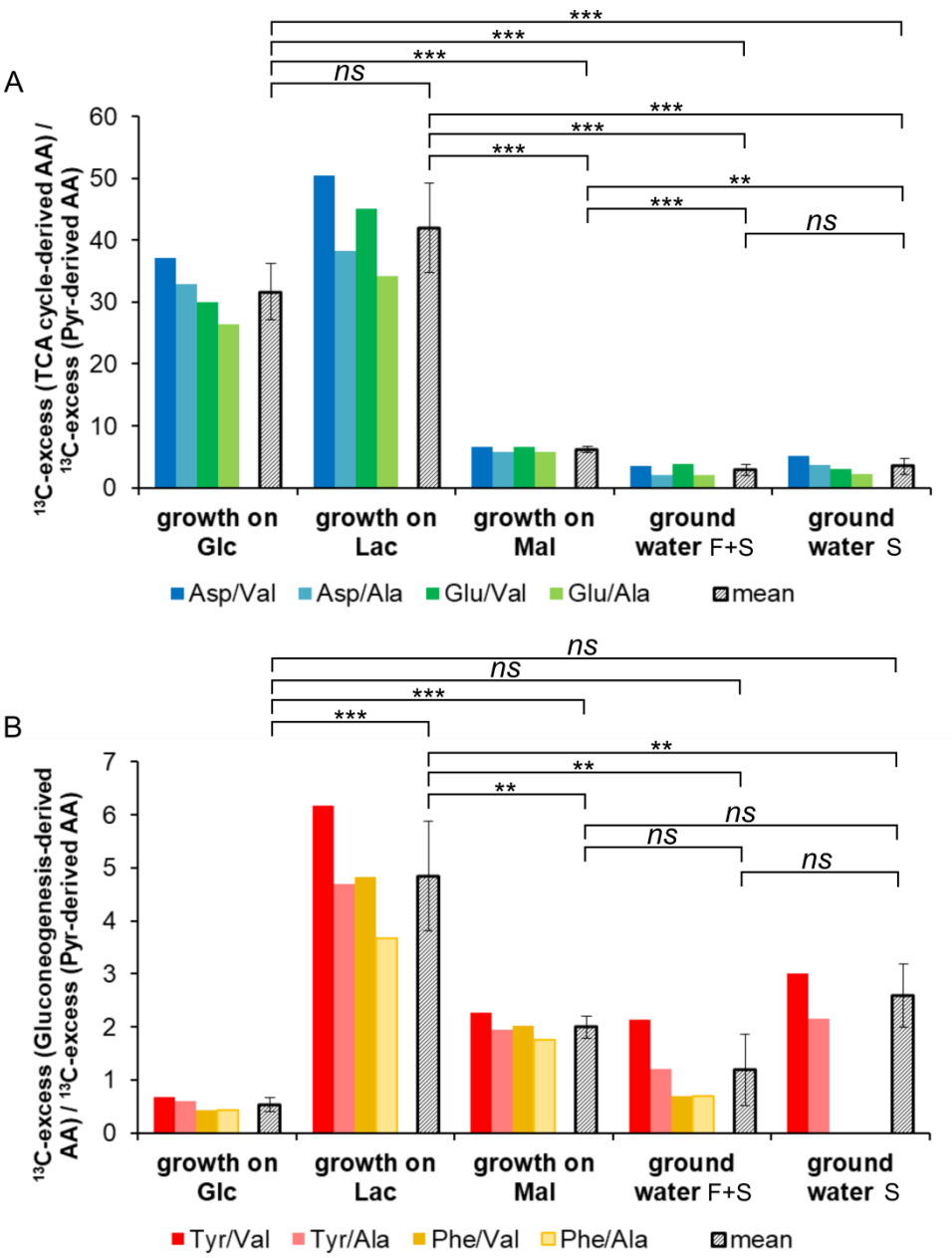

Figure 3.3: Marker ratios of ^{13}C-excess of the M+1 isotopomers between selected amino acids. (A) ^{13}C-excess (TCA cycle-derived amino acids)/ ^{13}C-excess (pyruvate-derived amino acids). The coloured bars depict the ratios of the chosen amino acids in the labelling experiments. The grey bars show the mean values of ^{13}C-ratios for these fractions. p-Values as calculated by Student's t-test (unpaired): p(Glc/Lac) = 0.05031, p(Glc/(Mal) = 0.00003, p(Glc/groundwater F+S) = 0.00002, p(Glc/groundwater S) = 0.00002, p(Lac/Mal) = 0.00006, p(Lac/groundwater F+S) = 0.00004, p(Lac/groundwater S) = 0.00004, p(Mal/groundwater F+S) = 0.00082, p(Mal/groundwater S) = 0.00668, p(groundwater F+S/groundwater S) = 0.48556. **(B) ^{13}C-excess (gluconeogenesis-derived amino acids)/ ^{13}C-excess (pyruvate-derived amino acids).** The coloured bars depict the ratios of the chosen amino acids in the labelling experiments and the grey bars show again the mean values of ^{13}C-ratios. p-Values as calculated by Student's t-test (unpaired): p(Glc/Lac) = 0.00017, p(Glc/(Mal) = 0.00002, p(Glc/groundwater F+S) = 0.10712, p(Glc/groundwater S) = 0.36039, p(Lac/Mal) = 0.00166, p(Lac/groundwater F+S) = 0.00103, p(Lac/groundwater S) = 0.00850, p(Mal/groundwater F+S) = 0.06284, p(Mal/groundwater S) = 0.39767, p(groundwater F+S /groundwater S) = 0.90246. (*For detailed calculation see SI excel file F5 m+1 and ratio of label_SI Paper*)

Discussion

The labelling experiments with a natural groundwater community feeding on organic fertiliser or soil extract and $H^{13}CO_3^-$ as tracer, revealed that groundwater microbes indeed incorporated ^{13}C-carbon into their biomass. The microorganisms (from the two initial bottles) performed ^{13}C-label incorporation mainly during the first period of the experiment (52 days) presumably using carbon from the organic fertiliser. Soil extract was added only during the second period of the experiment, where no additional $H^{13}CO_3^-$-incorporation took place. Whereas, microorganisms from the third bottle were only supplemented with soil extract and thus performed ^{13}C-label incorporation presumably using carbon from this source.

Meso-diaminopimelic acid (DAP, as a component of peptidoglycan) and lysine showed the highest ^{13}C-excess of the respective M+1 isotopomers during growth on organic fertiliser or soil extract, respectively. These amino acids play an important role in cell wall biosynthesis of bacteria [79]. DAP is the immediate precursor for lysine [80], which explained the similar ^{13}C-incorporation in the two amino acids. The fact that ^{13}C-label was detected in these amino acids showed (i) ^{13}C-label incorporation *via* anaplerosis, since DAP and lysine are derived from TCA cycle intermediates and (ii) active cell wall synthesis demonstrating growth of the microorganisms.

GC-MS analysis revealed information about the ^{13}C-carbon positions in amino acids and demonstrated that not only one anaplerotic enzyme – as it was the case in the experiments with *B. subtilis* W23 (*see chapter II*) – was responsible for the label incorporation.

As an example, the fragments with m/z of 432 and 286 for Glu and Pro, respectively, contained all five carbon atoms of the original amino acids. These fragments were accompanied by an amount of 4 % and 3 %, respectively, of the respective mass M+1 (namely m/z 433 for Glu and m/z 287 for Pro), as learned from analysing the mass spectrum. The fragments that had lost the C-1 position of these amino acids (i.e. m/z 404 and 330 for Glu and m/z 258 and 184 for Pro) were accompanied by an amount of the respective M+1 isotopomers of less than 2 % for Glu and less than 1 % for Pro. Thus, Glu and Pro carried the major share of the ^{13}C-label at C-1.

As another example, the fragments with m/z of 431 and 418 for Lys and Asp, respectively, contained all carbon atoms (six and four, respectively) of the original amino acids. The related M+1 isotopomers (namely m/z 432 for Lys and m/z 419 for Asp) were found with an amount of 12 % and 4 %, respectively. Interestingly, the ^{13}C-excess of the respective M+1 isotopomers of the fragments that had lost the C-1 position of these amino acids (i.e. m/z 329 for Lys, m/z 390 and 316 for Asp) was 3 % in both amino acids. Consequently, Lys carried the major share of the ^{13}C-label at C-1, whereas Asp carried only 1 % of the ^{13}C-label at the C-1 position. The localisation of ^{13}C-carbon in Glu, Pro and Asp pointed to an incorporation of ^{13}C-label from $H^{13}CO_3^-$ *via* anaplerosis because (i) the reaction of pyruvate carboxylase (or PEP-carboxylase) yields [4-^{13}C]oxaloacetate, (ii) Asp and Lys are derived from the TCA cycle intermediate oxaloacetate (leading to the [4-^{13}C]-isotopomers) and (iii) [4-^{13}C]oxaloacetate is converted into [1-^{13}C]α-ketoglutarate *via* the oxidative branch of the TCA cycle (leading to the detected [1-^{13}C]-isotopomers of Glu and Pro). The presence of ^{13}C-carbon in positions which are not captured by the above describe scenario shows that microbes from the groundwater community could use alternative pathways to incorporate the labelled inorganic carbon into their biomass.

To check whether it was still possible to reveal the main organic carbon substrate that was utilised by the groundwater community, we used a two-step procedure that was introduced by us in a previous work (*see chapter II*). We calculated and compared the ratios of ^{13}C-excess values for M+1 isotopomers in specific sets of amino acids. Remarkably, there was a striking similarity between these ratios and the corresponding ratios obtained from ^{13}C-labelling experiments with *B. subtilis* W23 growing on malate (Fig. 3.3). Consequently, we hypothesise (also with good statistical significance) that the microorganisms from the groundwater community mainly used organic matter which entered the central carbon metabolism at the stage of the TCA cycle – like malate. This result seems reasonable since the utilised organic fertiliser was mostly composed of humic substances, i.e. aromatic compounds, which are degraded to e.g. compounds comprising four carbon atoms, such as succinyl-CoA and succinate. These products could then serve as main substrates entering the central carbon metabolism *via* the TCA cycle, such as malate. Our experiments provide substantial evidence that GC-MS analysis of protein- and cell wall-derived amino acids could identify the type of the main organic carbon

substrate or at least the substrate family being used by the vast majority of heterotrophic organisms. Thus, labelling experiments using $H^{13}CO_3^-$ as a tracer bear high potential to generally assign the type of microbial DOC utilisation under various conditions.

IV

METABOLIC RESPONSE OF *B. SUBTILIS* TO LEUCINE AS UNFAVOURABLE SUBSTRATE – INSIGHT FROM ^{13}C-BICARBONATE LABELLING

Abstract

In a recent study, heterotrophic $^{13}CO_2$/ $H^{13}CO_3^-$-fixation was successfully used to identify the type of the main organic carbon source that was utilised by *Bacillus subtilis* (*B. subtilis*) W23. This study aimed to test whether heterotrophic CO_2-fixation could be applicable to analyse metabolic deficiencies and physiological adaptation in bacteria. Leucine is an unfavourable carbon source for *B. subtilis* W23 and was therefore used as test case. Experiments with *B. subtilis* W23 growing in the presence of $H^{13}CO_3^-$ (as tracer) and leucine or malate + leucine were conducted. Label incorporation from $H^{13}CO_3^-$ was analysed by elemental analysis-isotope ratio mass spectrometry (EA-IRMS) of microbial biomass and gas chromatography-mass spectrometry (GC-MS) of protein-derived amino acids. Bacterial growth stopped after a short initial growth phase and ^{13}C-label incorporation was only detected in tricarboxylic acid (TCA) cycle-derived amino acids when leucine was offered as substrate. The indicative labelling patterns of the amino acids revealed that the bacteria used organic matter leftovers from the inoculum, instead of leucine, for their initial growth. Leucine metabolism presumably stopped at the level of 3-methylbutanoyl-CoA, if metabolised at all. The results from the co-substrate experiment confirmed the known strict catabolite repression exhibited by malate, which was reflected in the amino acids' labelling patterns. Thus, heterotrophic $^{13}CO_2$/ $H^{13}CO_3^-$-fixation granted superior insights into the metabolic networks of *B. subtilis* W23 and has proven to be a useful tool to study metabolic bottlenecks as well as the phenomenon called carbon catabolite repression.

Introduction

Virtually all heterotrophic organisms – from microorganisms to humans – incorporate CO_2 *via* a variety of pathways involving at least 18 different carboxylases in the central and peripheral metabolism [27-29, 52]. Anaplerotic carboxylases are capable of efficiently incorporating CO_2 into (microbial) biomass [29] by replenishing intermediates of the tricarboxylic acid (TCA) cycle. Therefore, carbon from anaplerotic CO_2 incorporation accounts for a significant amount (i.e. 2-8 %) of the cell's biomass carbon abundance [30-34, 45].

Pyruvate carboxylase – the archetypical anaplerotic enzyme – catalyses the bicarbonate (HCO_3^-)-dependent conversion of pyruvate into oxaloacetate [35]. The enzyme is widely distributed across the three kingdoms of life and has also been retained in many heterotrophic organisms including the Gram-positive bacterium *Bacillus subtilis* (*B. subtilis*) W23. Pyruvate carboxylase is located at the "phosphoenolpyruvate-pyruvate-oxaloacetate node" [35, 37, 53], a metabolic hub that unites structurally entangled reactions of the major pathways of carbon metabolism, i.e. glycolysis (catabolism), gluconeogenesis (anabolism) and the TCA cycle (energy supply of the cell) [54]. The activity of pyruvate carboxylase depends on the available organic carbon source, leading to varying amounts of incorporated inorganic carbon even within the same organism [31-34, 45]. In a recent study, we explored this opportunity to identify the main type of the organic carbon substrate that is utilised by bacteria under given environmental conditions. By applying isotopically labelled bicarbonate ($H^{13}CO_3^-$) as tracer and analysing the ^{13}C-incorporation into bulk biomass and individual amino acids, we could directly observe up to which stage the label was distributed within the metabolic network (*see chapter II*). If bacteria primarily fed on substrates like lactate, then both the enzyme pyruvate carboxylase and the gluconeogenesis pathway were highly active and the label was found in the corresponding amino acids. In contrast, if bacteria utilised carbohydrates like glucose pyruvate carboxylase was active, but not gluconeogenesis so that the label was observed in a smaller subset of amino acids. Finally, if bacteria metabolised substrates like malate that correspond to intermediates of the TCA cycle, the activity

of pyruvate carboxylase was not needed to keep the TCA cycle running so that the overall label incorporation was significantly lower. Quantifying ^{13}C-incorporation from $H^{13}CO_3^-$ corresponds to ^{13}C-based metabolic pathway/flux analysis (46, 47), where carbon from $^{13}CO_2/H^{13}CO_3^-$ can be traced back through the metabolic network of the organism under study. Such tracer experiments grant insight into the mechanisms of CO_2-fixation. They also visualise the use and thereby the spreading of the labelled (carbon) atom in an organism's metabolism. This enables the reconstruction of the biosynthesis of metabolic products on a functional and quantitative basis [31, 40-42, 44-48, 58-63].

In our previous work we used, for the first time, the heterotrophic fixation of $^{13}CO_2/H^{13}CO_3^-$ as simple, inexpensive label to successfully identify the type of the main organic carbon source (carbohydrates *vs.* short chain sugars *vs.* short chain organic acids) that is utilised by heterotrophic microorganisms (*see chapter II*). In the current study we aim to take a next step and explore whether this simple approach – using heterotrophic fixation of $^{13}CO_2/H^{13}CO_3^-$ under *in vivo* conditions and without altering the dissolved organic carbon (DOC) pool – can provide answers also to questions that do not concern substrate availability, but rather metabolic deficiencies and physiological bacterial adaptation. To explore this capability, we addressed the metabolic bottleneck for *B. subtilis* W23, a well-known Gram-positive bacterium, during growth on leucine as a model case for an unfavourable substrate.

One characteristic of *B. subtilis* W23 is its capability to use many different organic carbon sources for growth [81]. However, looking at its metabolic network, it should hardly be possible for *B. subtilis* W23 to efficiently grow on the amino acid leucine as sole organic substrate. After leucine uptake into the bacterial cell, this amino acid is degraded into three molecules of acetyl-coenzyme A (Ac-CoA), which are channelled into the TCA cycle. There, citrate is formed from oxaloacetate and Ac-CoA by the activity of a (si)-specific citrate synthase [82]. Therefore, the use of leucine as growth substrate leads to a high demand of oxaloacetate, which in turn leads to the necessity of replenishing the oxaloacetate pool to ensure the continued function of the TCA cycle. The reaction of pyruvate carboxylase regenerates oxaloacetate *via* the carboxylation of pyruvate. However, leucine, or rather Ac-CoA, cannot be used to start gluconeogenesis, ruling out the possibility to replenish carbohydrates and – ultimately – pyruvate (Fig. 4.1A). Hence, at some point, *B. subtilis* W23 should run

into a shortage on carbohydrates and/or oxaloacetate, which will result in an arrest of cell growth. The addition of a TCA cycle intermediate to the growth medium, as co-substrate to leucine, should solve this shortage, however (Fig. 4.1B). Oxaloacetate can be regenerated from e.g. malate *via* the activity of malic enzymes. Thus, the continued function of the TCA cycle would again be ensured and gluconeogenesis could be operated providing the cell with carbohydrates. It is known that, next to glucose, malate is another preferred substrate of *B. subtilis* W23. The uptake of alternative substrates is strongly repressed in the presence of glucose or malate [2]. This phenomenon is known as carbon catabolite repression [2, 65, 83]. Hence, we wanted to explore whether leucine could nonetheless be used in a co-substrate experiment with malate and if not, whether our ^{13}C-labelling approach could visualise the catabolite repression imposed by malate.

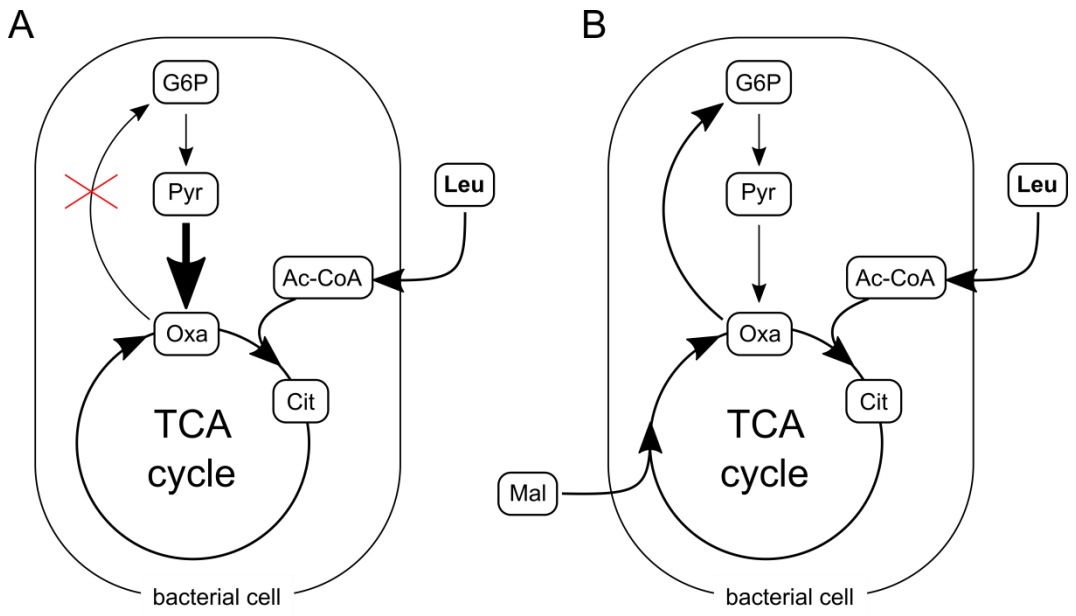

Figure 4.1: Simplified metabolic network of *B. subtilis* W23. (A) Bacterial growth on leucine as sole organic carbon source. Leucine, taken from the medium, is degraded to acetyl-coenzyme A and channelled into the TCA cycle. Bold arrows indicate main carbon fluxes, showing the vital need of the organism for an active pyruvate carboxylase, since the TCA cycle is highly active. **(B) Bacterial growth on leucine and malate as organic carbon sources.** Malate now also replenishes the TCA cycle metabolites and allows an active gluconeogenesis.

The aim of the current study was to investigate the underlying physiology with ^{13}C-incorporation from $H^{13}CO_3^-$ and ^{13}C-based metabolic pathway/flux analysis [56, 57] for the following concrete objectives: first, to experimentally verify that *B. subtilis* W23 is unable to grow on leucine; second, to explore if $^{13}CO_2/H^{13}CO_3^-$ labelling can reveal

the underlying metabolic reasons; third, to confirm that growth can be reconstituted by the simultaneous presence of malate; and, fourth, to explore with $^{13}CO_2/H^{13}CO_3^-$ labelling whether organisms would only grow on malate under these circumstances, or if the use of both carbon sources can be detected by the label incorporation into bulk biomass and individual amino acids.

Material and Methods

Strain and growth conditions

All experiments were performed with *B. subtilis* subsp. *spizizenii* W23 (DSM No.: 6395), a prototrophic derivative of the wild type, obtained from DSMZ (Leibnitz Institute DSMZ – German Collection of Microorganisms and Cell Cultures, Braunschweig, Germany). For pre-cultivation, 5 mL of M9 minimal growth medium, supplemented with 7.3 g/L leucine, 0.73 g/L leucine, 0.365 g/L leucine, 0.073 g/L leucine or 0.55 g/L malate and 0.365 g/L leucine (mixed substrate experiment), respectively, and preheated to 30 °C, were inoculated with 300 µL of a glycerol stock solution of the bacterium. The amounts of organic substrates (0.73 g/L leucine, 0.55 g/L malate and 0.365 g/L leucine) were chosen in order to ensure that the amount of C available to the bacteria (0.4 g/L) was the same in both setups. The other substrate concentrations were chosen to exclude limitations for bacterial growth due to the concentration of leucine in the medium. The pre-cultures were incubated for 20 h. In order to prevent the formation of biofilms, the culture tubes were shaken vigorously at 300 rpm on an orbital incubation shaker (IKA KS 4000i control, IKA-Werke, Staufen, Germany). Each pre-culture was used to inoculate 195 mL of M9 minimal growth medium, preheated to 30 °C, in 500 mL Schott bottles. The M9 minimal growth medium was a mixture of,

- 185 mL of M9 minimal medium and 1.46 g leucine added directly to the medium ($conc._{Leu}$ = 7.3 g/L),
- 165 mL of M9 minimal medium and 20 mL of a 7.3 g/L leucine stock solution ($conc._{Leu}$ = 0.73 g/L),
- 175 mL of M9 minimal medium and 10 mL of a 7.3 g/L leucine stock solution ($conc._{Leu}$ = 0.365 g/L),
- 183 mL of M9 minimal medium and 2 mL of a 7.3 g/L leucine stock solution ($conc._{Leu}$ = 0.073 g/L)
- or 165 mL of M9 minimal medium and 20mL of a 5.5 g/L malate and 3.65 g/L leucine stock solution ($conc._{Leu}$ = 0.365 g/L)
- and 10 mL of a 20 g/L sodium bicarbonate stock solution.

The bicarbonate was either $NaH^{13}CO_3$ (98 atom% ^{13}C, Sigma Aldrich, Darmstadt, Germany) in the ^{13}C-labelling experiments or unlabelled $NaHCO_3$ (i.e. at 1.1 % natural ^{13}C-abundance, Sigma Aldrich, Darmstadt, Germany) in the control experiments. The bottles were closed gastight after inoculation to block the release of $^{13}CO_2$. To avoid depletion of O_2, an aliquot of fresh (filter-sterilised) air that equals the volume of a taken sample, was added at every time point of sampling. The cultivations were performed at 30 °C and 150 rpm on an orbital incubation shaker.

The M9 minimal growth medium consisted of the following components (per litre): 8.5 g of $Na_2HPO_4 \cdot 2\ H_2O$, 3 g of KH_2PO_4, 1 g of NH_4Cl and 0.5 g of NaCl (=base salts solution). The following components were autoclaved separately before being added to the base salts solution in the given order (per litre): 1 mL of 0.1 M $CaCl_2$, 10 mL trace salts stock solution, 1 mL of 1 M $MgSO_4$ and 1 mL of 50 mM $FeCl_3 \cdot 6\ H_2O$ (filter-sterilised). The trace salts stock solution contained (per litre): 100 mg of $MnCl_2 \cdot 4\ H_2O$, 170 mg of $ZnCl_2$, 43 mg of $CuCl_2 \cdot 2\ H_2O$, 60 mg of $CoCl_2 \cdot 6\ H_2O$ and 60 mg of $Na_2MoO_4 \cdot 2\ H_2O$. The glucose, lactate, malate and sodium bicarbonate stock solutions were filter-sterilised before being added to the medium. All solutions were prepared using sterilised MilliQ water. All chemicals were purchased from Sigma Aldrich (St. Louis, USA).

^{13}C-Labelling experiments and microbial dry weight

B. subtilis subsp. *spizizenii* W23 was grown in M9 minimal growth medium supplemented with 7.3 g/L leucine, 0.73 g/L leucine, 0.365 g/L leucine, 0.073 g/L leucine or 0.55 g/L malate and 0.365 g/L leucine, respectively, and 1 g/L sodium bicarbonate. The ^{13}C-labelling experiments were conducted in triplicates and the control experiments with unlabelled bicarbonate in duplicates. After 6 h of incubation, one control experiment was spiked with sodium ^{13}C-bicarbonate (1 g/L); the second control experiment remained untouched. Bacterial growth was monitored by determining the optical density at 600 nm (OD_{600}). Samples for biomass and amino acid analysis were taken at intervals of 2 h after inoculation. At each of these time points, 20 mL of the bacterial culture were harvested by centrifugation (4 °C, 4000 rpm, 20 min). The supernatant was carefully removed. The cell pellet was re-suspended in 2 mL of sterile MilliQ water and transferred into an Eppendorf tube.

After this washing step, a second centrifugation step (4 °C, 14000 rpm, 20 min) pelleted the cells again. The supernatant was carefully discarded and the pellet was frozen at -80 °C. The frozen pellets were freeze-dried overnight using a VirTis Sentry 8L benchtop freeze dryer (SP Industries, Warminster, PA, USA). The freeze-dried bacterial pellets were weighed using a high-resolution balance (CP2P, Sartorius AG Göttingen, Germany) to determine the microbial dry weight.

Protein hydrolysis and amino acid derivatisation

For protein hydrolysis about 0.5 mg of the freeze-dried bacterial pellet was mixed with 500 µL of 6 M hydrochloric acid and heated at 105 °C for 24 h. After cooling to 70 °C, the residual hydrochloric acid was removed by a constant stream of nitrogen gas. The dried sample was then re-suspended in 50 % glacial acetic acid by sonication for 120 sec. A small column (1 mL pipet tip) of the cation exchanger Dowex 50WX8 [200-400 mesh (=37-74 µm), H^+ form] was prepared and washed with 1 mL of methanol followed by 1 mL of MilliQ water. After loading the sample onto the column, it was washed twice with 1 mL of MilliQ water. The bound amino acids were then eluted from the column by 1 mL of 4 M ammonium hydroxide. An aliquot of the eluate was dried under a constant stream of nitrogen gas at 70 °C. For derivatisation, the dry residue was dissolved in 50 µL of water-free acetonitrile and 50 µL of N-(tert-butyldimethylsilyl)-N-methyl-trifluoroacetamide containing 1 % tert-butyldimethylsilylchlorid. This mixture was kept at 70 °C for 30 min. The resulting N-tertbutyldimethylsilyl-derivatives of the amino acids (TBDMS-amino acid derivatives) were analysed by GC-MS following established protocols [18].

Gas chromatography/mass spectrometry of silylated amino acids

GC-MS analysis was performed using a 7890A GC system (Agilent Technologies, Santa Clara, CA, United States) equipped with a fused silica capillary column (Equity TM-5; 30 m x 0.25 mm, 0.25 µm film thickness; Supelco, Bellefonte, PA, United States). The mass detector worked with electron impact ionisation at 70 eV. An aliquot (1-3 µL) of the solution containing the TBDMS-amino acid derivatives was injected in a 1:10 split mode. The interface temperature was set to 260 °C. The column temperature was held at 140 °C for 3 min, heated with a temperature

gradient of 4 °C/ min to 165 °C, heated with a second temperature gradient of 15 °C/ min to 200 °C and heated with a third temperature gradient of 7 °C/ min to 280 °C where the temperature was held for 3 min. Selected ion monitoring data were acquired using a 0.3-sec sampling rate and the samples were analysed three times. Data collection was carried out *via* the GC-MSD Data Analysis software (Agilent Technologies, Santa Clara, CA, United States). The retention times and the detected mass fragments of the amino acids are listed in the supplementary Table T1. ^{13}C-Incorporation into amino acids was computed according to Lee et al. [64]. The steps include the determination of the contribution of the derivatisation reagent to the observed spectrum of the silylated amino acid and the correction for contribution from ^{13}C-carbon natural abundance using multiple linear regression analysis. The mass isotopomer distribution after this background subtraction provides fractional ^{13}C-excess values for amino acid isotopomers carrying one ^{13}C-carbon atom (M+1), two ^{13}C-carbon atoms (M+2), three ^{13}C-carbon atoms (M+3), and so on, where the sum over all isotopomers [M + (M+1) + (M+2) + (M+3) etc.] is defined as 100 %. As an example, amino acids with an M+1 excess value of 50 % are composed of 50 % unlabelled molecules (M) and 50 % molecules carrying one ^{13}C-carbon (M+1) from the ^{13}C-labelled precursor. Amino acids that carry at least one ^{13}C-carbon atom in excess are termed labelled amino acids in the following.

Carbon isotopic analysis of biomass

Carbon isotopic ratios were determined by an elemental analyser-isotope ratio mass spectrometer (EA-IRMS) consisting of a EuroEA (Euro vector, Milano, Italy) coupled to a FinniganTM MAT253 IRMS (Themo Fisher Scientific, Bremen, Germany) by a FinniganTM ConFlow III interface (Thermo Fisher Scientific, Bremen, Germany). For EA-IRMS analysis, a small amount of the freeze-dried pellet (100-400 µg) was put into tin capsules (3.3 x 5 mm, IVA Analysentechnik, Meerbusch, Germany) and subjected to elemental analysis by dropping them into a heated reactor which contained silvered cobalt oxide and chromium oxide (IVA Analysentechnik, Meerbusch, Germany and HEKA tech, Wegberg, Germany). The biomass pellets were combusted in a stream of O_2-containing He at 1000 °C to produce N_2, NO_x, H_2O and CO_2, where NO_x was directly converted to N_2 again in an online reduction reactor filled with metallic copper filings. The gases were subsequently transferred to the

isotope ratio mass spectrometer *via* a ConFlow III system using a continuous helium stream of 90 mL/ min. The CO_2 reference gas was provided by CARBO (Bad Hönningen, Germany). The resulting values from EA-IRMS analysis include the natural abundance of ^{13}C-carbon.

Statistical Analysis

A two-tailed unpaired Student's t-test was used for the analysis of differences between the mean values of ^{13}C-incorporation into selected pairs of amino acids from the experiments with leucine, malate and malate + leucine. Statistical significance is depicted as *ns* = not significant, *$p < 0.05$, **$p < 0.01$, or ***$p < 0.001$.

Results

Growth of *B. subtilis* in the presence of leucine and $H^{13}CO_3^-$

The four growth experiments with *B. subtilis* W23 in M9 medium containing different leucine concentrations and $H^{13}CO_3^-$ confirmed the inability of the bacteria to grow on leucine alone over an extended period of time (Fig. 4.2). Bacterial biomass increased until 6 h and stayed relatively constant until 10 h after inoculation, but then drastically decreased, almost leading to the initial OD_{600}-value. Identical growth curves, despite different leucine concentrations, demonstrated that the available amount of leucine did not influence this ephemeral bacterial growth.

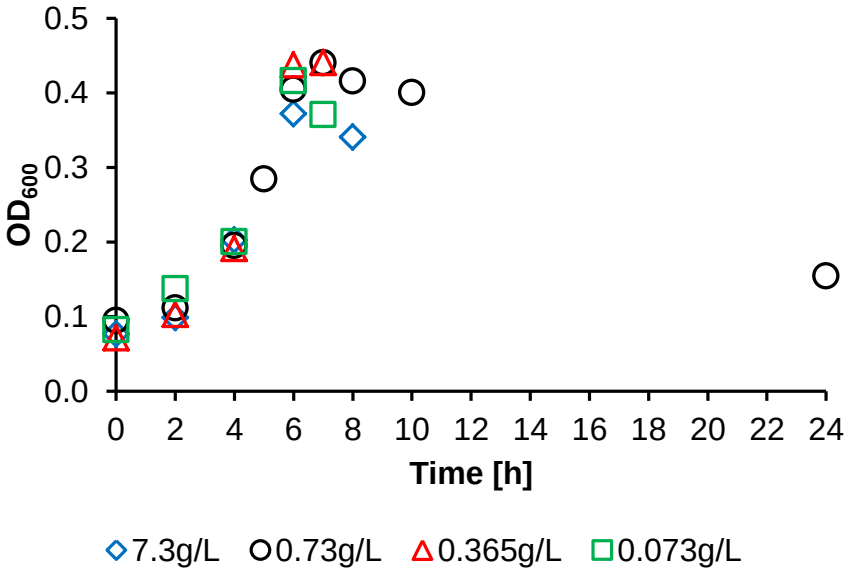

Figure 4.2: Growth curves of the four experiments with different leucine concentrations

Nevertheless, the bacteria were able to efficiently incorporate ^{13}C-carbon from $H^{13}CO_3^-$ during their short active growth phase: the ^{13}C-abundance of the biomass, as determined by EA-IRMS, steadily rose from 1.1 % (natural abundance of ^{13}C-carbon) to a maximum of 5 % at 6 h after inoculation (Fig. 4.3A). The ^{13}C-abundance of the biomass stayed constant until 8 h after inoculation, then levelled off and remained at about 4 % until the end of the experiment. The control experiment with

unlabelled HCO_3^- mirrored the natural abundance of ^{13}C-carbon (1.1 %) in the environment.

The ^{13}C-abundance of the biomass increased only by 0.3 % when ^{13}C-bicarbonate was spiked to a non-labelled control after exponential growth, i.e. 6 h after inoculation (Fig. 4.3B).

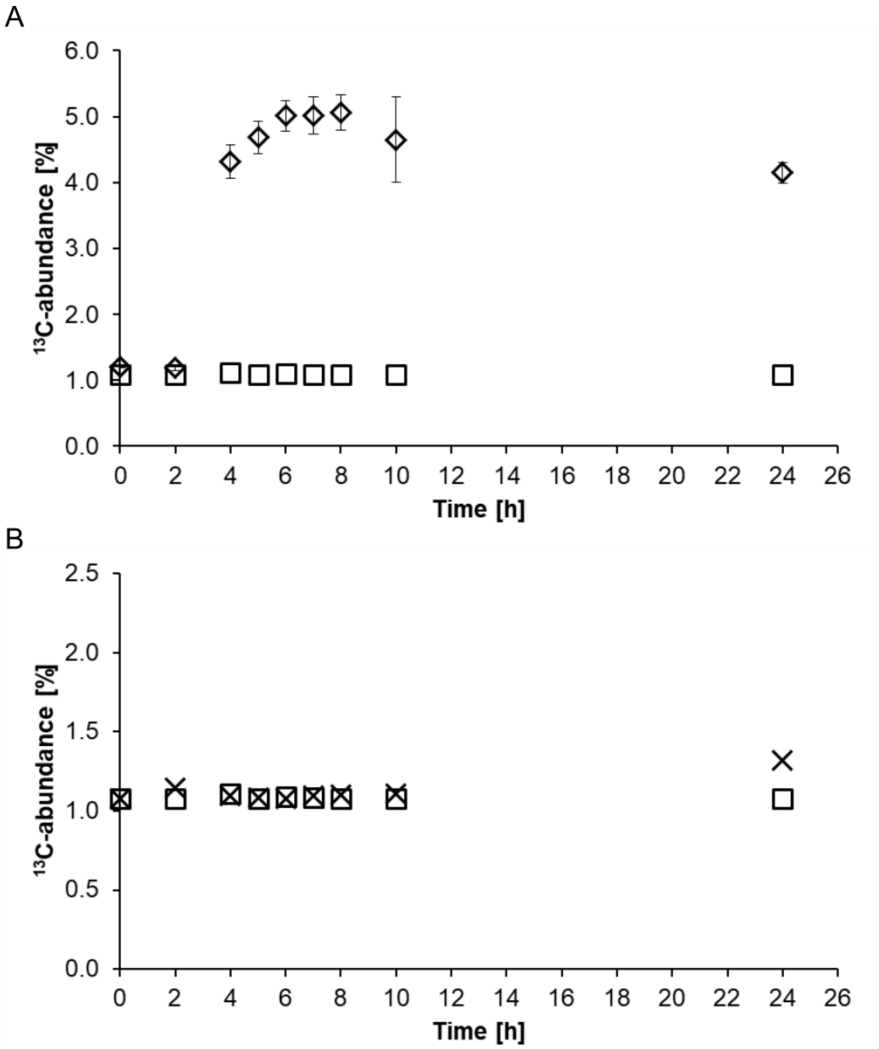

Figure 4.3: (A) Incorporation of ^{13}C-carbon into microbial biomass by *B. subtilis* W23 growing in M9 medium containing 0.73 g/L leucine and 1 g/L $NaH^{13}CO_3^-$. The diamonds represent the ^{13}C-incorporation into the biomass as determined by EA-IRMS measurements. The depicted values are mean values of three biological replicates. The squares represent the control experiment conducted with unlabelled bicarbonate which shows the natural abundance of ^{13}C-carbon of 1.1 % in the environment. **(B) Incorporation of ^{13}C-carbon into microbial biomass by *B. subtilis* W23 growing in M9 leucine medium containing 1 g/L $NaH^{13}CO_3^-$ after exponential growth.** The culture was supplied with the tracer 6 h after inoculation. The ^{13}C-abundance of the biomass (depicted as crosses) did almost not increase. In a control experiment, no $H^{13}CO_3^-$ was added. The ^{13}C-abundance of the biomass (depicted as squares) again mirrored the natural abundance of ^{13}C-carbon in the environment.

Growth of *B. subtilis* in the presence of malate, leucine and $H^{13}CO_3^-$

In a second experimental setup, *B. subtilis* W23 was grown in M9 medium supplemented with leucine, malate (as co-substrate) and $H^{13}CO_3^-$. The growth curve of the bacterial culture showed that growth could be restored in the presence of malate as co-substrate (Fig. 4.4). The bacteria were provided with half the amount per litre of malate and leucine compared to the single substrate experiments. By doing so, we could assure that the same amount of carbon (0.4 g/L) was available to the bacteria in all three setups. Until 10 h after inoculation the growth curve of the bacterial culture fed with malate + leucine overlapped with the growth curve of those bacteria growing only on malate. Afterwards, bacterial cell numbers started to decrease also in the co-substrate experiment, though the trend was not as pronounced as in the leucine experiment.

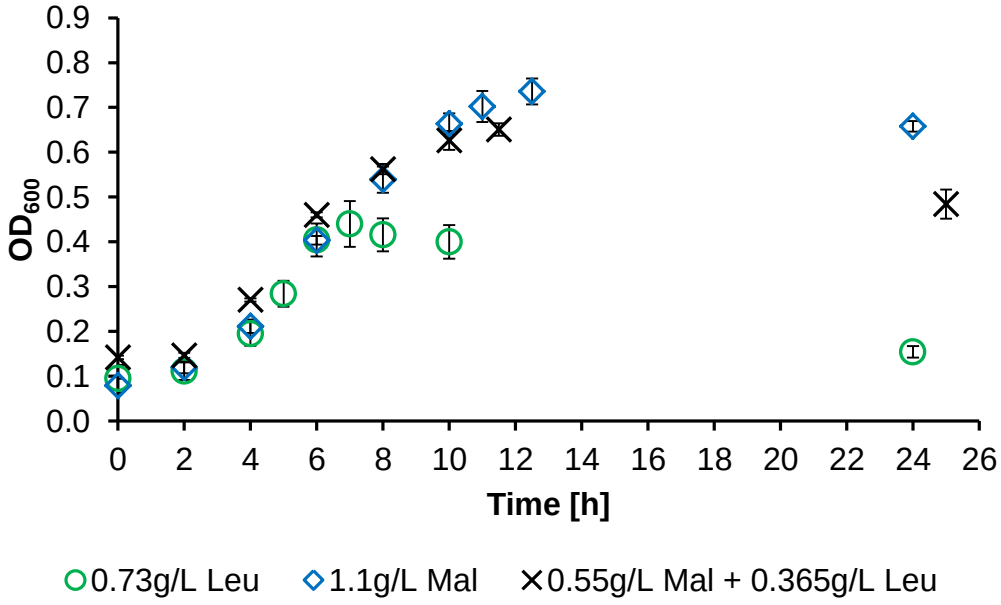

Figure 4.4: Growth curve of the co-substrate experiment with malate + leucine compared to the growth curves of the single substrate experiments with malate and leucine, respectively.

The ^{13}C-abundance of the biomass rose to a maximum of 3 % at 6 h after inoculation and stayed constant till the end of the experiment (Fig. 4.5A). Thus, ^{13}C-incorporation into bacterial biomass was exactly in the same range as during growth of *B. subtilis* W23 on malate alone (3.5 % *see chapter II,* Fig. S3B). The control experiment with unlabelled HCO_3^- mirrored again the natural abundance of ^{13}C-carbon (1.1 %) in the

environment. When ^{13}C-bicarbonate was spiked to an unlabelled control 8 h after inoculation, the ^{13}C-abundance of the biomass increased from 1.1 % to 2.5 % (Fig. 4.5B). Consequently, *B. subtilis* W23 was able to incorporate CO_2 into its biomass even in the absence of cell growth indicating active metabolism during the stationary phase. As a result, malate, added as co-substrate, was apparently able to rescue *B. subtilis* W23 from the limitations imposed by leucine offered as sole organic carbon source.

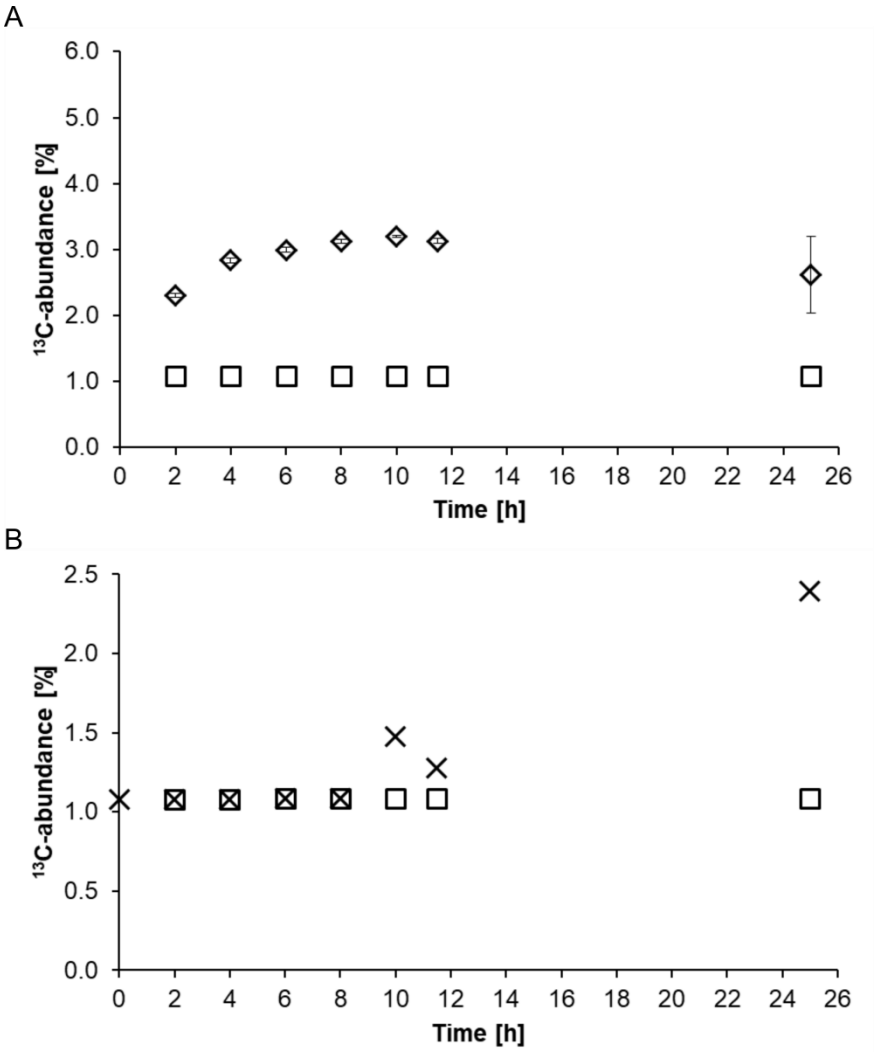

Figure 4.5: (A) Incorporation of ^{13}C-carbon into microbial biomass by *B. subtilis* W23 growing in M9 medium containing 0.55 g/L malate, 0.365 g/L leucine and 1 g/L $NaH^{13}CO_3^-$. The diamonds represent the ^{13}C-incorporation into the biomass as determined by EA-IRMS measurements. The depicted values are mean values of three biological replicates. The squares represent the control experiment conducted with unlabelled bicarbonate, which shows the natural abundance of ^{13}C-carbon of 1.1 % in the environment. **(B) Incorporation of ^{13}C-carbon into microbial biomass by *B. subtilis* W23 growing in M9 malate + leucine medium containing 1 g/L $NaH^{13}CO_3^-$ after exponential growth.** The culture was supplied with the tracer 8 h after inoculation. The ^{13}C-abundance of the biomass (depicted as crosses) increased up to 2.5 %. In a control experiment, no $H^{13}CO_3^-$ was added.

The ^{13}C-abundance of the biomass (depicted as squares) again mirrored the natural abundance of ^{13}C-carbon in the environment.

^{13}C-labelling patterns of amino acids

Our results confirmed that *B. subtilis* W23 was hardly able to grow on leucine as sole organic carbon source over a longer period of time. However, the universal label incorporation made it difficult to achieve the primary objective of this study, namely to identify the reason why an organism is unable to grow on a certain substrate. Therefore, we explored amino acids from the TCA cycle (e.g., Asp, Glu), gluconeogenesis (e.g., Tyr, Phe) and those derived from pyruvate (e.g., Val, Ala) with regard to their ^{13}C-label incorporation. Using established protocols [18], we could quantify the ^{13}C-incorporation in 14 amino acids obtained from acidic hydrolysis of the biomass. M+1 isotopomers, i.e. amino acid isotopomers that carried one ^{13}C-carbon atom, were predominantly found in all three experiments, and thus, discussed in the following.

Amino acids derived from intermediates of the TCA cycle, such as Asp, Thr, Lys, Glu and Pro, showed a ^{13}C-excess of the respective M+1 isotopomers of up to 35 % (Fig. 4.6A), when leucine was offered as growth substrate. In comparison, when grown on malate + leucine, the ^{13}C-excess of the respective M+1 isotopomers of the same amino acids only reached values up to 15 % (Fig. 4.6B). The ^{13}C-excess of the M+1 isotopomers of amino acids derived from gluconeogenetic intermediates was low for Ser and His (about 4 %), when *B. subtilis* W23 was grown on malate + leucine. These amino acids received no label at all, when leucine was offered as carbon source.

Glycine, which is also derived from gluconeogenetic intermediates, was moderately labelled in both cases (4 % (Leu) and 8 % (Mal + Leu)) most likely due to the reverse reaction of the glycine cleavage system [73] (*see chapter II*). Amino acids derived from pyruvate such as Ala, Val, and Leu received low ^{13}C-label in the co-substrate experiment (about 2 %) and very low ^{13}C-label (< 1.5 %) under leucine conditions. Finally, the ^{13}C-excess of the M+1 isotopomers of the amino acids Tyr and Phe, which are derived from erythrose-4-phosphate (an intermediate of the pentose phosphate pathway), reached values up to 3 % when *B. subtilis* W23 was grown on malate + leucine (Fig. 4.6B). The same amino acids received no label at all under leucine conditions (Fig. 4.6A).

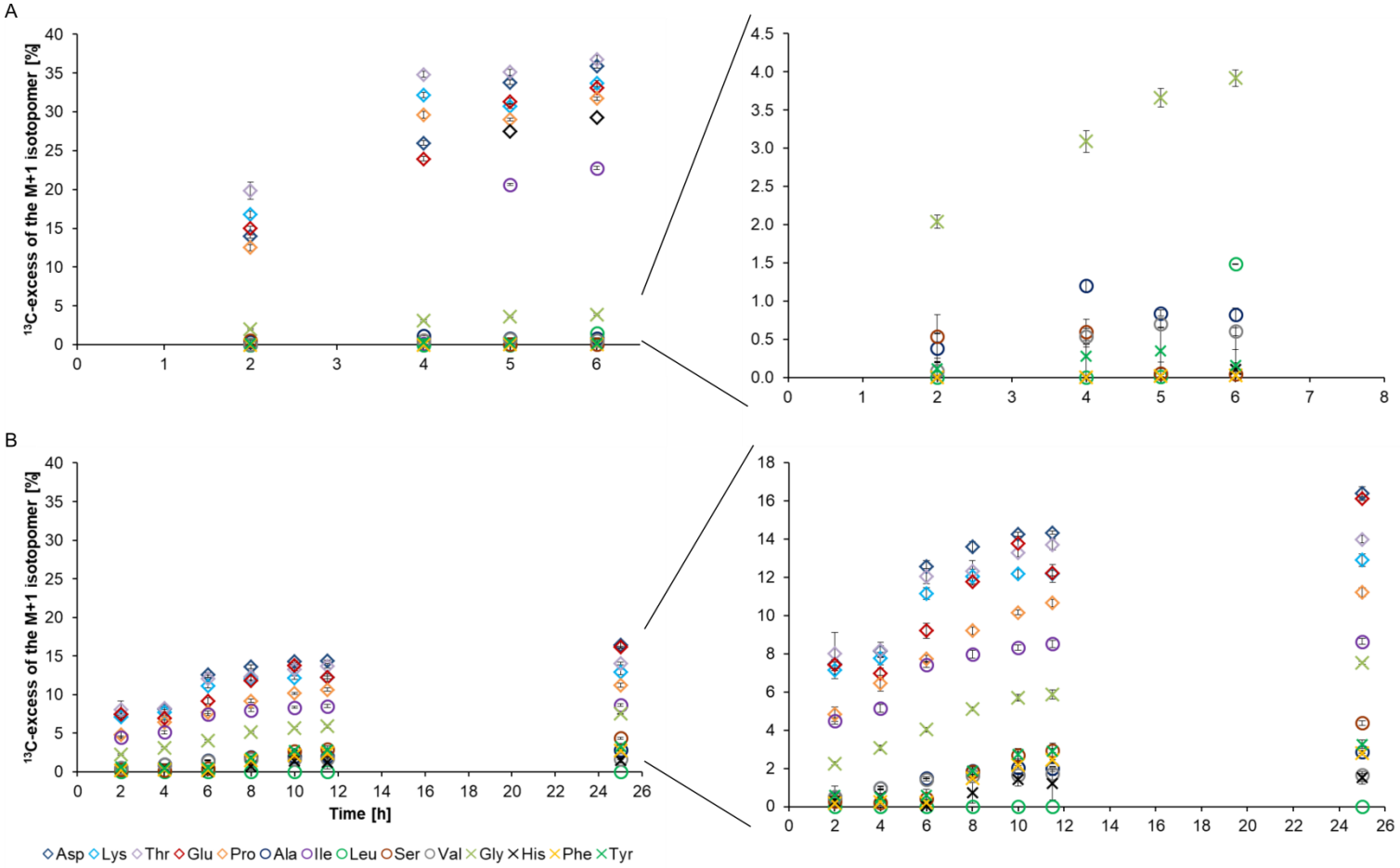

Figure 4.6: ^{13}C-excess of the M+1 isotopomers of specific amino acids produced by $H^{13}CO_3^-$-labelling experiments with leucine (A) and malate + leucine (B). Amino acids depicted as diamonds are derived from the TCA cycle. Amino acids depicted as circles are derived from pyruvate. Amino acids depicted as crosses are derived from the gluconeogenesis pathway. The ^{13}C-excess of the M+1 isotopomers of the amino acids derived from pyruvate and the gluconeogenesis pathway are also displayed with a different scaling to improve visibility.

From these comparisons it became visible that *B. subtilis* W23 was not able to pass on the label outside the TCA cycle, when leucine was offered as sole organic carbon source (only TCA cycle-derived amino acids were ^{13}C-labelled). To better visualise this observation, we calculated and compared ratios of ^{13}C-excess of the M+1 isotopomers in specific sets of amino acids (Fig. 4.7). The amino acids Ala and Val were chosen to represent the ^{13}C-incorporation *via* pyruvate. The amino acids Tyr and Phe were chosen to represent the ^{13}C-incorporation *via* gluconeogenesis and the pentose phosphate pathway. The amino aicds Asp and Glu were chosen to represent the ^{13}C-incorporation *via* the TCA cycle.

The ratios of the ^{13}C-excess of the M+1 isotopomers were calculated from samples taken during stationary phase of growth, i.e. from 6 h (Leu) and 8 h (Mal + Leu) after inoculation till the end of the experiment, respectively. The marker ratios calculated from the ^{13}C-excess of M+1 isotopomers in TCA cycle-derived amino acids and pyruvate-derived amino acids (i.e. Asp/Val, Asp/Ala, Glu/Val and Glu/Ala) yielded values above 30 for the leucine experiment and values below 10 for the co-substrate experiment (Fig. 4.7A). The marker ratios calculated from the ^{13}C-excess of M+1 isotopomers in gluconeogenesis-derived amino acids and pyruvate-derived amino acids (i.e., Tyr/Val, Tyr/Ala, Phe/Val and Phe/Ala) yielded values below 0.5 for the leucine experiment and values above 1 for the co-substrate experiment (Fig. 4.7B). The individual ratios as well as the corresponding mean values from the leucine experiment were very similar to the individual ratios and the respective mean values obtained from the ^{13}C-labelling experiment conducted with glucose as carbon source (*see chapter II*). The marker ratios calculated for the co-substrate experiment mirrored the marker ratios calculated for the ^{13}C-labelling experiment conducted with malate (*see chapter II*).

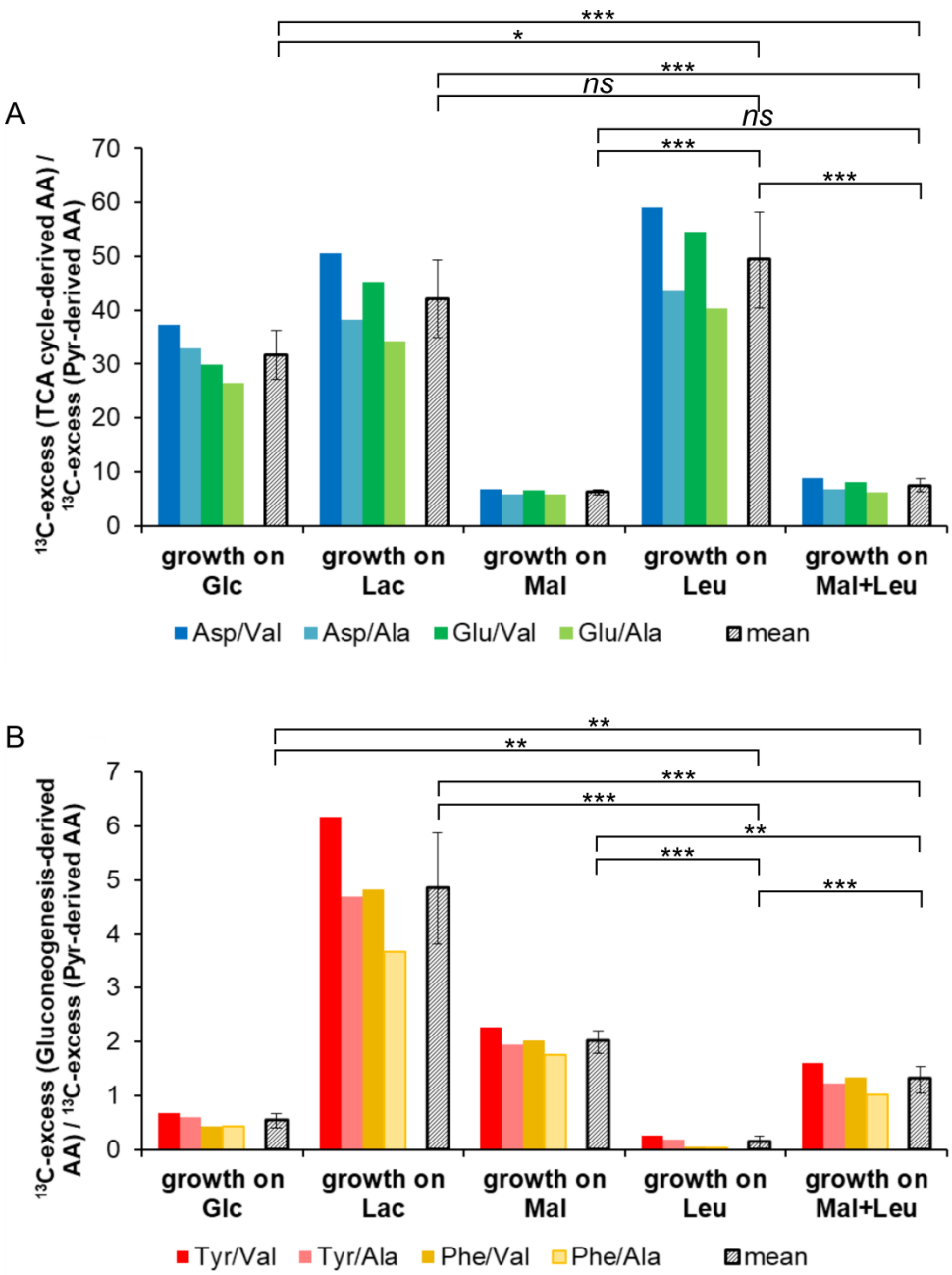

Figure 4.7: Marker ratios of ^{13}C-excess of the M+1 isotopomers between selected amino acids. (A) ^{13}C-excess (TCA cycle-derived amino acids)/ ^{13}C-excess (pyruvate-derived amino acids). The coloured bars depict the ratios of the chosen amino acids in the labelling experiments with glucose, lactate, malate, leucine or malate + leucine, respectively. The grey bars show the mean values of ^{13}C-ratios for these fractions. p-Values as calculated by Student's t-test (unpaired): p(Glc/(Mal+Leu)) = 0.0001, p(Glc/Leu) = 0.0121, p(Lac/(Mal+Leu)) = 0.0001, p(Lac/Leu) = 0.2480, p(Mal/(Mal+Leu)) = 0.1112 p(Mal/Leu) = 0.0001 **(B) ^{13}C-excess (gluconeogenesis-derived amino acids)/ ^{13}C-excess (pyruvate-derived amino acids).** The coloured bars depict the ratios of the chosen amino acids in the labelling experiments with glucose, lactate, malate, leucine or malate + leucine, respectively. The grey bars show the mean values of ^{13}C-ratios for these fractions. p-Values as calculated by Student's t-test (unpaired): p(Glc/(Mal+Leu)) = 0.0015, p(Glc/Leu) = 0.0028, p(Lac/(Mal+Leu)) = 0.0005, p(Lac/Leu) = 0.0001, p(Mal/(Mal+Leu)) = 0.0051 p(Mal/Leu) = 0.000004 (*For detailed calculation see SI excel file F5 m+1 and ratio of label_SI Paper*)

Discussion

Growth experiments with *B. subtilis* W23 and leucine, as sole source of carbon and energy, showed that 6 h after inoculation – regardless of the leucine concentration – biomass increase did not only stop, but was followed by a drastic decrease (Fig. 4.2). As expected, leucine was an unfavourable substrate for *B. subtilis* W23 to maintain growth. Moreover, it seemed that the use of leucine directed a subpopulation of the bacteria to differentiate into so-called cannibals. Cannibal cells are phenotypes that are able to lyse a fraction of their sensitive siblings, which release nutrients that feed the community. In case of need, *B. subtilis* W23 uses cannibalism as a strategy to delay the onset of sporulation and to overcome nutritional limitations [84, 85]. This behaviour would explain the observed drastic decrease in bacterial biomass after a short period of growth. Thus, based on this evidence, there exist two possible scenarios: (i) *B. subtilis* W23 was able to metabolise leucine as long as the nutrients released by lysed (unlabelled) siblings refilled the TCA cycle or (ii) *B. subtilis* W23 did not at all metabolise the offered leucine.

Spiking of ^{13}C-bicarbonate to a non-labelled control at the end of the exponential growth phase lead to almost no ^{13}C-incorporation (< 0.3 %) when leucine was offered as growth substrate to *B. subtilis* W23 (Fig. 4.3B). This means that, under maintenance conditions, metabolic turnover of oxaloacetate involving the reaction of pyruvate carboxylase was considerably reduced. On the contrary, when glucose, lactate or malate, respectively, were the organic carbon sources the metabolic turnover of oxaloacetate remained important, most likely to maintain the energy balance in non-growing *B. subtilis* W23.

The addition of the TCA cycle intermediate malate as co-substrate to leucine rescued *B. subtilis* W23 from the limitations imposed by leucine (Fig. 4.4). EA-IRMS analysis revealed that during growth on malate + leucine up to 3 % of labelled inorganic carbon was incorporated into microbial biomass, just as during growth on malate alone. Additionally, the results from spiking ^{13}C-labelled bicarbonate to a non-labelled control in the co-substrate experiment mirrored again the results from *B. subtilis* W23 growing on malate alone. In summary, *B. subtilis* W23 cultures growing on malate + leucine exhibited highly similar growth behaviour and ^{13}C-label incorporation into bulk biomass compared to growth on malate alone. Thus, these results

demonstrate an effective repression of leucine utilisation by malate, i.e. the expected strict catabolite repression. The ^{13}C-excess values of the M+1 isotopomers of the amino acids further stressed the repression of leucine. The values obtained from the co-substrate experiment and from the malate experiment were nearly identical (Fig. 4.6B and Fig. 2.4C).

EA-IRMS analysis of bacterial biomass grown in the presence of ^{13}C-labelled bicarbonate and two substrates could clearly show that malate repressed the utilisation of leucine in the co-substrate experiment. However, EA-IRMS analysis alone could not elucidate the reason why leucine (offered as sole organic carbon source) was an unsuitable substrate to maintain cell growth and which source of carbon was used by the bacteria during their initial exponential growth. To answer these questions and to follow the labelled inorganic carbon through the metabolic network of the microbial cell, we used GC-MS analysis to reveal information about the carbon positions in amino acids having acquired the label. On the basis of the detected fragmentation patterns of the silylated amino acids (for details, see Table T1), some positional assignments of the ^{13}C-label were possible. As an example, the fragments with m/z of 432 and 286 for Glu and Pro, respectively, contained all five carbon atoms of the original amino acids. The analysis of the respective mass spectra revealed that these fragments were accompanied by an amount of up to 35 % of the respective M+1 isotopomers (namely m/z 433 for Glu and m/z 287 for Pro). The fragments that had lost the C-1 position of these amino acids (i.e. m/z 404 and 330 for Glu and m/z 258 and 184 for Pro), however, did not show a significant ^{13}C-excess of the M+1 isotopomers (< 1 %). Therefore, we concluded that Glu and Pro carried the ^{13}C-label at C-1. The mass distribution in the fragments observed for Asp, Thr and Lys showed a similar amount of up to 35 % of the respective M+1 isotopomers. The ^{13}C-carbon atom was mainly present in C-4, however, lower amounts of ^{13}C-label (2-4 %) could also be assigned to C-1 of these amino acids. This label distribution could be explained because (i) the reaction of pyruvate carboxylase transfers the ^{13}C-label from $H^{13}CO_3^-$ to C-4 of oxaloacetate (ii) the oxidative branch of the TCA cycle converts [4-^{13}C]oxaloacetate into [1-^{13}C]α-ketoglutarate (leading to the detected [1-^{13}C]-isotopomers of Glu and Pro), (iii) Asp, Thr and Lys are synthesised from the TCA cycle intermediate oxaloacetate (leading to the detected [4-^{13}C]-isotopomers), and (iv) reversible reactions in the reductive

branch of the TCA cycle – between oxaloacetate and succinate – lead to a scrambling of label between C-1 and C-4 of the symmetric intermediates fumarate and succinate. Consequently, the ^{13}C-label got also into C-1 of oxaloacetate and its downstream products Asp, Thr and Lys. The ^{13}C-excess of the M+1 isotopomers of the TCA cycle-derive amino acids (i.e. Glu, Pro, Asp, Thr and Lys) reached values up to 35 %, when leucine was offered to *B. subtilis* W23 as the only carbon substrate. This label incorporation was accomplished by the reaction catabolised by pyruvate carboxylase as learned from the positions of the ^{13}C-carbon atoms in the respective amino acids. Notably, amino acids derived from gluconeogenetic intermediates (i.e. His, Phe, Tyr) or pyruvate (i.e. Ala, Leu, Ser, Val) received virtually no ^{13}C-label (< 1 %), when leucine was offered as substrate, indicating an inactive gluconeogenesis. Thus, altogether, these results exhibited a high similarity to the results obtained from $H^{13}CO_3^-$-labelling experiments with *B. subtilis* W23 cultures growing on glucose.

Moreover, a significant ^{13}C-excess of M+2 isotopomers of the above mentioned amino acids was not detected, when leucine was offered as substrate. This was interesting, because in leucine metabolism a decarboxylation step is followed by a carboxylation step, in which a molecule of bicarbonate is attached onto 3-methylbut-2-enoyl-CoA. Hence, this reaction represents a second possibility to introduce the ^{13}C-label to the metabolic network of *B. subtilis* W23. The ^{13}C-label would be found in one out of three Ac-CoA molecules, when leucine degradation is completed (Fig. 4.8). The (si)-specific citrate synthase could then synthesise a citrate molecule that carries two ^{13}C-atoms – one originating from Ac-CoA and one originating from oxaloacetate (Fig. 4.9). This in turn should give rise to M+2 isotopomers in the amino acids derived from TCA cycle intermediates (in particular [1,5-$^{13}C_2$]-isotopomers for Glu and Pro and [1,4-$^{13}C_2$]-isotopomers for Asp, Thr and Lys). However, no isotopomers of TCA cycle-derived amino acids could be identified that carried two ^{13}C-carbon atoms. Consequently, either the bicarbonate utilised during metabolism of leucine was not labelled (which is hardly possible due to our experimental settings) or the relevant reaction did not take place. Interestingly, the genes for leucine degradation are united in two regulons: the SigE and SigL regulons [86-88]. The enzymes catalysing the first four reactions of leucine degradation, and thus also the decarboxylation step, are encoded in the SigL regulon. Expression of these genes is induced in the presence of branched chain amino acids (like leucine). The end

product of these four reactions is 3-methylbutanoyl-CoA, which in turn is a starting point for branched chain fatty acid biosynthesis (Fig. 4.8 yellow box). The enzymes encoded in the SigE regulon are expressed during sporulation of the mother cell. We hypothesise that the genes united in the SigE regulon were not expressed, because there were no indications that *B. subtilis* W23 has begun to build spores. Consequently, the enzymes catalysing the carboxylation step were not synthesised and the carboxylation reaction did not happen (Fig. 4.8 blue box). This would explain why we only see [$^{13}C_1$]-isotopomers in the amino acids derived from TCA cycle intermediates. Thus, ^{13}C-label incorporation was only accomplished *via* the anaplerotic reaction of pyruvate carboxylase, when leucine was offered as carbon substrate.

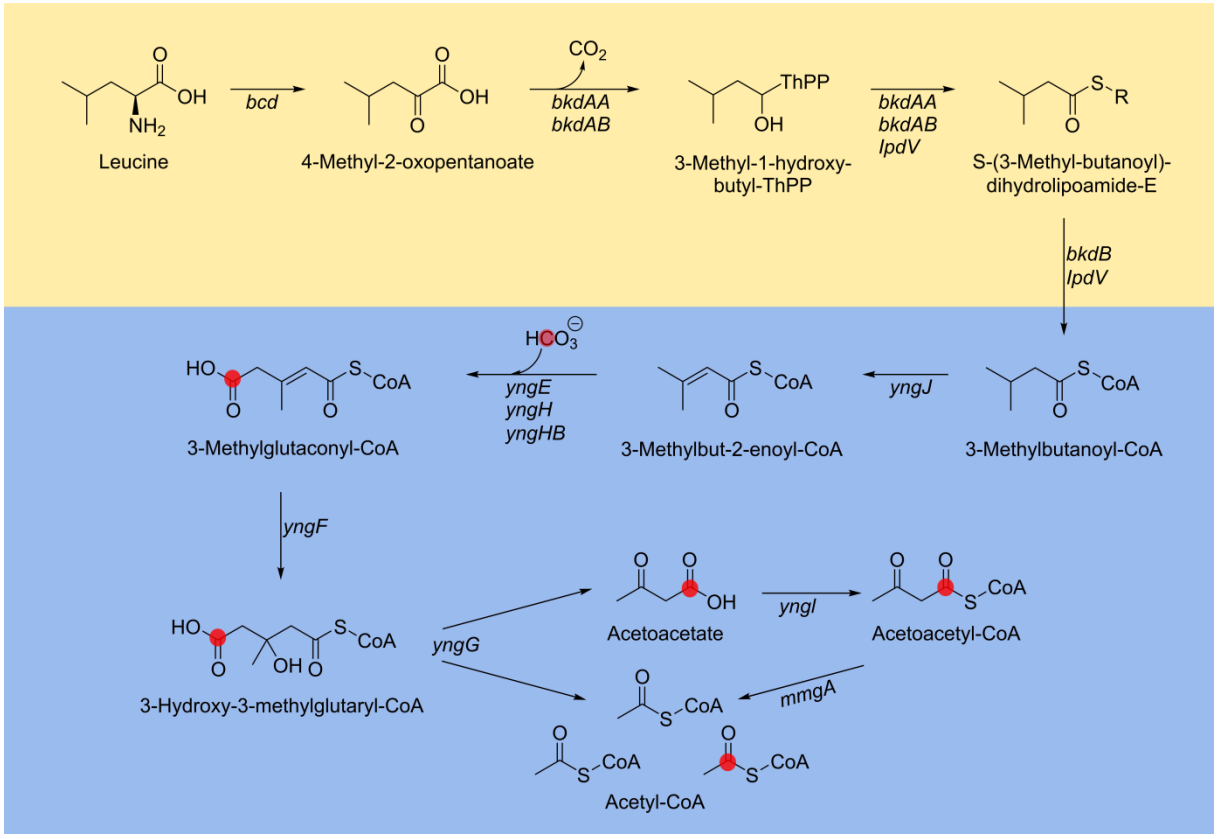

Figure 4.8: Leucine degradation in *B. subtilis*. Reactions and enzymes that are assigned to the SigL regulon are highlighted by the yellow box. Reactions and enzymes that are assigned to the SigE regulon are highlighted by the blue box.

Therefore, we concluded that *B. subtilis* W23 was neither able to channel leucine into the TCA cycle (as metabolism of leucine presumably stopped at the level of 3-methylbutanoyl-CoA, if metabolised at all), nor to utilise leucine together with

nutrients released by lysed unlabelled siblings. This was experimentally confirmed by the absence of amino acid isotopomers carrying two ^{13}C-carbon atoms.

Taking into account the results from GC-MS analysis of ^{13}C-incorporation into individual amino acids, it therefore seems safe to assume that leucine was not used at all by *B. subtilis* W23. In our previous work we introduced a two-step procedure to distinguish (main) utilised organic carbon sources: the marker ratios of ^{13}C-excess values for M+1 isotopomers in specific sets of amino acids were calculated and compared against each other (*see chapter II*). When we apply this procedure to the data obtained from the leucine experiment, the already observed similarity to the glucose experiment (concerning ^{13}C-incorporation into bulk biomass and no detected ^{13}C-label in gluconeogenesis-derived amino acids) becomes even more striking. As shown in Fig. 4.7, the resultant amino acid ratios obtained from *B. subtilis* W23 cultures growing on glucose came closest to those ratios obtained from the leucine experiment – also with good statistical significance. This suggests that the bacteria metabolised remains of the nutrients from the medium of the glycerol stock solution, which was used to inoculate the pre-cultures. Calculations showed that 0.46 g/L of organic matter (14.2 mg/L from tryptone soya broth, 0.45 g/L from glycerol solution) was left from the inoculum and present in the growth medium. This organic matter is mainly composed of carbohydrates that enter the central carbon metabolism *via* glycolysis. This explains the similarity to the ^{13}C-incorporation patterns obtained from growth on glucose and why *B. subtilis* W23 was able to grow up to an OD_{600} of 0.4 in the leucine experiments.

The detailed analysis of amino acid isotopomer patterns granted insight into the core metabolic network of *B. subtilis* W23. The comparison of the marker ratios of ^{13}C-excess values for M+1 isotopomers in specific sets of amino acids demonstrated that no ^{13}C-label could be spread outside the TCA cycle at high statistical significance. Hence, it became evident that *B. subtilis* W23 was not able to use leucine for growth. Instead, the bacteria metabolised the organic matter leftover from the inoculum until this carbon source became exhausted. This resulted in an arrest of cell growth and even drove a subpopulation to differentiate into cannibal-cells.

Labelling experiments using $H^{13}CO_3^-$ as a tracer and *B. subtilis* W23 as a model organism in combination with EA-IRMS analysis of the biomass and GC-MS analysis of protein-derived amino acids was able to provide superior insight into the functional metabolic networks of the living organism. The technique bears the advantage of studying an organism *in vivo* and without altering the (dissolved) organic carbon pool. By applying this technique, we were able to elucidate that *B. subtilis* W23 was unable to metabolise the offered leucine. *B. subtilis* W23 metabolised organic matter leftovers from the inoculum, instead, which was also revealed by our labelling approach. Furthermore, heterotrophic CO_2-fixation granted insights into specific pathways such as leucine degradation and was able to show that, under the chosen conditions, leucine metabolism presumably stopped at the level of 3-methylbutanoyl-CoA.

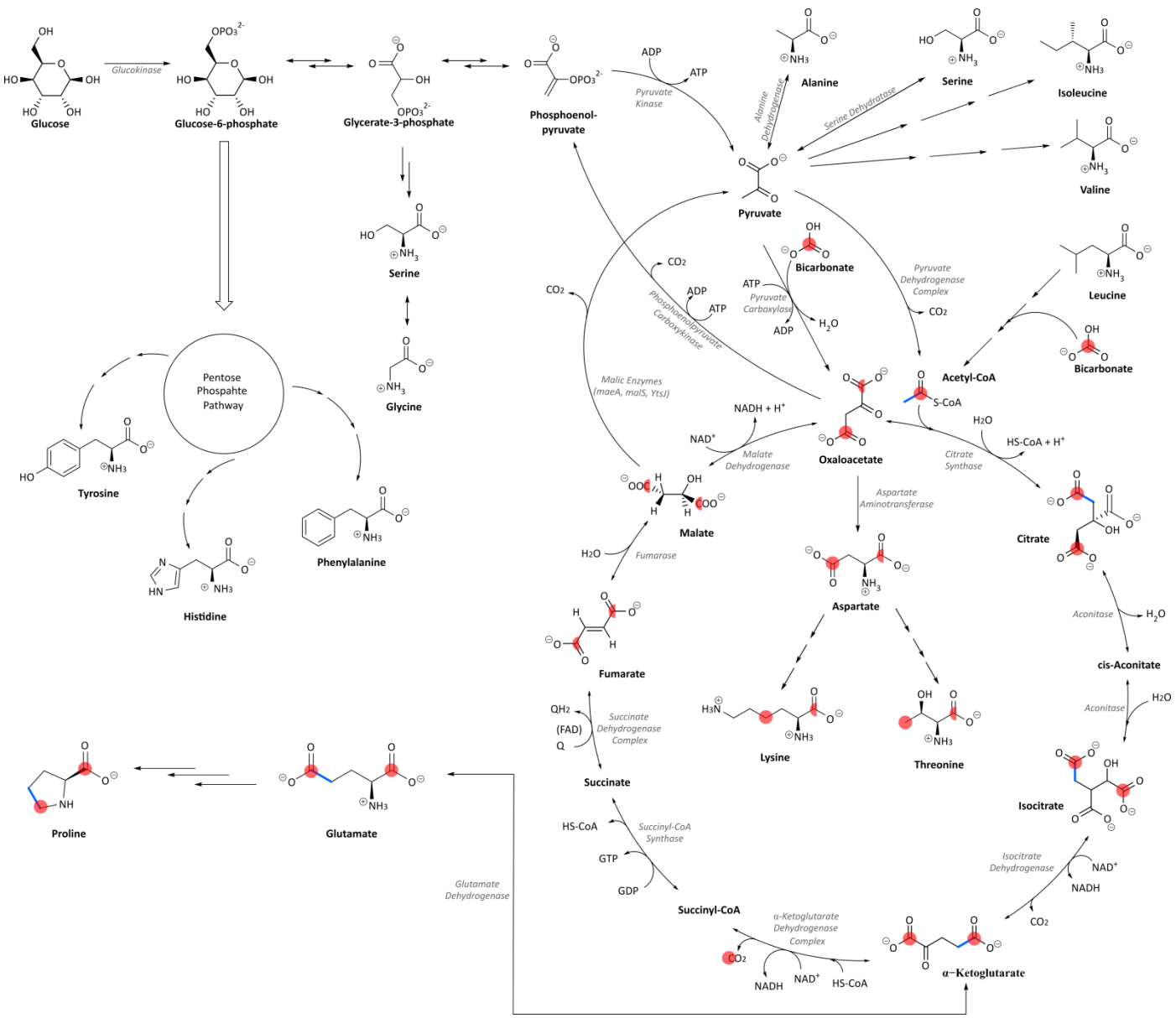

Figure 4.9: Hypothetical metabolic network for *B. subtilis* W23 growing in M9 medium containing $H^{13}CO_3^-$ as a tracer and leucine as carbon source. The full red circles mark the location of the ^{13}C-atom detected in amino acids due to anaplerosis. The carbon atoms originating from Ac-CoA are marked in blue and the ^{13}C-atom is again marked with a red circle. The equilibrium between the reactions of the reductive branch of the TCA cycle could transfer the ^{13}C-label from oxaloacetate to malate, fumarate and succinate. The intrinsic symmetry of fumarate leads to the formation of a 0.5:0.5 mixture of [1-^{13}C]- and [4-^{13}C]malate as well as [1-^{13}C]- and [4-^{13}C]oxaloacetate, respectively. This is indicated by the red half circles. The same is true for the label acquired *via* ^{13}C-labeld Ac-CoA.

V

GENERAL CONCLUSION

Heterotrophic organisms, from microorganisms to humans, have one thing in common: they incorporate CO_2/HCO_3^- into their biomass, although they rely on complex organic substrates as nutrients. This incorporation of inorganic carbon is achieved by the activity of carboxylases that reside in the metabolism of heterotrophs. This thesis is focussed on pyruvate carboxylase, one of the most prominent anaplerotic enzymes, which catalyses the bicarbonate-dependent conversion of pyruvate into oxaloacetate. The activity of pyruvate carboxylase depends on the main organic carbon substrate that is available to bacteria as shown for the model organism *Bacillus subtilis* and bacterial communities living in groundwater samples. Substrates belonging to different chemical families (e.g. sugars, amino acids or carboxylic acids) have specific entry points to the network of central carbon metabolism (e.g. glycolysis, gluconeogenesis, TCA cycle), either upstream or downstream from the pyruvate carboxylase reaction. Therefore, the use of substrates belonging to different chemical families results in different levels of ^{13}C-incorpration in metabolic products, due to the activity of pyruvate carboxylase, when the bacteria are grown in the presence of isotopically labelled bicarbonate ($H^{13}CO_3^-$). Consequently, by ^{13}C-tracing the substrate-dependent activity of pyruvate carboxylase, it is possible to identify the main organic carbon substrate utilised by microorganisms, without perturbing the natural (dissolved) organic carbon pool.

Our experiments with *Bacillus subtilis* W23 (a well-known, heterotrophic, Gram-positive model organism) grown on glucose, lactate or malate, respectively, and $H^{13}CO_3^-$ as tracer, indeed yielded characteristic ^{13}C-incorporation patterns of the bulk biomass and of individual protein- and cell wall-derived amino acids for each substrate (*see chapter II*). For the simplified data interpretation, marker ratios between the ^{13}C-excess values of specific sets of amino acids were established as sensitive and selective markers to assign the type of the main utilised organic carbon source. The results obtained from a labelling experiment with a natural groundwater community proved that this approach is also applicable to environmental samples. Again, the marker ratios of ^{13}C-incorporation into amino acids revealed the type of the main organic carbon source that was used by the vast majority of heterotrophic organisms in these environmental samples (*see chapter III*). Thus, labelling experiments using $H^{13}CO_3^-$ as a tracer could assign the type of microbial substrate

utilisation and thus could characterise the bioavailable components of dissolved organic matter.

Furthermore, this novel approach based on heterotrophic CO_2-fixation seems to be suitable to investigate microbial metabolism and physiology in general. As an example, we were able to reveal the reason behind the fact that leucine is an unfavourable carbon substrate for *B. subtilis* W23: the bacteria could neither use the offered leucine for their protein biosynthesis, nor channel the amino acid into the TCA cycle or into gluconeogenesis, as leucine metabolism presumably stopped at the level of 3-methylbutanoyl-CoA. Heterotrophic CO_2-fixation could also be used to study carbon catabolite repression in co-substrate experiments: we could confirm that malate efficiently repressed leucine utilisation. Hence, next to gene expression studies, the labelling approach *via* heterotrophic CO_2-fixation represents a welcome method to study carbon catabolite repression in co-substrate settings (*see chapter IV*).

Notably, the ^{13}C-labelling experiments conducted with $H^{13}CO_3^-$ as tracer, yielded equally valuable information about the utilisation of an organic carbon substrate compared to experiments conducted with the ^{13}C-labelled organic substrates themselves. Moreover, the great advantage of the novel approach is that $^{13}CO_2/H^{13}CO_3^-$ is a very simple, inexpensive and readily available labelled precursor that is efficiently taken up by many, if not all organisms, and that this inorganic tracer does not perturb the occurring natural (dissolved) organic carbon pool.

Thus, based on the results presented in this thesis, heterotrophic CO_2-fixation is a useful tool in fundamental research to study the metabolism of microorganisms *in vivo* as well as to reveal the type of the main utilised organic carbon source in environmental samples. Possible areas of application might be microbial ecology (in the environment) or medical biology.

For example, labelling experiments based on heterotrophic CO_2-fixation using environmental Gram-negative or methanotrophic microorganisms as well as model microbial communities, originating from groundwater that was subjected to different landscape, could further confirm the validity of the experimental approach to indicate

surface condition and quality (e.g. agricultural use, forest, meadow, rocks). Thus, “indicator ratios” would emerge from these experiments - in the ideal case. A significant deviation from the “indicator ratios” could then be an indication for a contamination. Additionally, the “indicator ratios” would help to identify the type of the main utilised organic carbon source, for example in studies that aim to characterise the metabolised (dissolved) organic matter in soil or groundwater systems. This is of great interest when it comes to groundwater contamination (with e.g. pesticides, herbicides or aromatic compounds originating from oil production (BTEX)) and remediation. Microbial degradation of pollutants is studied by scientist from the field of ecological microbiology: here, our approach could help to answer the question which pollutant was metabolised and thus degraded by the microbial community.

As another example, the elucidation of early stages of diabetes type 2 using $H^{13}CO_3^-$-fixation is possible. During the early stages of this disease, glucose production and thus blood sugar levels are already slightly elevated, but no physical consequences are noticeable yet. Bicarbonate is a building block in gluconeogenesis; consequently the application of ^{13}C-labelled bicarbonate (e.g. drinking of sparkling water) would uncover glucose production, if ^{13}C-label is found in glucose isolated from blood or saliva samples. Thus, the presence of ^{13}C-labelled glucose, when no active gluconeogenesis is required, would be an indication for early diabetes type 2.

References

1. Gleixner, G., *Soil organic matter dynamics: a biological perspective derived from the use of compound-specific isotopes studies.* Ecological Research, 2013. **28**(5): p. 683-695.
2. Kleijn, R.J., et al., *Metabolic Fluxes during Strong Carbon Catabolite Repression by Malate in Bacillus subtilis.* Journal of Biological Chemistry, 2010. **285**(3): p. 1587-1596.
3. Shen, Y., et al., *Origins and bioavailability of dissolved organic matter in groundwater.* Biogeochemistry, 2014. **122**(1): p. 61-78.
4. Hedges, J.I., et al., *Origins and processing of organic matter in the Amazon River as indicated by carbohydrates and amino acids.* Limnol. Oceanogr., 1994. **39**: p. 743-761.
5. Risse-Buhl, U., et al., *Dynamics, chemical properties and bioavailability of DOC in an early successional catchment.* Biogeosciences, 2013. **10**(7): p. 4751-4765.
6. Zhang, F., et al., *Molecular and structural characterization of dissolved organic matter during and post cyanobacterial bloom in Taihu by combination of NMR spectroscopy and FTICR mass spectrometry.* Water Research, 2014. **57**: p. 280-294.
7. Lam, B., et al., *Major Structural Components in Freshwater Dissolved Organic Matter.* Environmental Science & Technology, 2007. **41**(24): p. 8240-8247.
8. McDonough, L.K., et al., *Changes in groundwater dissolved organic matter character in a coastal sand aquifer due to rainfall recharge.* Water Research, 2020. **169**: p. 115201.
9. Niu, X.-Z., et al., *Characterisation of dissolved organic matter using Fourier-transform ion cyclotron resonance mass spectrometry: Type-specific unique signatures and implications for reactivity.* Science of The Total Environment, 2018. **644**: p. 68-76.
10. Townsend-Small, A., M.E. McClain, and J.A. Brandes, *Contributions of carbon and nitrogen from the Andes Mountains to the Amazon River: Evidence from an elevational gradient of soils, plants, and river material.* Limnol. Oceanogr., 2005. **50**: p. 672–685.
11. Meredith, K.T., et al., *Isotopic and chromatographic fingerprinting of the sources of dissolved organic carbon in a shallow coastal aquifer.* Hydrology and Earth System Sciences, 2020. **24**(4): p. 2167-2178.
12. Kaiser, K., et al., *Origins and transformations of dissolved organic matter in large Arctic rivers.* Sci Rep, 2017. **7**(1): p. 1-11.
13. Peter, S., et al., *Bioavailability and diagenetic state of dissolved organic matter in riparian groundwater.* Journal of Geophysical Research: Biogeosciences, 2012. **117**(G4): p. 1-10.
14. Winter, G. and J.O. Kromer, *Fluxomics - connecting 'omics analysis and phenotypes.* Environ Microbiol, 2013. **15**(7): p. 1901-1916.
15. Antoniewicz, M.R., *Methods and advances in metabolic flux analysis: a mini-review.* J Ind Microbiol Biotechnol, 2015. **42**(3): p. 317-325.

16. Eisenreich, W., et al., *^{13}C isotopologue perturbation studies of Listeria monocytogenes carbon metabolism and its modulation by the virulence regulator PrfA.* Proc. Natl. Acad. Sci., 2006. **103**: p. 2040–2045.
17. Eylert, E. and W. Eisenreich, *Auf der Suche nach den Achillesfersen pathogener Bakterien.* BIOspektrum, 2010. **16**: p. 435-437.
18. Eylert, E., et al., *Carbon metabolism of Listeria monocytogenes growing inside macrophages.* Molecular Microbiology, 2008. **69**(4): p. 1008-1017.
19. Willenborg, J., et al., *Characterization of the pivotal carbon metabolism of Streptococcus suis serotype 2 under ex vivo and chemically defined in vitro conditions by isotopologue profiling.* J Biol Chem, 2015. **290**(9): p. 5840-5854.
20. Eylert, E., et al., *Isotopologue profiling of Legionella pneumophila: role of serine and glucose as carbon substrates.* J Biol Chem, 2010. **285**(29): p. 22232–22243.
21. Berg, I.A., *Ecological aspects of the distribution of different autotrophic CO_2 fixation pathways.* Appl Environ Microbiol, 2011. **77**(6): p. 1925-1936.
22. Fuchs, G., *Alternative pathways of carbon dioxide fixation: insights into the early evolution of life?* Annu Rev Microbiol, 2011. **65**: p. 631-658.
23. Giovannoni, S.J. and U. Stingl, *Molecular diversity and ecology of microbial plankton.* Nature, 2005. **437**(7057): p. 343-348.
24. Bassham, J.A. and M. Calvin, *The way of CO_2 in plant photosynthesis.* Comparative Biochemistry and Physiology, 1962. **4**(2-4): p. 187-192.
25. Wood, H.G. and C.H. Werkman, *The Utilisation of CO_2 in the Dissimilation of Glycerol by the Propionic Acid Bacteria.* Biochem. 1936, 1935: p. 48-53.
26. Middelburg, J.J., *Chemoautotrophy in the ocean.* Geophysical Research Letters, 2011. **38**(24): p. 1-4.
27. Baltar, F., et al., *Significance of non-sinking particulate organic carbon and dark CO_2 fixation to heterotrophic carbon demand in the mesopelagic northeast Atlantic.* Geophysical Research Letters, 2010. **37**(9): p. 1-6.
28. Dijkhuizen, L. and W. Harder, *Microbial metabolism of carbon dioxide.* Comprehensive Biotechnology, 1985. **1**: p. 409-423.
29. Erb, T.J., *Carboxylases in natural and synthetic microbial pathways.* Appl Environ Microbiol, 2011. **77**(24): p. 8466-8477.
30. Herndl, G.J. and T. Reinthaler, *Microbial control of the dark end of the biological pump.* Nature Geoscience, 2013. **6**: p. 718-724.
31. Miltner, A., et al., *Assimilation of CO_2 by soil microorganisms and transformation into soil organic matter.* Organic Geochemistry, 2004. **35**(9): p. 1015-1024.
32. Perez, R.C. and A. Matin, *Carbon dioxide assimilation by Thiobacillus novellus under nutrient-limited mixotrophic conditions.* Journal of bacteriology, 1982. **150**(1): p. 46-51.
33. Romanenko, V.I., *Heterotrophic CO_2 assimilation by water bacterial flora.* Mikrobiologiia, 1964. **33**: p. 679-683.
34. Doronia, N.V. and Y.A. Trotsenko, *Levels of carbon dioxide assimilation in bacteria with different pathways of C1 metabolism.* Mikrobiologiya, 1985. **53**: p. 885-889.
35. Owen, O.E., S.C. Kalhan, and R.W. Hanson, *The key role of anaplerosis and cataplerosis for citric acid cycle function.* Journal of Biological Chemistry, 2002. **277**(34): p. 30409-30412.
36. Jitrapakdee, S. and J.C. Wallace, *Structure, function and regulation of pyruvate carboxylase.* Biochem. J., 1999. **340**: p. 1-16.

37. Jitrapakdee, S., et al., *Structure, mechanism and regulation of pyruvate carboxylase.* Biochemical Journal, 2008. **413**: p. 369-387.
38. Giovannelli, D., et al., *Insight into the evolution of microbial metabolism from the deep-branching bacterium, Thermovibrio ammonificans.* Elife, 2017. **6**: p. 1-31.
39. Lombard, J. and D. Moreira, *Early evolution of the biotin-dependent carboxylase family.* BMC Evol Biol, 2011. **11**: p. 1-22.
40. Alonso-Saez, L., et al., *High bicarbonate assimilation in the dark by Arctic bacteria.* ISME J, 2010. **4**(12): p. 1581-1590.
41. Miltner, A., et al., *Non-phototrophic CO_2 fixation by soil microorganisms.* Plant and Soil, 2005. **269**(1-2): p. 193-203.
42. Wegener, G., et al., *Assessing sub-seafloor microbial activity by combined stable isotope probing with deuterated water and ^{13}C-bicarbonate.* Environ Microbiol, 2012. **14**(6): p. 1517-1527.
43. Wegener, G., M.Y. Kellermann, and M. Elvert, *Tracking activity and function of microorganisms by stable isotope probing of membrane lipids.* Curr Opin Biotechnol, 2016. **41**: p. 43-52.
44. Hesselsoe, M., et al., *Isotope labeling and microautoradiography of active heterotrophic bacteria on the basis of assimilation of $^{14}CO_2$.* Appl Environ Microbiol, 2005. **71**(2): p. 646-655.
45. Roslev, P., et al., *Use of heterotrophic CO_2 assimilation as a measure of metabolic activity in planktonic and sessile bacteria.* Journal of Microbiological Methods, 2004. **59**(3): p. 381-393.
46. DeLorenzo, S., et al., *Ubiquitous dissolved inorganic carbon assimilation by marine bacteria in the Pacific Northwest coastal ocean as determined by stable isotope probing.* PLoS One, 2012. **7**(10): p. 1-15.
47. Yakimov, M.M., et al., *Heterotrophic bicarbonate assimilation is the main process of de novo organic carbon synthesis in hadal zone of the Hellenic Trench, the deepest part of Mediterranean Sea.* Environmental Microbiology Reports, 2014. **6**(6): p. 709-722.
48. Šantrůčková, H., et al., *Heterotrophic Fixation of CO_2 in Soil.* Microbial Ecology, 2005. **49**(2): p. 218-225.
49. Huber, C., et al., *Elements of metabolic evolution.* Chemistry, 2012. **18**: p. 2063-2080.
50. Bassham, J.A. and M. Calvin, *The way of CO_2 in plant photosynthesis.* Comp Biochem Physiol, 1962. **4**: p. 187-204.
51. Wood, H.G. and C.H. Werkman, *The utilisation of CO_2 in the dissimilation of glycerol by the propionic acid bacteria.* Biochem J, 1936. **30**: p. 48-53.
52. Middelburg, J.J., *Chemoautotrophy in the ocean.* Geophy Res Lett, 2011. **38**: p. 1-4.
53. Attwood, P.V., *The structure and the mechanism of action of pyruvate carboxylase.* The International Journal of Biochemistry & Cell Biology, 1995. **27**(3): p. 231-249.
54. Sauer, U. and B.J. Eikmanns, *The PEP-pyruvate-oxaloacetate node as the switch point for carbon flux distribution in bacteria.* FEMS Microbiol Rev, 2005. **29**(4): p. 765-794.
55. Kleijn, R.J., et al., *Metabolic fluxes during strong carbon catabolite repression by malate in Bacillus subtilis.* J Biol Chem, 2010. **285**: p. 1587-1596.
56. Nielsen, J., *Systems biology of metabolism.* Annu Rev Biochem, 2017. **86**: p. 245-275.

57. Heux, S., et al., *Recent advances in high-throughput ^{13}C-fluxomics.* Curr Opin Biotechnol, 2017. **43**: p. 104-109.
58. Bacher, A., F. Chen, and W. Eisenreich, *Decoding biosynthetic pathways in plants by pulse-chase strategies using $^{13}CO_2$ as a universal tracer.* Metabolites, 2016. **6**: p. 1-24.
59. Römisch-Margl, W., et al., *$^{13}CO_2$ as a universal metabolic tracer in isotopologue perturbation experiments.* Phytochemistry, 2007. **68**: p. 2273-2289.
60. Schramek, N., et al., *Artemisinin biosynthesis in growing plants of Artemisia annua. A $^{13}CO_2$ study.* Phytochemistry, 2010. **71**: p. 179-187.
61. Ishihara, H., et al., *Quantifying protein synthesis and degradation in Arabidopsis by dynamic $^{13}CO_2$ labeling and analysis of enrichment in individual amino acids in their free pools and in protein.* Plant Physiol, 2015. **168**: p. 74-93.
62. Cegelski, L. and J. Schaefer, *NMR determination of photorespiration in intact leaves using in vivo $^{13}CO_2$ labeling.* J Magn Reson, 2006. **178**: p. 1-10.
63. Johnson, B.T. and V.I. Romanenko, *Xenobiotic perturbation of microbial growth as measured by CO_2 uptake in aquatic heterotrophic bacteria.* J. Great Lakes Res., 1984. **10**: p. 245-250.
64. Lee, W.N., et al., *Mass isotopomer analysis: theoretical and practical considerations.* Biol Mass Spectrom, 1991. **20**: p. 451-458.
65. Meyer, F.M. and J. Stülke, *Malate metabolism in Bacillus subtilis: distinct roles for three classes of malate-oxidizing enzymes.* FEMS Microbiol Lett, 2013. **339**(1): p. 17-22.
66. Laboratories, K., *Glycine, serine and threonine metabolism - Bacillus subtilis subsp. spizizenii W23*. 2019.
67. Schilling, O., et al., *Transcriptional and metabolic responses of Bacillus subtilis to the availability of organic acids: transcription regulation is important but not sufficient to account for metabolic adaptation.* Appl Environ Microbiol, 2007. **73**: p. 499-507.
68. Mirouze, N., et al., *Genome-wide mapping of TnrA-binding sites provides new insights into the TnrA regulon in Bacillus subtilis.* Microbiologyopen, 2015. **4**: p. 423-435.
69. Cazzulo, J.J. and A.O. Stoppani, *Effects of adenosine phosphates and nicotinamide nucleotides on pyruvate carboxylase from baker's yeast.* Biochem J, 1969. **112**: p. 755-762.
70. Zhu, B. and J. Stülke, *SubtiWiki in 2018: from genes and proteins to functional network annotation of the model organism Bacillus subtilis.* Nucleic Acids Res, 2018. **46**: p. 743-748.
71. Diesterhaft, M.D. and E. Freese, *Role of pyruvate carboxylase, phosphoenolpyruvate carboxykinase, and malic enzyme during growth and sporulation of Bacillus subtilis.* J Biol Chem, 1973. **248**: p. 6062-6070.
72. Chubukov, V., et al., *Transcriptional regulation is insufficient to explain substrate-induced flux changes in Bacillus subtilis.* Mol Syst Biol, 2013. **9**: p. 1-13.
73. Kikuchi, G., et al., *Glycine cleavage system: reaction mechanism, physiological significance, and hyperglycinemia.* Proc Jpn Acad Ser B Phys Biol Sci, 2008. **84**: p. 246-263.

74. Baker, M.A., H.M. Valett, and C.N. Dahm, *Organic Carbon Supply and Metabolism in a Shallow Groundwater Ecosystem.* Ecology, 2000. **81**(11): p. 3133-3148.
75. Aiken, G., *Organic Matter in Ground Water*. 2002: Artificial Recharge Workshop Proceedings open file report 02–89 (ed US Geological Survey). p. 21-23.
76. Baker, A. and R.G. Spencer, *Characterization of dissolved organic matter from source to sea using fluorescence and absorbance spectroscopy.* Sci Total Environ, 2004. **333**(1-3): p. 217-232.
77. Graham, P.W., A. Baker, and M.S. Andersen, *Dissolved Organic Carbon Mobilisation in a Groundwater System Stressed by Pumping.* Sci Rep, 2015. **5**: p. 1-12.
78. Lendenmannt, U. and T. Egli, *Is Escherichia coli growing in glucose-limited chemostat culture able to utilize other sugars without lag?* Microbiology, 1995. **141**: p. 71-78.
79. Born Timothy L. and B.J. S., *Structure/function studies on enzymes in the diaminopimelate pathway of bacterial cell wall biosynthesis.* Current Opinion in Chemical Biology, 1999. **3**: p. 607-613.
80. Laboratories, K., *Lysine biosynthesis - Reference pathway*. 2020.
81. Holger Ludwig, et al., *Transcription of glycolytic genes and operons in Bacillus subtilis: evidence for the presence of multiple levels of control of the gapA operon.* Molecular Microbiology, 2001. **41**: p. 409-422.
82. Laboratories, K., *Citrate cycle (TCA cycle) - Bacillus subtilis subsp. spizizenii W23*. 2020, Kanehisa Laboratories.
83. Gorke, B. and J. Stülke, *Carbon catabolite repression in bacteria: many ways to make the most out of nutrients.* Nat Rev Microbiol, 2008. **6**(8): p. 613-624.
84. Lopez, D., et al., *Cannibalism enhances biofilm development in Bacillus subtilis.* Mol Microbiol, 2009. **74**(3): p. 609-618.
85. González-Pastor J. E., Hobbs E. C., and L. R., *Cannibalism by sporulating bacteria.* Science, 2003. **301**: p. 510-513.
86. Zhu, B. and J. Stülke, *SubtiWiki in 2018: from genes and proteins to functional network annotation of the model organism Bacillus subtilis.* Nucleic Acids Res, 2018. **46**(D1): p. 743-748.
87. Zhu, B. and J. Stülke, *SigE Regulon*.
88. Zhu, B. and J. Stülke, *SigL Regulon*.

Abbreviations

%	per centum (Latin) – percent; parts per hundred
°C	degree Celsius
Ac-CoA	acetyl coenzyme A
AKG	alpha-ketoglutarate
Ala	alanine
Asp	aspartate
B. subtilis	*Bacillus subtilis*
$CaCl_2$	calcium chloride
Cit	citrate
CO_2	carbon dioxide
$CoCl_2$	cobalt(II) chloride
conc.	concentration
$CuCl_2$	copper(II) chloride
DAD	Diode Array Detector
DAP	diaminopimelic acid
DNA	deoxyribonucleic acid
DOC	dissolved organic carbon
DOM	dissolved organic matter
EA-IRMS	Elemental Analysis-Isotope Ratio Mass Spectrometry
et al.	et alii (Latin) – and others
$FeCl_3$	iron(III) chloride
Fum	fumarate
g; mg; µg	gram; milligram; microgram
G6P	glucose 6-phosphate
GAP	glyceraldehyde 3-phosphate
GC-MS	Gas Chromatography-Mass Spectrometry
Glc	glucose
Glu	glutamate
Gly	glycine
GTP	guanosine triphosphate
h; min; sec	hour; minute; second

H_2O	water
H_2SO_4	sulfuric acid
HCO_3^-	bicarbonate ion
His	histidine
HPLC	High Performance Liquid Chromatography
Ile	isoleucine
kDa	kilo dalton (dalton = unified atomic mass unit)
KH_2PO_4	potassium dihydrogen phosphate
L; mL; µL	litre; millilitre; microliter
Lac	lactate
Leu	leucine
LOD	Limit Of Detection
Lys	lysine
m/ z	ratio of molecular/atomic mass to the charge number of the ion
M; mM	molar (1 mol/ L); millimolar
Mal	malate
Met	methionine
MFA	metabolic flux analysis
$MgSO_4$	magnesium sulphate
mm; µm; nm	millimetre; micrometre; nanometre
$MnCl_2$	manganese(II) chloride
N_2	nitrogen
Na_2HPO_4	disodium hydrogen phosphate
Na_2MoO_4	sodium molybdate
NaCl	sodium chloride
NADH	nicotinamide adenine dinucleotide
NADPH	Nicotinamide adenine dinucleotide phosphate
$NaHCO_3$	sodium bicarbonate
NH_4^+	ammonium cation
NH_4Cl	ammonium chloride
NMR	Nuclear Magnetic Resonance
NO_2^-	nitrite ion
NO_3^-	nitrate ion
NO_x	nitrogen oxides

ns	not significant
O_2	oxygen
OD	Optical Density
Oxa	oxaloacetate
PC	pyruvate carboxylase
PEP	phosphoenolpyruvate
Phe	phenylalanine
PO_4^{3-}	phosphate ion
Pro	proline
PRPP	phosphoribosyl pyrophosphate
Pyr	pyruvate
RID	Refractive Index Detector
RNA	ribonucleic acid
rpm	rounds per minute
RT	retention time
Ser	serine
SIM	selected ion monitoring
Suc	succinate
TBDMS-	*tert*-Butyldimethylsilyl-
TCA cycle	tricarboxylic acid cycle
Thr	threonine
Tyr	tyrosine
Val	valine
$ZnCl_2$	zinc(II) chloride

Appendix

A1 Calculation of the label dilution

Detailed calculations of the carbon use efficiency (CUE), the dilution of the ^{13}C-label and the t-test for growth of *B. subtilis* W23 on glucose, lactate and malate:

Excel file *F1 CUE, biomass_Glc_SI Paper*

Excel file *F2 CUE, biomass_Lac_SI Paper*

Excel file *F3 CUE, biomass_Mal_SI Paper*

Excel file *F4 Calculation 13C bicarbonate dilution_SI Paper*

Excel file *F5 m+1 and ratio of label_SI Paper*

<u>Calculation of the label dilution caused by the production of unlabelled bicarbonate</u>

The ratio of ^{13}C-bicarbonate to unlabelled bicarbonate was calculated at each sampling time point taking into account the uptake of $H^{13}CO_3^-$ and production of unlabelled bicarbonate. To this end, the substrate consumption data were used together with a carbon use efficiency (CUE) of 47 %, 44 % or 34 % (for growth on glucose, lactate or malate, respectively) for *B. subtilis* W23 (Fig. S1 and Excel files F1, F2 and F3). Until 7 h (Glc), 12 h (Lac) or 6 h (Mal), respectively, after inoculation, the concentration of $H^{13}CO_3^-$ exceeded the concentration of unlabelled bicarbonate, which led to a constant increase of the ^{13}C-content in the bacterial biomass. After that, unlabelled bicarbonate dominated over $H^{13}CO_3^-$ leading to the slight decline in the ^{13}C-content of the biomass.

The detailed calculations can be found in the following Excel file: *F4 Calculation 13C bicarbonate dilution_SI Paper*

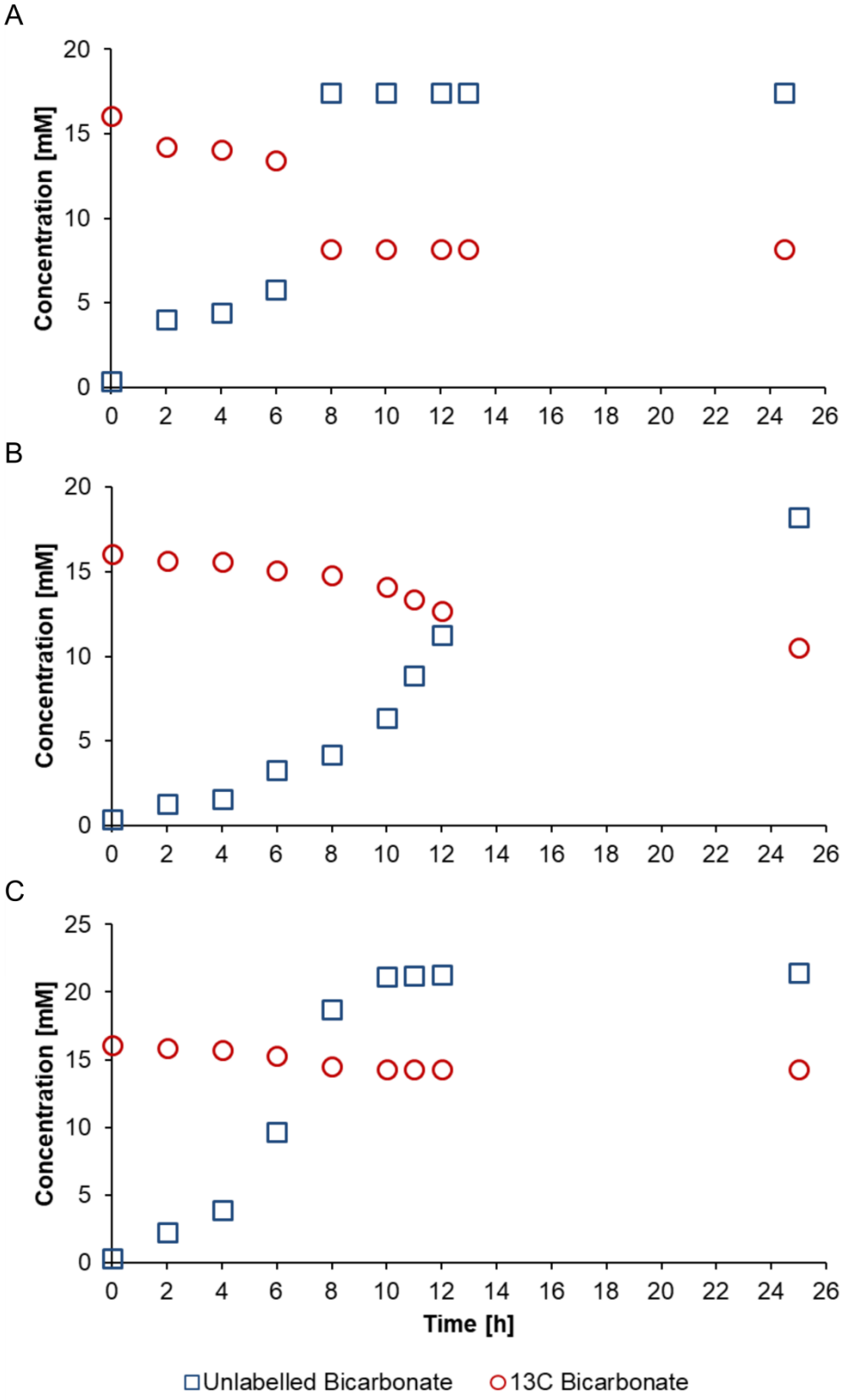

Figure S1: ^{13}C-Bicarbonate consumption vs. unlabelled bicarbonate production when growing on glucose (A), lactate (B) or malate (C), respectively, as the organic carbon source. Decreasing concentrations of ^{13}C-bicarbonate, as calculated from substrate consumption data and the CUE, are depicted as red circles. The evolution of unlabelled bicarbonate *via* respiration of unlabelled glucose, lactate or malate, respectively – also calculated from substrate consumption data and the CUE – is shown by blue squares.

A2 Lactate and malate experiments

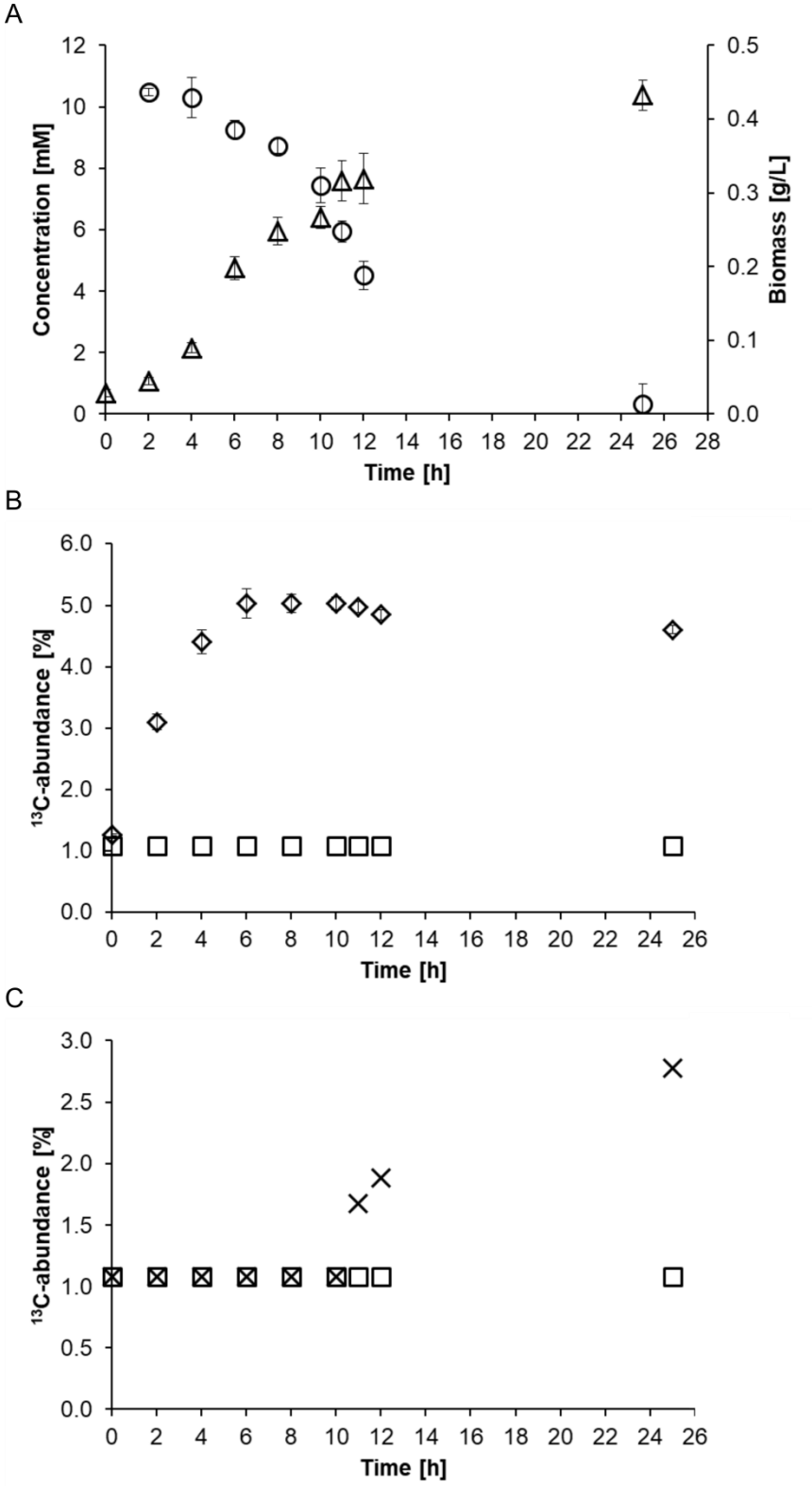

Figure S2: (A) Lactate consumption and biomass production by *B. subtilis* W23 growing in M9 medium containing 1 g/L lactate. The circles represent the lactate concentration and the triangles the biomass production over time. **(B) Incorporation of ^{13}C-carbon into microbial biomass by *B. subtilis* W23 growing in M9 medium containing 1 g/L lactate and 1 g/L $NaH^{13}CO_3^-$.** The diamonds represent the ^{13}C-incorporation into the

biomass as determined by EA-IRMS measurements. The depicted values are mean values of three biological replicates. The squares represent the control experiment conducted with unlabelled bicarbonate which shows the natural abundance of ^{13}C-carbon of 1.1 % in the environment. **(C) Incorporation of ^{13}C-carbon into microbial biomass by *B. subtilis* W23 growing in M9 lactate medium containing 1 g/L $NaH^{13}CO_3^-$ during the stationary phase.** The culture was supplied with the tracer 10 h after inoculation. The ^{13}C-abundance of the biomass (depicted as crosses) increased up to 3 %. In a control experiment, no $H^{13}CO_3^-$ was added. The ^{13}C-abundance of the biomass (depicted as squares) again mirrored the natural abundance of ^{13}C-carbon in the environment.

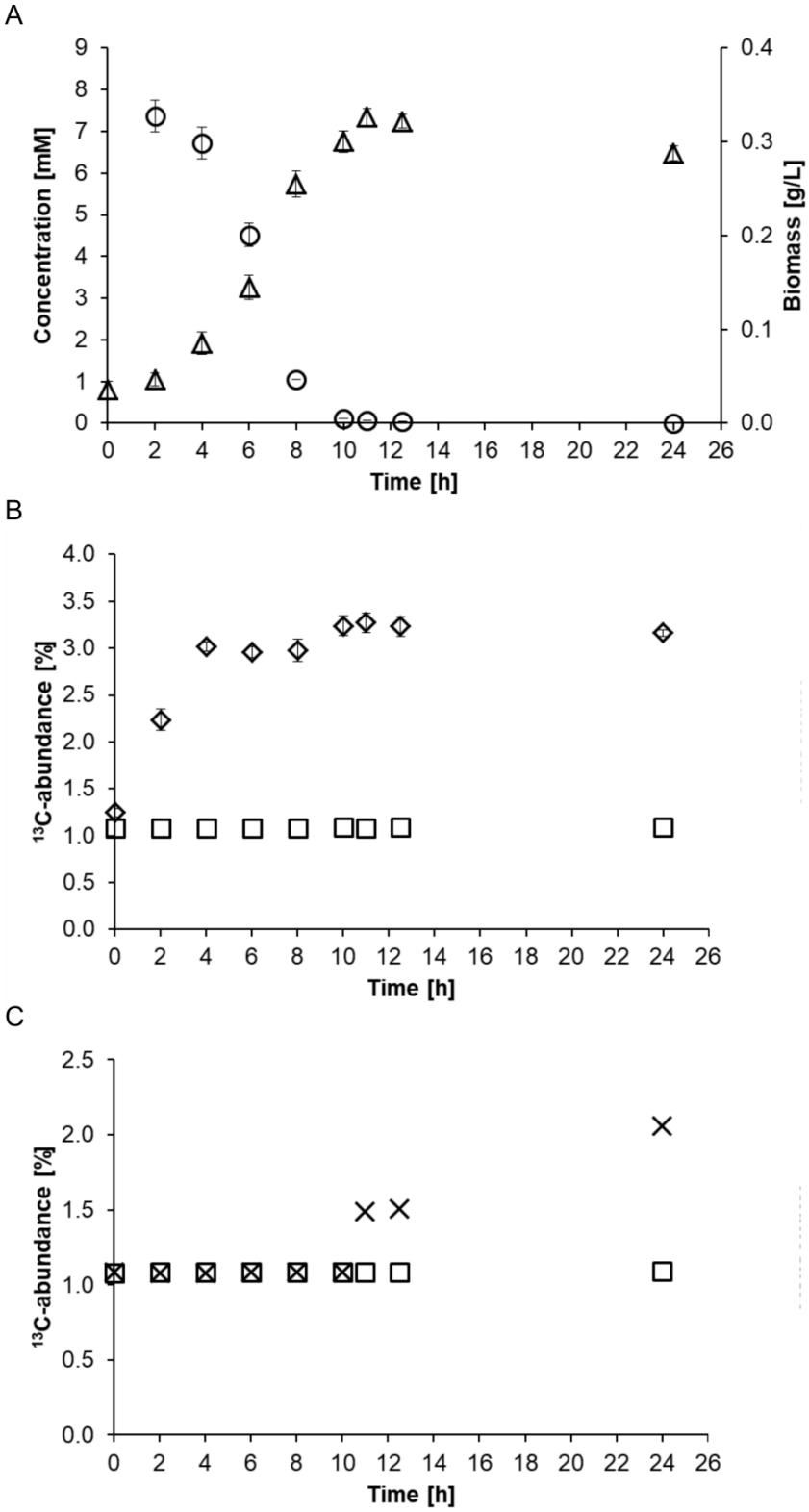

Figure S3: (A) Malate consumption and biomass production by *B. subtilis* W23 growing in M9 medium containing 1.1 g/L malate. The circles represent the malate concentration and the triangles the biomass production over time. **(B) Incorporation of ^{13}C-carbon into microbial biomass by *B. subtilis* W23 growing in M9 medium containing 1.1 g/L malate and 1 g/L $NaH^{13}CO_3^-$.** The diamonds represent the ^{13}C-incorporation into the biomass as determined by EA-IRMS measurements. The depicted values are mean values of three biological replicates. The squares represent the control experiment conducted with

unlabelled bicarbonate which shows the natural abundance of ^{13}C-carbon of 1.1 % in the environment. **(C) Incorporation of ^{13}C-carbon into microbial biomass by *B. subtilis* W23 growing in M9 malate medium containing 1 g/L $NaH^{13}CO_3^-$ during the stationary phase.** The culture was supplied with the tracer 10 h after inoculation. The ^{13}C-abundance of the biomass (depicted as crosses) increased up to 2 %. In a control experiment, no $H^{13}CO_3^-$ was added. The ^{13}C-abundance of the biomass (depicted as squares) again mirrored the natural abundance of ^{13}C-carbon in the environment.

A3 Retention times and fragmentation patterns of the detected amino acids

Table T1 Retention times and fragmentation patterns of the detected amino acids

RT [min]	Metabolite	$[m-57]^+$	$[m-85]^+$	$[m-159]^+$
11.5	**Ala**	**260.1** 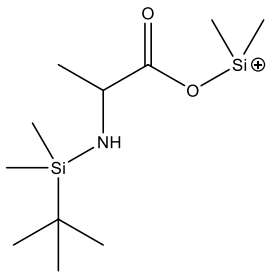 *<u>SIM-Ions:</u>* *259.1 – 264.1*	**232.2** 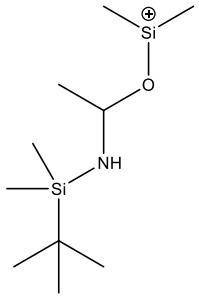 *<u>SIM-Ions:</u>* *231.2 – 235.2*	**158.1** 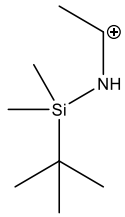 *<u>SIM-Ions:</u>* *157.1 – 161.1*
11.8	**Gly**	**246.1** 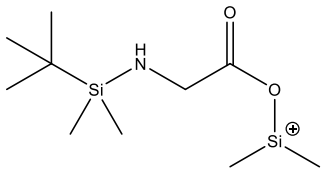 *245.1 – 249.1*	**218.1** 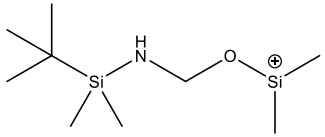 *217.1 – 220.1*	

13.2	**Val**	**288.2** 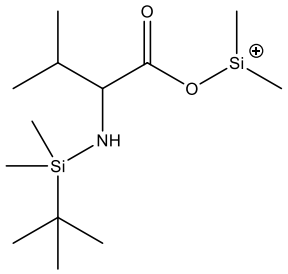 *287.2 – 294.2*	**260.2** 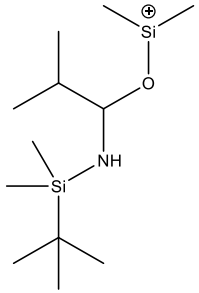 *259.2 – 265.2*	**186.2** 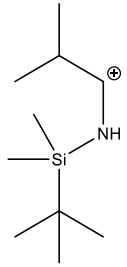 *185.2 – 191.2*
13.8	**Leu**	**302.2** 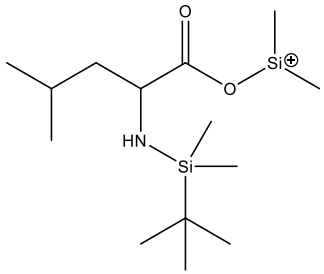 *301.2 – 309.2*	**274.2** 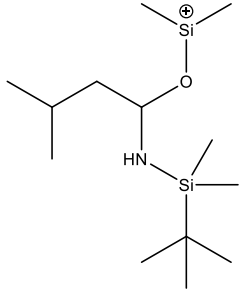 *273.2 – 280.2*	**200.2** 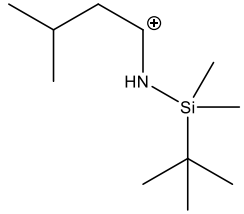 *199.2 – 206.2*

14.2	**Ile**	**302.2** 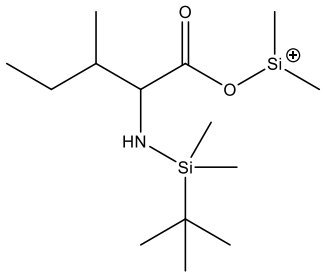 *301.2 – 309.2*	**274.2** 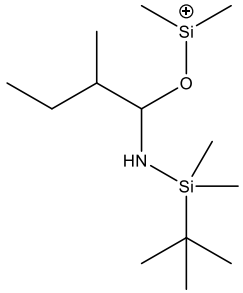 *273.2 – 280.2*	**200.2** 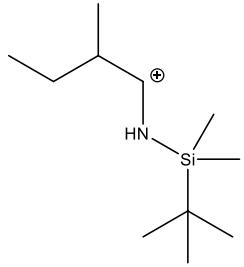 *199.2 – 206.2*
14.8	**Pro**	**286.2** 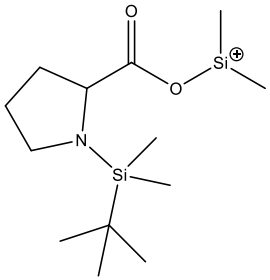 *285.2 – 292.2*	**258.2** 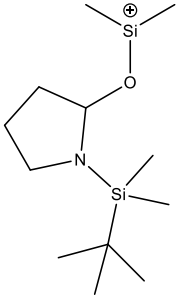 *257.2 – 263.2*	**184.2** 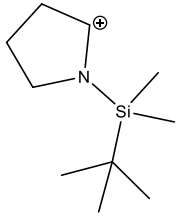 *183.2 – 189.2*

17.2	**Met**	**320.2** 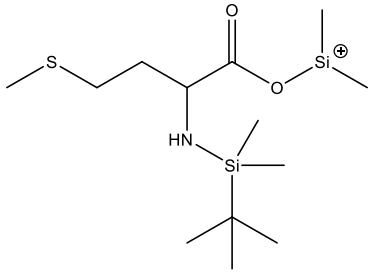 *319.2 – 325.2*	**292.1** 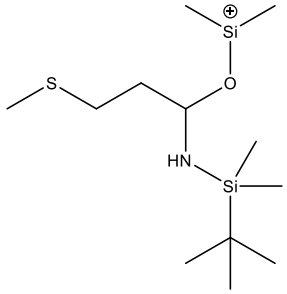 *291.1 – 297.1*	**218.1** 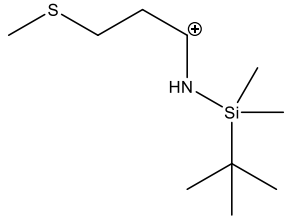 *217.1 – 223.1*
17.6	**Ser**	**390.2** 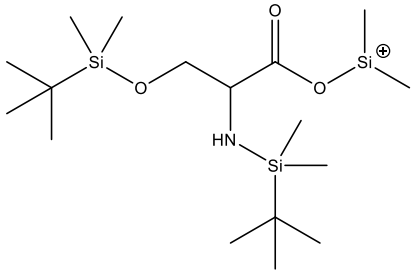 *389.2 – 394.2*	**362.2** 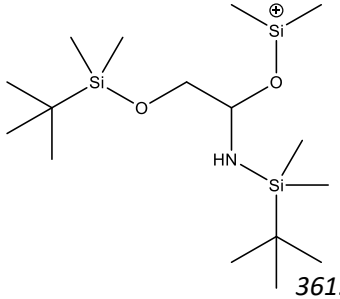 *361.2 – 365.2*	**288.2** 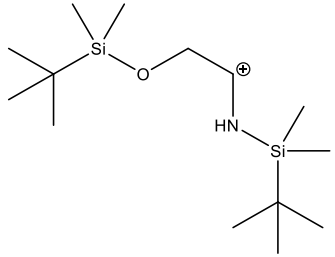 *287.2 – 291.2*

18.1	**Thr**	**404.2** 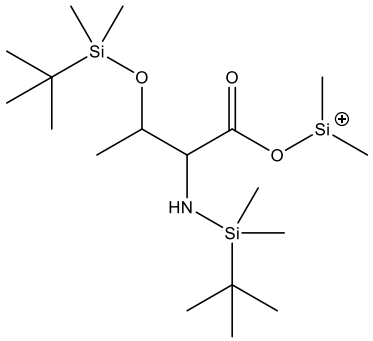 *403.2 – 409.2*	**376.3** 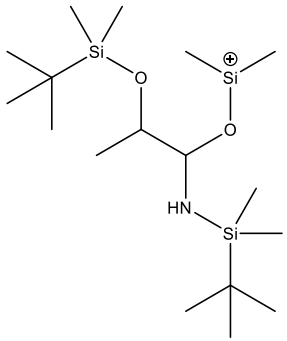 *375.3 – 380.3*	**302.2** 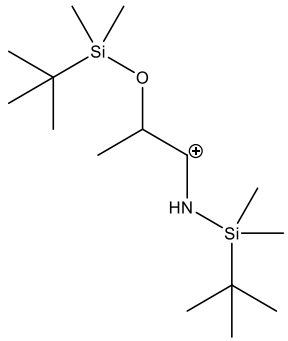 *301.2 – 306.2*
18.9	**Phe**	**336.2** 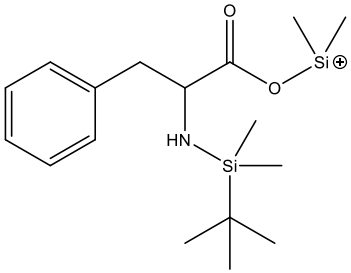 *335.2 – 346.2*	**308.2** 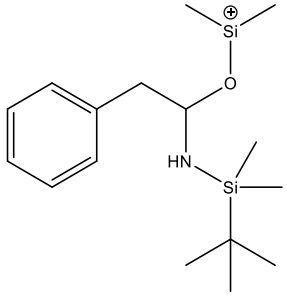 *307.2 – 317.2*	**234.2** 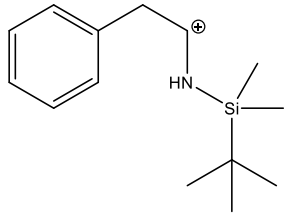 *233.2 – 243.2*

19.6	**Asp**	**418.2** 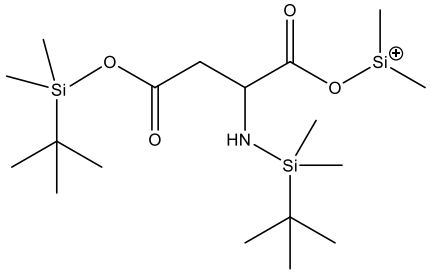 *417.2 – 423.2*	**390.2** 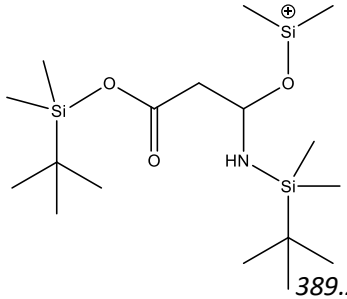 *389.2 – 394.2*	**316.2** 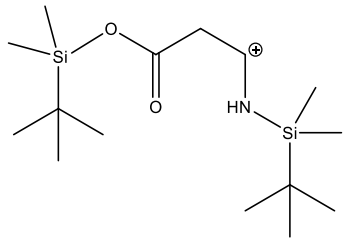 *315.2 – 320.2*
21.0	**Glu**	**432.2** 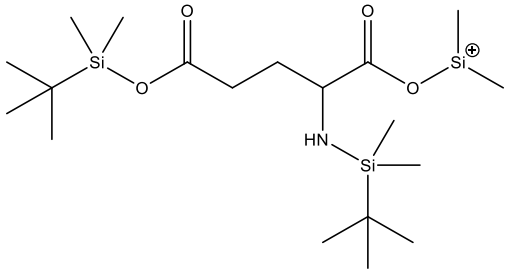 *431.2 – 438.2*	**404.2** 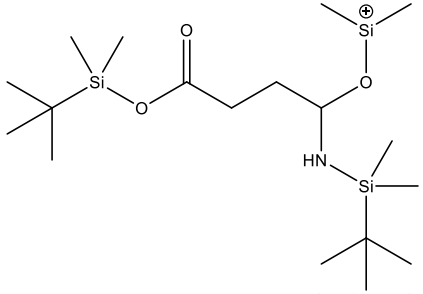 *403.2 – 409.2*	**330.2** 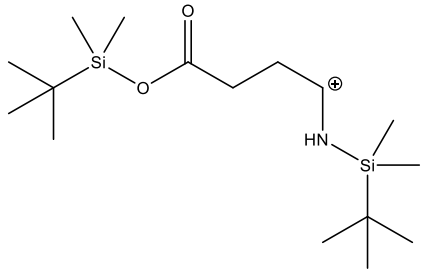 *329.2 – 335.2*

22.2	**Lys**	**431.3** 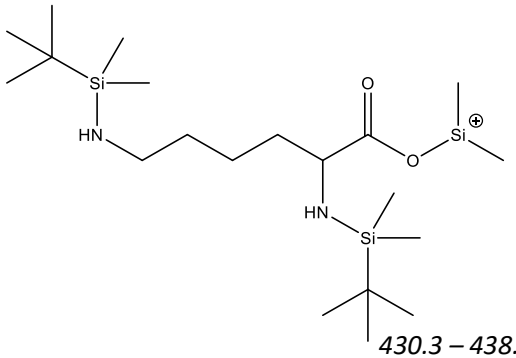 *430.3 – 438.3*	**403.3** 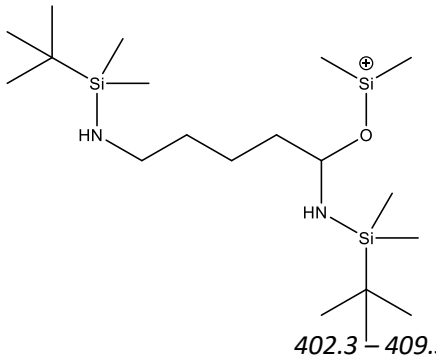 *402.3 – 409.3*	**329.3** 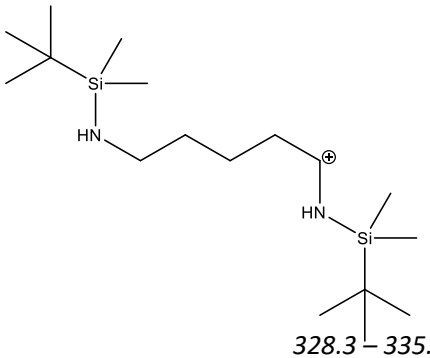 *328.3 – 335.3*
24.7	**His**	**440.3** 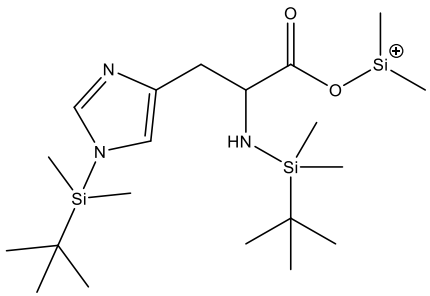 *439.3 – 447.3*	**412.3** 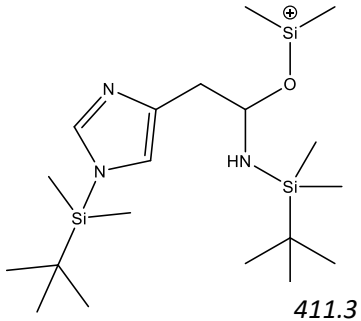 *411.3 – 418.3*	**338.2** 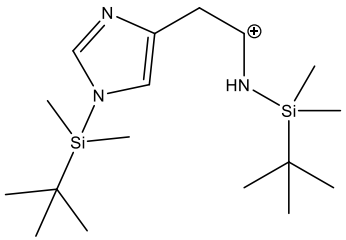 *337.3 – 344.3*

25.4	**Tyr**	**466.3** 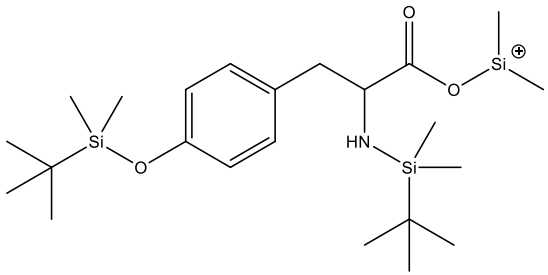 *465.3 – 476.3*	**438.3** 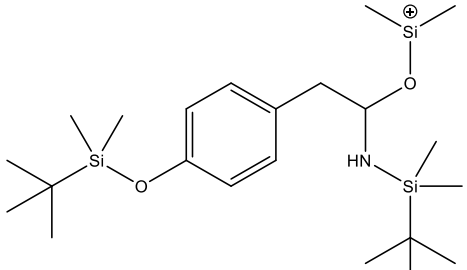 *437.3 – 447.3*	**364.2** 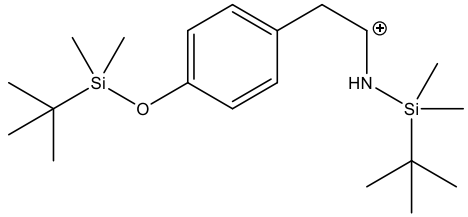 *363.2 – 373.2*

A4 Paper *Substrate-dependent CO_2 fixation in heterotrophic bacteria revealed by stable isotope labelling*

FEMS Microbiology Ecology, 96, 2020, fiaa080

doi: 10.1093/femsec/fiaa080
Advance Access Publication Date: 2 May 2020
Research Article

RESEARCH ARTICLE

Substrate-dependent CO_2 fixation in heterotrophic bacteria revealed by stable isotope labelling

Marina Spona-Friedl[1], Alexander Braun[1], Claudia Huber[2], Wolfgang Eisenreich[2,*], Christian Griebler[1,3], Andreas Kappler[4] and Martin Elsner[1,5,*,†]

[1]Institute of Groundwater Ecology, Helmholtz Zentrum München, Ingolstädter Landstr. 1, 85764 Neuherberg, Germany, [2]Chair of Biochemistry, Technische Universität München, Lichtenbergstr. 4, 85747 Garching, Germany, [3]Department of Functional and Evolutionary Ecology, Universität Wien, Althanstr. 14, A-1090 Wien, Austria, [4]Geomicrobiology, Eberhard-Karls-University Tuebingen, Sigwartstr. 10, 72076 Tuebingen, Germany and [5]Chair of Analytical Chemistry and Water Chemistry, Technische Universität München, Marchioninistr. 17, 81377 München, Germany

*Corresponding author: Chair of Analytical Chemistry and Water Chemistry, Technische Universität München, Marchioninistr. 17, 81377 München. Tel: +49 89 2180 78231, E-mail: m.elsner@tum.de and Chair of Biochemistry, Technische Universität München, Lichtenbergstr. 4, 85747 Garching, Germany. Tel: +49 89 289 13336, E-mail: wolfgang.eisenreich@mytum.de

One sentence summary: Incorporation of labelled carbon dioxide reveals what type of organic substrate (glucose, lactate, malate) the bacterium Bacillus subtilis utilises.

Editor: Lee Kerkhof

†Martin Elsner, http://orcid.org/0000-0003-4746-9052

ABSTRACT

Virtually all heterotrophs incorporate carbon dioxide by anaplerotic fixation. Little explored, however, is the interdependency of pathways and rates of CO_2 fixation on the concurrent usage of organic substrate(s). Potentially, this could reveal which substrates out of a pool of dissolved organic carbon are utilised by environmental microorganisms. To explore this possibility, *Bacillus subtilis* W23 was grown in a minimal medium with normalised amounts of either glucose, lactate or malate as only organic substrates, each together with 1 g/L $NaH^{13}CO_3$. Incorporation of $H^{13}CO_3^-$ was traced by elemental analysis-isotope ratio mass spectrometry of biomass and gas chromatography-mass spectrometry of protein-derived amino acids. Until the late logarithmic phase, ^{13}C incorporation into the tricarboxylic acid cycle increased with time and occurred via [4–^{13}C]oxaloacetate formed by carboxylation of pyruvate. The levels of ^{13}C incorporation were highest for growth on glucose and lowest on malate. Incorporation of ^{13}C into gluconeogenesis products was mainly detected in the lactate and malate experiment, whereas glucose down-regulated this path. A proof-of-principle study with a natural groundwater community confirmed the ability to determine incorporation from $H^{13}CO_3^-$ by natural communities leading to specific labelling patterns. This underlines the potential of the labelling approach to characterise carbon sources of heterotrophic microorganisms in their natural environments.

Keywords: heterotrophic CO_2 fixation; isotope labelling; organic substrate use; dissolved organic matter; bacterial substrate usage; isotope analysis

Received: 3 December 2019; Accepted: 30 April 2020

INTRODUCTION

Reductive carbon fixation under volcanic conditions played a key role in a potential chemoautotrophic origin of life (Huber et al. 2012), and CO_2 fixation by autotrophic organisms including plants is among the most important biosynthetic processes in the biosphere (Bassham and Calvin 1962; Giovannoni and Stingl 2005; Berg 2011; Fuchs 2011). However, the presence and diversity of carboxylating (CO_2-fixing) enzymes in nature are not restricted to autotrophs alone. Already 80 years ago, utilisation of CO_2 was reported for heterotrophic bacteria producing propionic acid (*Propionibacteria*) (Wood and Werkman 1936). Today, it is recognised that virtually all heterotrophic organisms—from microorganisms to humans—incorporate CO_2 via a variety of pathways involving at least 18 different carboxylases in the central and peripheral metabolism (Dijkhuizen and Harder 1985; Baltar et al. 2010; Erb 2011; Middelburg 2011). Among these enzymes, anaplerotic carboxylases incorporate CO_2 into biomass and replenish intermediates of the tricarboxylic acid (TCA) cycle, which are constantly withdrawn for the biosynthesis of amino acids and other metabolic products (Erb 2011). It is therefore not surprising that carbon from anaplerotic CO_2 incorporation accounts for a significant amount (i.e. 2–8%) of the cell's biomass carbon abundance (Romanenko 1964; Perez and Matin 1982; Doronia and Trotsenko 1985; Miltner et al. 2004; Roslev et al. 2004; Herndl and Reinthaler 2013).

Among the protein family of carboxylases, pyruvate carboxylase, an anaplerotic carboxylase, catalyses the bicarbonate (HCO_3^-)-dependent conversion of pyruvate into oxaloacetate. As a component of a putative ancestral reverse TCA cycle, the enzyme is also present in chemolitho-autotrophic bacteria (Giovannelli et al. 2017), which are considered as one of the most ancient forms of life. The reaction of pyruvate carboxylase could therefore represent a metabolic feature that goes back to the early evolution of life (Lombard and Moreira 2011).

The enzyme is widely distributed across the three kingdoms of life and has also been retained in many heterotrophic organisms including the Gram-positive bacterium *Bacillus subtilis* W23. Generally, pyruvate carboxylase occupies a vital position in the central carbon metabolism, since it is located at the 'phosphoenolpyruvate-pyruvate-oxaloacetate node' (Attwood 1995; Owen, Kalhan and Hanson 2002; Jitrapakdee et al. 2008). This metabolic hub unites structurally entangled reactions that interconnect the major pathways of carbon metabolism, i.e. glycolysis (catabolism), gluconeogenesis (anabolism) and the TCA cycle (energy supply of the cell) (Sauer and Eikmanns 2005). However, the direction of the carbon fluxes at this metabolic hub (towards catabolism, anabolism or energy supply) primarily depends on the type of the available dissolved organic carbon (DOC) and it can be expected that the amount of incorporated CO_2 (or $^{13}CO_2/H^{13}CO_3^-$ in tracer experiments, respectively) varies even within the same organism depending on the assimilated organic carbon source (Romanenko 1964; Perez and Matin 1982; Doronia and Trotsenko 1985; Miltner et al. 2004; Roslev et al. 2004). Given a typical metabolic network of a heterotrophic organism capable of carrying out the reaction of pyruvate carboxylase using $H^{13}CO_3^-$ as a substrate, the following simplified scenarios A–C may be distinguished (Fig. 1).

Scenario A: During growth on carbohydrates like glucose (Glc), the glycolytic flux constantly produces pyruvate (Pyr), which is further oxidised to acetyl coenzyme A (Ac-CoA). Ac-CoA requires oxaloacetate (Oxa) to form citric acid (Cit) in the first reaction of the TCA cycle. The TCA cycle serves, on the one hand, to catabolise substrates to CO_2. On the other hand, intermediates of the TCA cycle are used as building blocks for biosynthesis. Hence, equivalents of Oxa are constantly withdrawn from the TCA cycle for the formation of Asp and related amino acids. Therefore, the pool of Oxa must be replenished to keep the cycle running. To this end, in *B. subtilis* W23, pyruvate carboxylase directly converts Pyr to Oxa via the addition of $H^{13}CO_3^-$. Consequently, TCA cycle metabolites and any products derived thereof, e.g. amino acids like Asp, Lys, Thr, Glu or Pro, are expected to carry this label from $H^{13}CO_3^-$.

Scenario B: When substrates such as lactate (Lac) enter the metabolic network somewhere between glycolysis and the TCA cycle, Oxa must also be replenished via the reaction catalysed by pyruvate carboxylase, in the same way as in the first scenario. In this case, however, also gluconeogenesis via Oxa and phosphoenolpyruvate (PEP) would be expected to become active in order to satisfy the need of the organism for glucose and its derivatives (e.g. for building up membranes and the cell wall of the Gram-positive bacterium). As a result, the ^{13}C-label from $H^{13}CO_3^-$ is expected not only in the metabolites and the products of the TCA cycle (like in the first scenario) but also in those derived from gluconeogenesis or the pentose phosphate pathway, such as Ser, Gly, His, Phe or Tyr.

Scenario C: When cells grow on TCA cycle intermediates like malate (Mal), the substrate directly replenishes the TCA cycle. Hence, Pyr carboxylation seems not to be necessary *per se* and central carbon metabolites are not expected to show ^{13}C incorporation in labelling experiments with $H^{13}CO_3^-$.

However, the assumption that heterotrophic fixation of CO_2/HCO_3^- depends on the organic substrate has not been fully exploited yet. This is surprising since this dependency also has the potential to assign the main carbon source that is utilised by heterotrophic microorganisms. Our study aims to close this gap of knowledge by investigating $H^{13}CO_3^-$ incorporation into *B. subtilis* W23, a well-known model for a heterotrophic bacterium, during growth on glucose, lactate and malate, respectively. These carbon substrates are indicative of the three different entry points to the central carbon metabolism as depicted in the simplified scenarios in Fig. 1. Additionally, these substrates also represent naturally occurring components in soil and DOC (Šantrůčková et al. 2005; Kleijn et al. 2010; Gleixner 2013).

To assess and to quantify ^{13}C incorporation from $H^{13}CO_3^-$ in our experiments, we used ^{13}C-based metabolic pathway/flux analysis as a key method (Heux et al. 2017; Nielsen 2017). Using this technology, carbon from $^{13}CO_2/H^{13}CO_3^-$ can be traced back through the metabolic network of the organism under study. On this basis, not only mechanisms of CO_2 fixation but also downstream fluxes via the TCA cycle or gluconeogenesis into metabolic products can be reconstructed on a functional and quantitative basis as shown earlier for plants (Cegelski and Schaefer 2006; Römisch-Margl et al. 2007; Schramek et al. 2010; Ishihara et al. 2015; Bacher, Chen and Eisenreich 2016) or microorganisms (Johnson and Romanenko 1984; Miltner et al. 2004; Roslev et al. 2004; Hesselsoe et al. 2005; Miltner et al. 2005; Alonso-Saez et al. 2010; Wegener et al. 2012). Indeed, the latter experiments also pointed at the crucial role of CO_2 fixation in heterotrophic environmental microbes (Šantrůčková et al. 2005; Alonso-Saez et al. 2010; DeLorenzo et al. 2012; Yakimov et al. 2014).

In the present study with *B. subtilis* W23, $H^{13}CO_3^-$-labelling experiments were monitored by elemental analysis-isotope

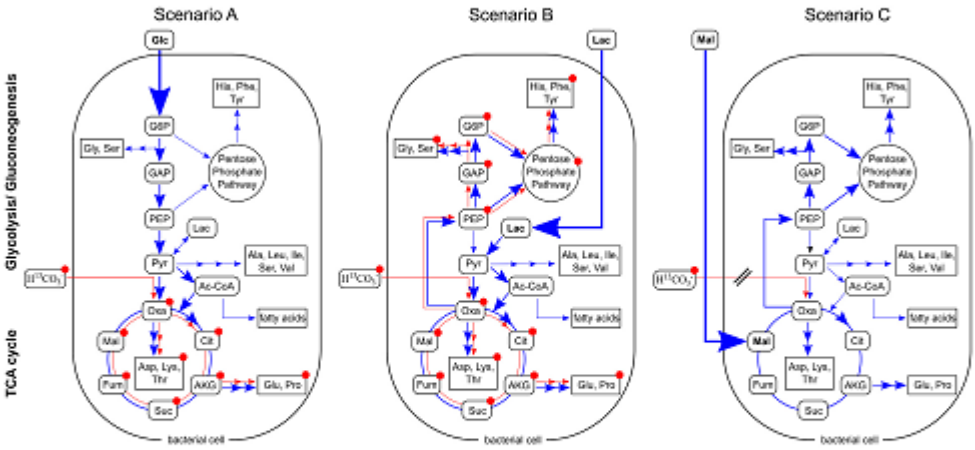

Figure 1. Metabolic routes of ^{13}C-labelled bicarbonate after anaplerotic fixation during growth on different substrates. Scenarios A, B and C show the expected labelling patterns from $H^{13}CO_3^-$ when using unlabelled glucose (Glc), lactate (Lac) or malate (Mal) as main organic carbon substrates. The bold arrows indicate main carbon fluxes. Red arrows show the respective fluxes from the supplied $H^{13}CO_3^-$ tracer through the metabolic network; blue arrows depict the carbon fluxes from the unlabelled organic substrates, respectively. Metabolites and products marked with a red circle are expected to receive ^{13}C-label originating from $H^{13}CO_3^-$.

ratio mass spectrometry (EA-IRMS) of total biomass and by gas chromatography-mass spectrometry (GC-MS) of amino acids to show an example of how to assign main (unlabelled) organic substrates on this basis. Subsequently, $H^{13}CO_3^-$-labelling experiments with a natural microbial community from groundwater were conducted to provide a proof of principle that this approach indeed opens a new avenue to elucidate substrate usages in complex environmental samples.

MATERIALS AND METHODS

Strain and growth conditions

All experiments were performed with *B. subtilis* subsp. *spizizenii* W23 (DSM No.: 6395), a prototrophic derivative of the wild type, obtained from DSMZ (Leibnitz Institute DSMZ—German Collection of Microorganisms and Cell Cultures, Braunschweig, Germany). For pre-cultivation, 5 mL of M9 minimal growth medium, supplemented with 1 g/L glucose, 1 g/L lactate or 1.1 g/L malate, respectively, and preheated to 30°C, were inoculated with 300 µL of a glycerol stock solution of the bacterium. The amounts of organic substrates were chosen in order to ensure that the amount of carbon available to the bacteria (0.4 g/L) was the same in all three set-ups. The pre-cultures were incubated for 20 h. In order to prevent the formation of biofilms, the culture tubes were shaken vigorously at 300 rpm on an orbital incubation shaker (IKA KS 4000i control, IKA-Werke, Staufen, Germany). Each pre-culture was used to inoculate 195 mL of M9 minimal growth medium, preheated to 30°C, in 500 mL Schott bottles. The M9 minimal growth medium was a mixture of 165 mL of M9 minimal medium, 20 mL of a 10 g/L glucose, 10 g/L lactate or 11 g/L malate stock solution, respectively, and 10 mL of a 20 g/L sodium bicarbonate stock solution. The bicarbonate was either $NaH^{13}CO_3$ (98 atom% ^{13}C, Sigma Aldrich, Darmstadt, Germany) in the ^{13}C-labelling experiments or unlabelled $NaHCO_3$ (1.1% natural ^{13}C-abundance, Sigma Aldrich, Darmstadt, Germany) in the control experiments. The bottles were closed gastight after inoculation to block the release of $^{13}CO_2$. To avoid depletion of O_2, an aliquot of fresh air (filter-sterilised using a 0.22-µm syringe filter) that equals the volume of a taken sample was added at every time point of sampling. The cultivations were performed at 30°C and 150 rpm on an orbital incubation shaker.

The M9 minimal growth medium consisted of the following components (per litre): 8.5 g of $Na_2HPO_4 \cdot 2\,H_2O$, 3 g of KH_2PO_4, 1 g of NH_4Cl and 0.5 g of NaCl (= base salts solution). The following components were autoclaved separately before being added to the base salts solution in the given order (per litre): 1 mL of 0.1 M $CaCl_2$, 10 mL trace salts stock solution, 1 mL of 1 M $MgSO_4$ and 1 mL of 50 mM $FeCl_3 \cdot 6\,H_2O$ (filter-sterilised using a 0.22-µm syringe filter). The trace salts stock solution contained (per litre): 100 mg of $MnCl_2 \cdot 4\,H_2O$, 170 mg of $ZnCl_2$, 43 mg of $CuCl_2 \cdot 2\,H_2O$, 60 mg of $CoCl_2 \cdot 6\,H_2O$ and 60 mg of $Na_2MoO_4 \cdot 2\,H_2O$. The glucose, lactate, malate and sodium bicarbonate stock solutions were filter-sterilised, using a 0.22-µm syringe filter, before being added to the medium. All solutions were prepared using sterilised MilliQ water. All chemicals were purchased from Sigma Aldrich (Darmstadt, Germany).

^{13}C-Labelling experiments and microbial dry weight

Bacillus subtilis subsp. *spizizenii* W23 was grown in M9 minimal growth medium supplemented with 1 g/L glucose, 1 g/L lactate or 1.1 g/L malate, respectively, and 1 g/L sodium bicarbonate. The ^{13}C-labelling experiments were conducted in triplicates and the control experiments with unlabelled bicarbonate in duplicates. After 10 h of incubation, one control experiment was spiked with sodium ^{13}C-bicarbonate (1 g/L); the second control experiment remained untouched. Bacterial growth was monitored by determining the optical density at 600 nm (OD_{600}). Samples for biomass and amino acid analysis were taken at intervals of 2 h after inoculation. At each of these time points, 20 mL of the bacterial culture was harvested by centrifugation

(4°C, 4000 rpm, 20 min). The supernatant was carefully removed, filter-sterilised, using a 0.22-µm syringe filter and stored at −20°C for high performance liquid chromatography (HPLC) analysis (see below). The cell pellet was re-suspended in 2 mL of sterile MilliQ water and transferred into an Eppendorf tube. After this washing step, a second centrifugation step (4°C, 14 000 rpm, 20 min) pelleted the cells again. The supernatant was carefully discarded and the pellet was frozen at −80°C. The frozen pellets were freeze-dried overnight using a VirTis Sentry 8 L benchtop freeze dryer (SP Industries, Warminster, PA, USA). The freeze-dried bacterial pellets were weighed using a high-resolution balance (CP2P, Sartorius AG, Göttingen, Germany) to determine the microbial dry weight.

Testing of the $H^{13}CO_3^-$ method with a microbial groundwater community

Natural oligotrophic and oxic groundwater samples were collected from a shallow unconsolidated quaternary aquifer composed of fluvio-glacial carbonate gravel and sands at Neuherberg/Munich, Germany. The freshly collected groundwater contained 1.5 ± 0.2 mg/L DOC, 1.5 ± 0.15 mg/L nitrate (NO_3^-) and ~15 µg/L phosphate (PO_4^{3-}), whereas the concentrations of nitrite (NO_2^-) and ammonium (NH_4^+) were below the detection limit of ion chromatography (LOD of 0.1 mg/L) (Dionex ICS-1100; Thermo Fisher Scientific, Bremen, Germany): 200 µL of the filter-sterilised samples were analysed to determine the concentrations of the nutrients. A stock solution of an organic fertiliser (DOC content 300 mg/L) was prepared by dissolving the lyophilised substrates at a pH of 9 in ultrapure water, followed by a neutralisation and a centrifugation step. The supernatant was filter-sterilised using a 0.22-µm syringe filter. The organic fertiliser was mainly composed of humic substances of varying molecular size (PhytoGreen®-HumusWP, PhytoSolution, Freyburg, Germany).

Each of two bottles with 400 mL groundwater were loaded with 30 and 50 mL, respectively, of the organic fertiliser, spiked with 1 g/L ^{13}C-sodium bicarbonate ($NaH^{13}CO_3$, 98 atom% ^{13}C, Sigma Aldrich, Darmstadt, Germany) and closed with a screw cap. The bottles were incubated in the dark at room temperature for 52 days (13 September 2018–3 November 2018) and gently mixed once a week. Growth of the bacterial groundwater community was monitored by optical density measurements at 595 nm.

To enhance biomass yield, the two bottles were combined (on 3 November 2018), filled with fresh groundwater to a volume of 1000 mL and supplemented with 25 mL of a soil extract, which was prepared from a dark conifer forest soil by solvent extraction: soil from a coniferous wood was extracted with ultrapure water on a stirrer in darkness at 37°C overnight. The extract was filter-sterilised using a 0.22-µm syringe filter to remove microbes. The DOC content of the sterile soil extract stock solution was 100 mg/L. On 20 December 2018, the bottle was again loaded with 25 mL sterile soil extract. Bacterial growth was monitored by optical density measurements at 595 nm.

The experiment was ended on 18 January 2019 by sacrificing the whole bottle via centrifugation. Biomass was concentrated using centrifugal filter units (30 kDa cut-off; Amicon® Ultra-15, Sigma Aldrich, Darmstadt, Germany) to a final volume of 2 mL. The sample was frozen at −80°C and freeze-dried overnight to remove the residual water.

Protein hydrolysis and amino acid derivatisation

For protein hydrolysis, ~0.5 mg of the freeze-dried bacterial pellet was mixed with 500 µL of 6 M hydrochloric acid and heated at 105°C for 24 h. After cooling to 70°C, the residual hydrochloric acid was removed by a constant stream of nitrogen gas. The dried sample was then re-suspended in 50% glacial acetic acid by sonication for 120 s. A small column (1 mL pipet tip) of the cation exchanger Dowex 50WX8 [200–400 mesh (= 37–74 µm), H^+ form] was prepared and washed with 1 mL of methanol followed by 1 mL of MilliQ water. After loading the sample onto the column, it was washed twice with 1 mL of MilliQ water. The bound amino acids were then eluted from the column by 1 mL of 4 M ammonium hydroxide. An aliquot of the eluate was dried under a constant stream of nitrogen gas at 70°C. The dry residue was dissolved in 50 µL of water-free acetonitrile and 50 µL of *N*-(tert-butyldimethylsilyl)-*N*-methyl-trifluoroacetamide containing 1% tert-butyldimethylsilylchlorid. This mixture was kept at 70°C for 30 min. The resulting *N*-tert-butyldimethylsilyl derivatives of the amino acids (TBDMS-amino acid derivatives) were analysed by GC-MS following established protocols (Eylert *et al.* 2008).

Gas chromatography/mass spectrometry of silylated amino acids

GC-MS analysis was performed using a 7890A GC system (Agilent Technologies, Santa Clara, CA, USA) equipped with a fused silica capillary column (Equity TM-5; 30 m x 0.25 mm, 0.25-µm film thickness; Supelco, Bellefonte, PA, USA). The mass detector worked with electron impact ionisation at 70 eV. An aliquot (1–3 µL) of the solution containing the TBDMS-amino acid derivatives was injected in a 1:10 split mode. The interface temperature was set to 260°C. The column temperature was held at 140°C for 3 min, heated with a temperature gradient of 4°C/min to 165°C, heated with a second temperature gradient of 15°C/min to 200°C and heated with a third temperature gradient of 7°C/min to 280°C where the temperature was held for 3 min. Selected ion monitoring data were acquired using a 0.3-s sampling rate and the samples were analysed three times. Data collection was carried out via the GC-MSD Data Analysis software (Agilent Technologies, Santa Clara, CA, USA). The retention times and the detected mass fragments of the amino acids are listed in Table T1 in the Supporting Information. Incorporation of ^{13}C into amino acids was computed according to Lee *et al.* (1991). The steps include the determination of the contribution of the derivatisation reagent to the observed spectrum of the silylated amino acid and the correction for contribution from ^{13}C-carbon natural abundance using multiple linear regression analysis. The mass isotopomer distribution after this background subtraction provides fractional ^{13}C-excess values for amino acid isotopomers carrying one ^{13}C-carbon atom (M+1), two ^{13}C-carbon atoms (M+2), three ^{13}C-carbon atoms (M+3) and so on, where the sum over all isotopomers [M + (M+1) + (M+2) + (M+3) etc.] is defined as 100%. As an example, amino acids with an M+1 excess value of 50% are composed of 50% unlabelled molecules (M) and 50% molecules carrying one ^{13}C-carbon (M+1) from the ^{13}C-labelled precursor. Amino acids that carry at least one ^{13}C-carbon atom in excess are termed labelled amino acids in the following.

Carbon isotopic analysis of biomass

Carbon isotopic ratios were determined by an elemental analyser-isotope ratio mass spectrometer (EA-IRMS) consisting

of a EuroEA (Euro vector, Milano, Italy) coupled to a Finnigan MAT253 IRMS (Thermo Fisher Scientific, Bremen, Germany) by a Finnigan ConFlow III interface (Thermo Fisher Scientific, Bremen, Germany). For EA-IRMS analysis, a small amount of the freeze-dried pellet (100–400 µg) was put into tin capsules (3.3 × 5 mm; IVA Analysentechnik, Meerbusch, Germany) and subjected to elemental analysis by dropping them into a heated reactor that contained silvered cobalt oxide and chromium oxide (IVA Analysentechnik, Meerbusch, Germany and HEKA tech, Wegberg, Germany). The biomass pellets were combusted in a stream of O_2-containing He at 1000°C to produce N_2, NO_x, H_2O and CO_2, where NO_x was directly converted to N_2 again in an online reduction reactor filled with metallic copper filings. The gases were subsequently transferred to the isotope ratio mass spectrometer via a ConFlow III system using a continuous helium stream of 90 mL/min. The CO_2 reference gas was provided by CARBO (Bad Hönningen, Germany). The resulting values from EA-IRMS analysis include the natural abundance of ^{13}C-carbon.

Analysis of substrate consumption (HPLC)

The frozen, filter-sterilised supernatant was used for substrate consumption analysis by HPLC. Briefly, glucose, lactate and malate, respectively, were separated and quantified by HPLC using a ligand exchange Aminex HPX 87H column (300 × 7.8 mm) plus pre-column (30 × 4.6 mm) (Bio-Rad Laboratories GmbH, Feldkirchen, Germany). Aliquots of 20 µL were injected per run. The column oven was set to 40°C. The eluent was 5 mM H_2SO_4 at a flow rate of 0.6 mL/min. Glucose was detected using an RID-10A detector; lactate and malate were detected using the RID-10A and the DAD-SPD-M10Avp detector operating at 210 nm. The retention times of glucose, malate and lactate were 9.1, 9.9 and 12.8 min, respectively.

Statistical analysis

A two-tailed unpaired Student's t-test was used for the analysis of differences between the mean values of ^{13}C incorporation into selected pairs of amino acids from the experiments with glucose, lactate and malate. Statistical significance is depicted as ns = not significant, *$P < 0.05$, **$P < 0.01$ or ***$P < 0.001$.

RESULTS

Growth of *B. subtilis* in the presence of glucose and $H^{13}CO_3^-$

The growth experiment with *B. subtilis* W23 in M9 medium containing glucose and $H^{13}CO_3^-$ displayed the usages of both substrates over time for building up its biomass. The glucose concentration in the medium constantly decreased from 5.6 mM to below the analytical detection limit (3 mM in this set-up) at 8 h after inoculation (Fig. 2A). With declining substrate concentration, bacterial biomass increased from 0.03 to 0.44 g/L during the experiment until glucose became limiting. The ^{13}C-abundance of the biomass, as determined by EA-IRMS, steadily rose from 1.1% (natural abundance of ^{13}C-carbon) to a maximum of 6% at 6 h after inoculation (Fig. 2B). Then, the ^{13}C-abundance levelled off and stayed constant at ~5% until the end of the experiment. The control experiment with unlabelled HCO_3^- mirrored the natural abundance of ^{13}C-carbon (1.1%) in the environment. In the labelling experiment, the maximum of ^{13}C-abundance of 6% at 6 h and the subsequent decline to 5%

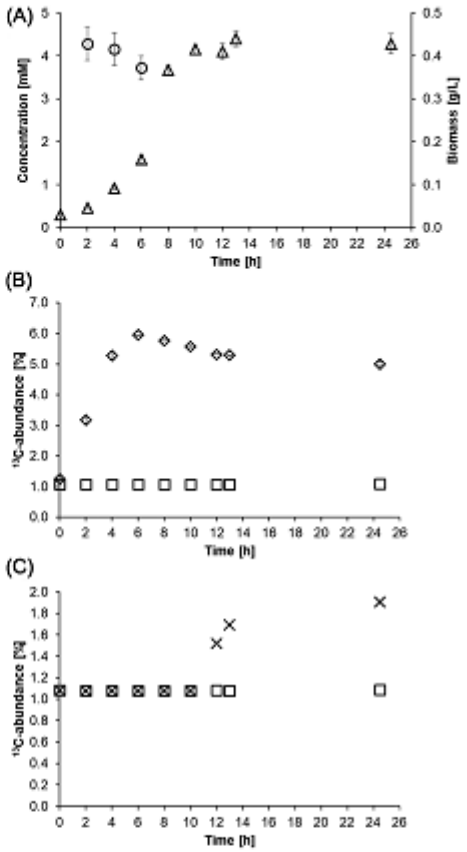

Figure 2. (A) Glucose consumption and biomass production by *B. subtilis* W23 growing in M9 medium containing 1 g/L glucose. The circles represent the glucose concentration and the triangles the biomass production over time. (B) Incorporation of ^{13}C-carbon into microbial biomass by *B. subtilis* W23 growing in M9 medium containing 1 g/L glucose and 1 g/L $NaH^{13}CO_3^-$. The diamonds represent the ^{13}C incorporation into the biomass as determined by EA-IRMS measurements. The depicted values are mean values of three biological replicates. The squares represent the control experiment conducted with unlabelled bicarbonate that shows the natural abundance of ^{13}C-carbon of 1.1% in the environment. (C) Incorporation of ^{13}C-carbon into microbial biomass by *B. subtilis* W23 growing in M9 glucose medium containing 1 g/L $NaH^{13}CO_3^-$ during the stationary phase. The culture was supplied with the tracer 10 h after inoculation. The ^{13}C-abundance of the biomass (depicted as crosses) increased up to 2%. In a control experiment, no $H^{13}CO_3^-$ was added. The ^{13}C-abundance of the biomass (depicted as squares) again mirrored the natural abundance of ^{13}C-carbon in the environment.

could be explained by the production of unlabelled CO_2 via respiration of unlabelled glucose, which led to the formation of unlabelled CO_2/bicarbonate in the medium as growth occurred. This production of unlabelled bicarbonate led over time to a dilution of the supplied $H^{13}CO_3^-$ as indicated by model calculations (see data files F1–F4 for details and Figure S1 in the Supporting Information). In addition, glucose became limiting so that microbial growth slowed down. Nevertheless, $H^{13}CO_3^-$ was still present

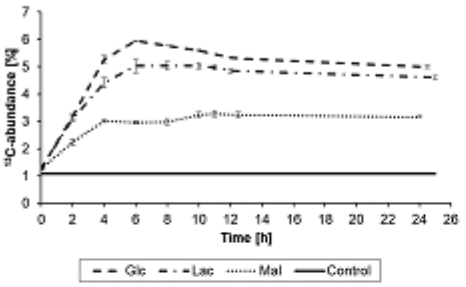

Figure 3. Incorporation of ^{13}C-carbon from $H^{13}CO_3^-$ into the biomass of B. subtilis W23 growing in M9 containing unlabelled glucose, lactate or malate as carbon sources, respectively. The control shows the natural abundance of ^{13}C-carbon. The depicted values are mean values of three biological replicates. The error bars represent the calculated standard deviation; in case of the control, the error bars are too small to be visible.

in the medium and was used by B. subtilis W23 for anaplerosis even during the stationary phase of growth finally leading to a stable ^{13}C-abundance of the bacterial biomass till the end of the experiment (Fig. 2B). Specifically, when ^{13}C-bicarbonate was spiked to a non-labelled control after exponential growth in the stationary phase, i.e. after 10 h of inoculation, the ^{13}C-abundance of the biomass still increased up to ~2% (Fig. 2C). This clearly demonstrated that CO_2 fixation took place even in the absence of cell growth indicating active metabolism during the stationary phase. In similar experiments, we added $H^{13}CO_3^-$ to B. subtilis W23 during the stationary phase when grown on lactate or malate, respectively (see also below). The ^{13}C-abundance of the respective biomass was again determined by EA-IRMS and accounted for 3% in the lactate experiment (Figure S2C, Supporting Information) and 2% in the malate experiment (Figure S3C, Supporting Information). Thus, irrespective of the used carbon substrate and the physiological state (growth phase or stationary phase), metabolic turn-over of oxaloacetate involving the reaction of pyruvate carboxylase remained important, probably to maintain the energy balance also in non-growing B. subtilis W23.

Growth of B. subtilis in the presence of lactate and $H^{13}CO_3^-$

The trends for substrate consumption and biomass production for growth on lactate and $H^{13}CO_3^-$ were similar to the experiment with glucose. Briefly, the concentration of lactate decreased from 11.2 to 0.3 mM, while the biomass increased from 0.03 to 0.43 g/L during the experiment (Figure S2A, Supporting Information). Again, the formation of unlabelled bicarbonate caused a dilution of the ^{13}C-label at the end of the experiment. EA-IRMS showed that under these conditions B. subtilis W23 incorporated 5% of labelled inorganic carbon into its biomass, which is 1% less compared to the glucose experiment (Figure S2B, Supporting Information) (see also Fig. 3).

Growth of B. subtilis in the presence of malate and $H^{13}CO_3^-$

In the third experimental set-up, B. subtilis W23 was grown in M9 medium supplemented with malate and $H^{13}CO_3^-$. Measured substrate consumption demonstrated efficient uptake of malate (Meyer and Stülke 2013) that was accompanied by an increase of biomass from 0.04 to 0.29 g/L during the experiment. The concentration of malate in the medium decreased from 8.2 mM to below the analytical detection limit of 0.05 mM (Figure S3A, Supporting Information). When using ^{13}C-bicarbonate in the malate medium, the ^{13}C-abundance of the biomass of the bacteria accounted for 3% under these conditions, as measured by EA-IRMS (Figure S3B, Supporting Information). Notably, this value was significantly lower compared to the glucose and lactate experiments (Fig. 3). Nevertheless, the detection of ^{13}C incorporation came as a surprise, since exogenous malate could have fully refilled the TCA cycle without the need for anaplerotic replenishment, introducing the ^{13}C-label (see simplified scenario C in Fig. 1).

^{13}C-Labelling patterns of amino acids

The ^{13}C-EA-IRMS results demonstrated the general importance of heterotrophic CO_2 fixation by pyruvate carboxylase. However, the universal label incorporation under different conditions makes it difficult to achieve the primary objective of our study, namely to identify the use of different substrates. In a next step, we therefore focused on amino acid-specific incorporation of ^{13}C, which should provide more specific data concerning substrate usage. As an example, amino acids from the TCA cycle (e.g. Asp, Glu) or gluconeogenesis (e.g. Tyr, Phe) were expected to acquire a greater fraction of ^{13}C-carbon as compared to those amino acids derived from pyruvate (e.g. Val, Ala), where the incorporation of ^{13}C-carbon should be low (see Fig. 1). Using established protocols (Eylert et al. 2008), we quantified the ^{13}C-excess (mol%) in 14 amino acids obtained from acidic hydrolysis of the biomass. Among the labelled amino acids, ^{13}C-excess was found especially for isotopomers carrying one ^{13}C-carbon atom (M+1 isotopomers) as expected for a labelling experiment with $H^{13}CO_3^-$.

During growth on glucose, ^{13}C-excess of the M+1 isotopomers of amino acids derived from intermediates of the TCA cycle, such as Asp, Thr, Lys, Glu and Pro (see also Fig. 1), reached values up to 50% (Fig. 4A). The ^{13}C-excess of the same isotopomers reached values up to 40% when the bacteria were grown on lactate (Fig. 4B) and values up to 15% during growth on malate (Fig. 4C). The ^{13}C-excess of the M+1 isotopomers of amino acids derived from gluconeogenetic intermediates was low for Ser (~4%) and apparently absent for His (derived from the pentose phosphate pathway intermediate, phosphoribosyl pyrophosphate, PRPP) when B. subtilis W23 was grown on glucose, lactate or malate, respectively. Glycine, which is also derived from gluconeogenetic intermediates, showed a moderate ^{13}C-excess of the M+1 isotopomer under all three conditions (6–8%). Amino acids derived from pyruvate such as Ala, Val and Leu received very low ^{13}C-label under all three conditions (<3%). Amino acids (Tyr and Phe) that were synthesised from the pentose phosphate pathway intermediate, erythrose-4-phosphate, showed moderate ^{13}C-excess of the respective M+1 isotopomers (~5%) when B. subtilis W23 was grown on lactate or malate (Fig. 4B and C), and no ^{13}C-excess of the same M+1 isotopomers when grown on glucose (Fig. 4A).

From these comparisons, it becomes already evident that the ^{13}C-patterns in amino acids specifically reflected the (unlabelled) organic carbon substrate used by B. subtilis W23 in our model experiments. However, to better visualise the differences in the respective substrate usages, we now compared ratios of ^{13}C-excess of the M+1 isotopomers in specific sets of amino acids (Fig. 5). More specifically, Ala and Val were used as rep-

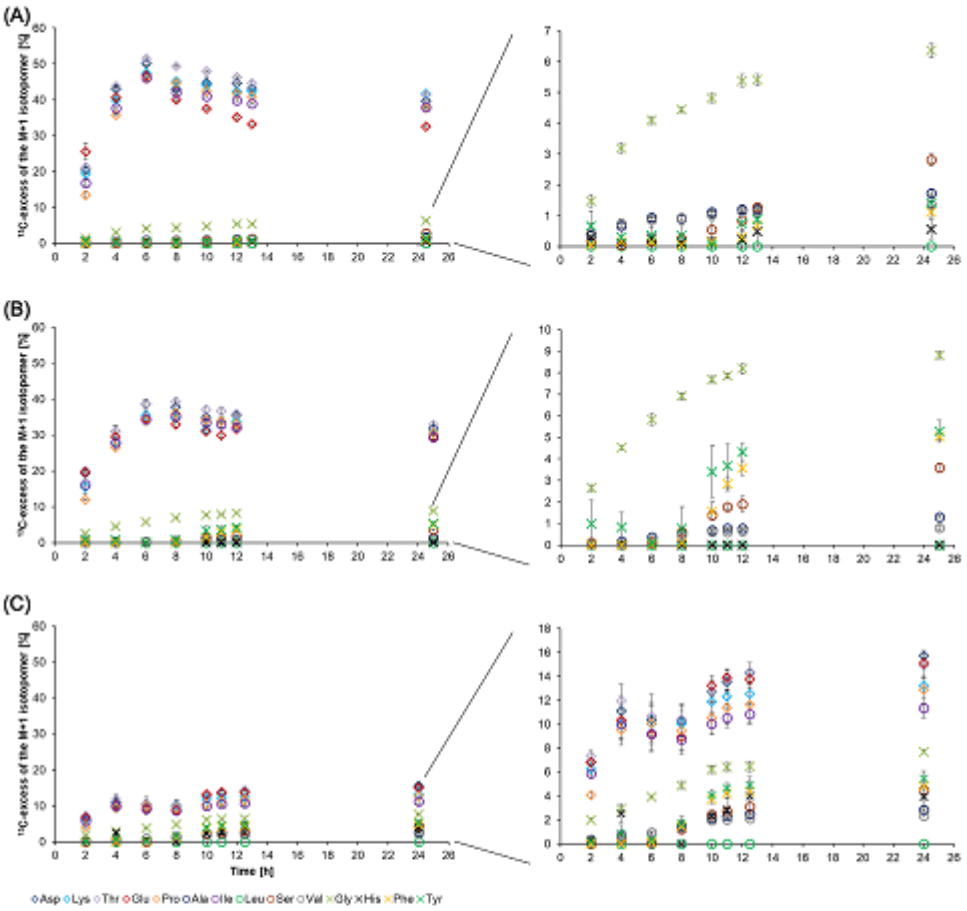

Figure 4. ^{13}C-excess (mol%) of the M+1 isotopomers of specific amino acids produced in $H^{13}CO_3^-$-labelling experiments with glucose (A), lactate (B) and malate (C), respectively. Amino acids depicted as diamonds are derived from the TCA cycle. Amino acids depicted as circles are derived from pyruvate. Amino acids depicted as crosses are derived from the gluconeogenesis pathway. The ^{13}C-excess of the amino acids derived from pyruvate and the gluconeogenesis pathway are also displayed with a different scaling to improve visibility.

resentatives for ^{13}C incorporation *via* pyruvate (i.e. displaying only very low ^{13}C-excess of the M+1 isotopomers in the experimental settings). Tyr and Phe served as representatives for ^{13}C-bicarbonate incorporation *via* gluconeogenesis and the pentose phosphate pathway, whereas Asp and Glu were used as representatives for ^{13}C incorporation *via* the TCA cycle (see also Fig. 1). The ratios of the ^{13}C-excess of the M+1 isotopomers at quasi steady-state conditions (from 10 h after inoculation till the end of the experiment) gave clear diagnostic trends that uniquely allowed discerning the three different scenarios shown in Fig. 1. When calculating the ratios between the ^{13}C-excess of the M+1 isotopomers in TCA cycle-derived amino acids and those of pyruvate-derived amino acids (i.e. Asp/Val, Asp/Ala, Glu/Val and Glu/Ala), values above 20 were obtained in the experiments with glucose or lactate, where TCA cycle metabolites must be replenished, whereas ratios below 10 were obtained for the same sets of amino acids in the experiments with malate, where anaplerosis is not needed (Fig. 5A). When calculating the ratios between the ^{13}C-excess of the M+1 isotopomers in gluconeogenesis-derived amino acids and those in pyruvate-derived amino acids (i.e. Tyr/Val, Tyr/Ala, Phe/Val and Phe/Ala), ratios above 4 were obtained for experiments with lactate (i.e. under apparently active gluconeogenesis), whereas ratios of 1 or lower were observed for growth on glucose where gluconeogenesis is not needed (Fig. 5B). Thus, ratios of ^{13}C-excess of the M+1 isotopomers between these selected groups of amino acids provided highly selective markers to distinguish the main organic carbon substrates in our model experiments.

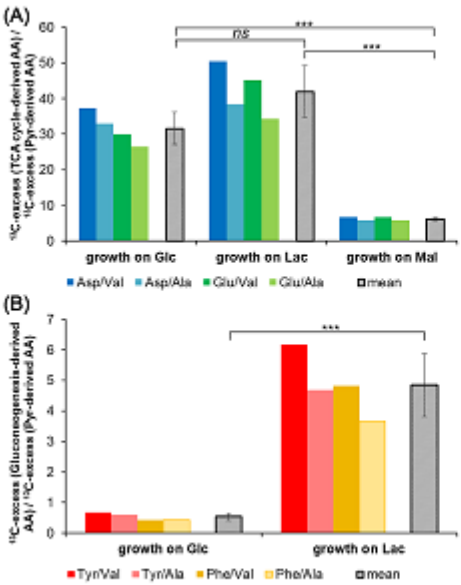

Figure 5. Marker ratios of ^{13}C-excess between selected amino acids. (A) ^{13}C-excess (TCA cycle-derived amino acids)/^{13}C-excess (pyruvate-derived amino acids). The coloured bars depict the ratios of the chosen amino acids in three independent labelling experiments with each of the three substrates, glucose (Glc), lactate (Lac) or malate (Mal). The grey bars show the mean values of ^{13}C-ratios for these fractions. The individual ratios as well as the mean values are significantly higher when an active CO_2 fixation is required in the experiments with Glc and Lac compared to a background or random fixation of CO_2 in the experiment with Mal. *P*-values were calculated by Student's *t*-test (unpaired): *P*(Glc/Lac) = 0.05031, *P*(Glc/Mal) = 0.00003, *P*(Lac/Mal) = 0.00006. (B) ^{13}C-excess (gluconeogenesis-derived amino acids)/^{13}C-excess (pyruvate-derived amino acids). The coloured bars depict the ratios of the chosen amino acids when glucose or lactate were the growth substrates, respectively, and the grey bars show again the mean values of ^{13}C-ratios. *P*-value was calculated by Student's *t*-test (unpaired): *P*(Glc/Lac) = 0.00017 (for detailed calculation, see the excel file F5 m+1 and ratio of label_SI Paper in the Supporting Information).

Incorporation of ^{13}C-carbon from $H^{13}CO_3^-$ by a natural groundwater community

To test whether this approach can also be used to assign unknown substrates for microbes growing in environmental samples, a proof-of-principle experiment was conducted. Specifically, a natural groundwater microbial community was grown for 124 days in water containing organic fertiliser/soil extract and 1 g/L $H^{13}CO_3^-$ (Fig. 6A and B). Indeed, significant ^{13}C incorporation was found in the biomass of the harvested bacteria (Fig. 6C).

To more specifically assign potential substrates that were used by the microbial community under these conditions, we again analysed amino acids obtained from acidic hydrolysis of the biomass. Overall ^{13}C incorporation and ^{13}C-excess of the M+1 isotopomers were quantified in 16 amino acids. Meso-diaminopimelic acid (DAP, as a component of peptidoglycan) and lysine reached values up to 12% ^{13}C-excess of the M+1 isotopomers (Fig. 6C). These amino acids play important roles in cell wall biosynthesis of bacteria (Born Timothy and Blanchard 1999). DAP is the immediate precursor for lysine (Lysine biosynthesis—Reference pathway 2020), which explained the similar ^{13}C incorporation into these two amino acids. The detected ^{13}C-label of these amino acids showed (i) ^{13}C incorporation via anaplerosis, since DAP and lysine are derived from TCA cycle intermediates and (ii) active cell wall synthesis demonstrating multiplication of the microorganisms under these conditions. Amino acids that are derived from TCA cycle intermediates showed a ^{13}C-excess of the M+1 isotopomers of 3–6%, i.e. Asp (4%), Thr (3%), Met (6%), Glu (4%) and Pro (4%).

To check whether it is possible to reveal the type of organic carbon that has been utilised by the groundwater community, we also calculated the ratios of ^{13}C-excess of the M+1 isotopomers between TCA cycle-derived amino acids and pyruvate-derived amino acids (<10) (Fig. 6D) and the ratios of ^{13}C-excess of the M+1 isotopomers between gluconeogenesis-derived amino acids and pyruvate-derived amino acids (<2) (Fig. 6E). Remarkably, there was a striking similarity between these values and the corresponding values in the model experiments when *B. subtilis* W23 was grown on malate. Consequently, we hypothesise (also with good statistical significance) that the microorganisms from the groundwater community mainly used organic matter that entered the central carbon metabolism at the stage/level of the TCA cycle, like malate. This result seems reasonable since the utilised organic fertiliser was mostly composed of humic substances, i.e. aromatic compounds, which are degraded to compounds comprising four carbon atoms, such as succinyl-CoA and succinate. These products could then serve as main substrates entering the central carbon metabolism via the TCA cycle such as malate in our model experiment.

DISCUSSION

By means of anaplerotic CO_2 fixation, *B. subtilis* W23 incorporated ^{13}C-labelled bicarbonate to a different extent into its biomass depending on the main organic carbon source being present in the minimal medium (i.e. glucose, lactate or malate, respectively). Indeed, the data from EA-IRMS analyses alone could already show significant differences between the three carbon substrates tested in this study, as illustrated in Fig. 3. Incorporation of $H^{13}CO_3^-/^{13}CO_2$ to an extent of 6 and 5% into microbial biomass during growth on glucose and lactate, respectively, reflected biomass formation involving anaplerotic carboxylation of pyruvate, which was in some agreement with our simplified scenarios A and B in Fig. 1. Notably, however, in comparison with the glucose experiment, the ^{13}C-abundance of the biomass was lower in the lactate experiment (6 vs 5%). At first glance, this came as a surprise since we expected the same or an even higher ^{13}C-abundance of the bacterial biomass, when lactate was used as the organic substrate. Under lactate conditions, ^{13}C incorporation should also have occurred via ^{13}C-labelled oxaloacetate into products derived from intermediates of the TCA cycle as well as into those derived from gluconeogenesis and the pentose phosphate pathway (see scenario B in Fig. 1). The latter routes did not play a major role in the lactate experiment as confirmed by the low levels or the apparent absence of label in His, Ser, Tyr and Phe, respectively. Rather, lactate seemed to be directly channelled via pyruvate and Ser into glycerate-3-phosphate and triose phosphates (Glycine, serine and threonine metabolism 2019) and then serving as unlabelled precursors for glucose formation and the pentose phosphate pathway in our experimental setting (Kleijn et al. 2010). Following this metabolic flux, cell wall sugars and other gluconeogenetic

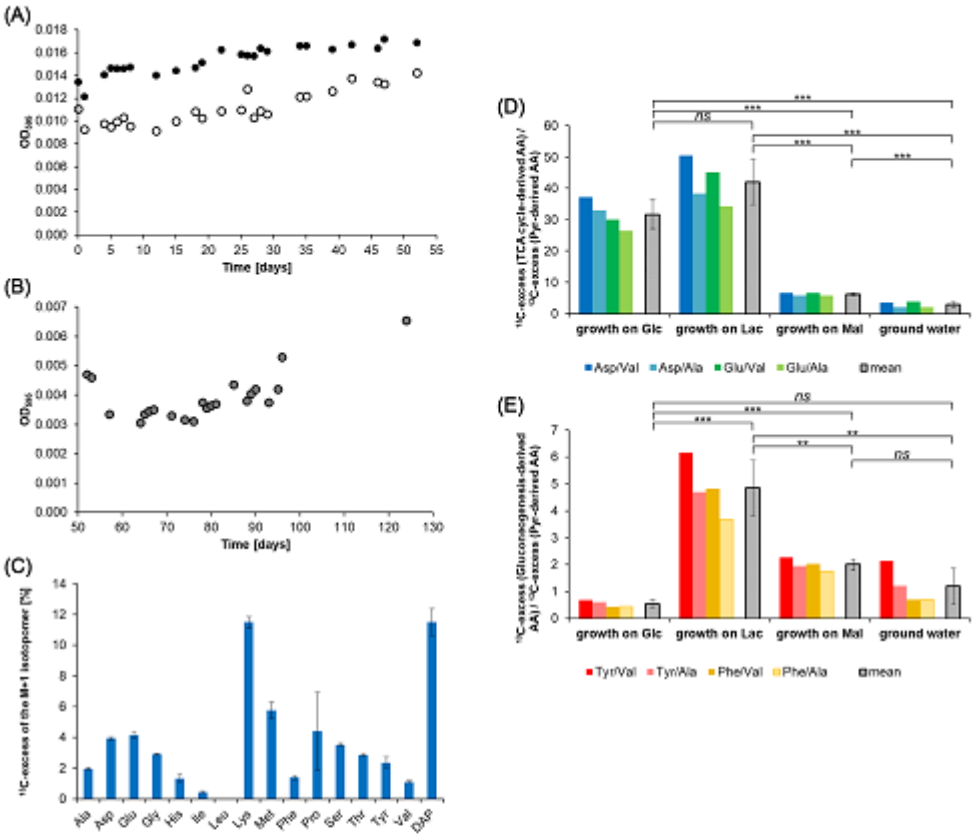

Figure 6. Labelling experiment with a natural groundwater community and $H^{13}CO_3^-$ as a tracer. (A) Growth curves of the bacterial groundwater communities growing on different concentrations of organic fertiliser. The microorganisms that were supplemented with 30 mL of organic fertiliser are depicted as open circles. The microorganisms that were supplemented with 50 mL of organic fertiliser are depicted as full circles. (B) Growth curve of the combined bacterial groundwater community growing on organic fertiliser and soil extract. (C) ^{13}C-excess of the M+1 isotopomers of specific amino acids produced by $H^{13}CO_3^-$-labelling experiments. (D) Marker ratios of ^{13}C-excess between selected amino acids: ^{13}C-excess (TCA cycle-derived amino acids)/^{13}C-excess (pyruvate-derived amino acids). The coloured bars depict the ratios of the chosen amino acids in the labelling experiments. The grey bars show the mean values of ^{13}C-ratios for these fractions. P-values as calculated by Student's t-test (unpaired): P(Glc/Lac) = 0.05031, P(Glc/Mal) = 0.00003, P(Glc/groundwater) = 0.00002, P(Lac/Mal) = 0.00006, P(Lac/groundwater) = 0.00004, P(Mal/groundwater) = 0.00082. (E) Marker ratios of ^{13}C-excess between selected amino acids: ^{13}C-excess (gluconeogenesis-derived amino acids)/^{13}C-excess (pyruvate-derived amino acids). The coloured bars depict the ratios of the chosen amino acids in the labelling experiments and the grey bars show again the mean values of ^{13}C-ratios. P-values as calculated by Student's t-test (unpaired): P(Glc/Lac) = 0.00017, P(Glc/Mal) = 0.00002, P(Glc/groundwater) = 0.10712, P(Lac/Mal) = 0.00166, P(Lac/groundwater) = 0.00103, P(Mal/groundwater) = 0.06284.

metabolites would not acquire label from $H^{13}CO_3^-/^{13}CO_2$ via ^{13}C-oxaloacetate, thus leading to the observed lower ^{13}C incorporation. Interestingly, transcriptional, translational and post-translational down-regulation of anaplerotic reactions might be triggered by the presence of exogenous organic acids in the medium (Schilling et al. 2007; Mirouze et al. 2015). Against the background of lactate, as the only organic carbon source in the medium, it seemed safe to assume that anaplerosis was restrained. Similarly, nicotinamide adenine dinucleotide (NADH) in excess produced by lactate dehydrogenase in the presence of lactate would also down-regulate the TCA cycle and its anaplerotic reactions (Cazzulo and Stoppani 1969). Together, less ^{13}C-carbon is incorporated into gluconeogenetic products and the overall biomass when the bacteria grow on lactate compared to growth on glucose.

The occurrence of the ^{13}C-label in amino acids also clearly assigned pyruvate carboxylase as the $H^{13}CO_3^-/^{13}CO_2$-binding enzyme in all of our settings including the experiment with malate (for details, see below). The unexpected incorporation of 3% ^{13}C-carbon into microbial biomass during growth on malate suggests that, even under this condition, pyruvate carboxylase was still actively transforming pyruvate to oxaloacetate, even though the organism could have directly refilled the oxaloacetate pool of the TCA cycle by taking excess malate from the growth medium (see scenario C in Fig. 1). Thus, although being

characterised as non-essential for *B. subtilis* W23 in SubtiWiki (Zhu and Stülke 2018), the constantly expressed gene for pyruvate carboxylase implies a permanent activity for this enzyme (Sauer and Eikmanns 2005; Jitrapakdee et al. 2008)—possibly to be able to quickly react when growth conditions change and anaplerosis becomes necessary for survival (Diesterhaft and Freese 1973; Chubukov et al. 2013). Interestingly, metabolic activity of pyruvate carboxylase could also be detected during the stationary growth phase of *B. subtilis* W23 irrespective of the main organic substrate being used from the medium (Fig. 2C; Figures S2C and S3C, Supporting Information). This also indicates the important role of the constantly present enzyme pyruvate carboxylase in the metabolism of *B. subtilis* W23.

EA-IRMS analysis alone could not clearly pinpoint the metabolic history of the incorporated inorganic carbon under the different conditions, nor could it exclude that multiple enzymes contributed to the observed label incorporation. To further confirm that pyruvate carboxylase is responsible for ^{13}C incorporation into microbial biomass and to follow the labelled inorganic carbon through the metabolic network of the microbial cell, we used GC-MS analysis to reveal information about the carbon positions in amino acids having acquired the label. On the basis of the detected fragmentation patterns of the silylated amino acids (for details, see Table T1 in the Supporting Information), some positional assignments of the ^{13}C-label, especially those involving C-1 of the amino acids, were possible (Fig. 7). As an example, the fragments with m/z of 432 and 286 for Glu and Pro, respectively, contained all five carbon atoms of the original amino acid. When analysing the mass spectra, we found that these fragments were accompanied by a high amount (up to 50%) of the respective M+1 isotopomer (namely, m/z 433 for Glu and m/z 287 for Pro). In contrast, the fragments that had lost the C-1 carbon atom of these amino acids (i.e. m/z 404 and 330 for Glu and m/z 258 and 184 for Pro) were not accompanied by a significant excess of the respective M+1 isotopomers (<1%). On this basis, it can be safely concluded that Glu and Pro carried the ^{13}C-label at C-1. Similarly, the mass distribution in the fragments observed for Asp, Thr and Lys signalled high amounts of the respective M+1 isotopomers (up to 50%). Here, the ^{13}C-labelled carbon atom was mainly present at C-4 of these amino acids, as learned from the analysis of the respective fragments. However, lower amounts of ^{13}C-label (1–5%) could also be assigned to C-1 of these amino acids. As illustrated in Fig. 7, this label distribution can be explained because (i) C-4 of oxaloacetate acquires the ^{13}C-label from $H^{13}CO_3^-$ by the reaction of pyruvate carboxylase, (ii) [4-^{13}C]oxaloacetate is converted into [1-^{13}C]α-ketoglutarate *via* the oxidative branch of the TCA cycle (leading to the detected [1-^{13}C]-isotopomers of Glu and Pro), (iii) the biosynthesis of Asp, Thr and Lys is based on the TCA cycle intermediate oxaloacetate (leading to the detected [4-^{13}C]-isotopomers) and (iv) reversible reactions between oxaloacetate and succinate, in the reductive branch of the TCA cycle, lead to a scrambling of label between C-1 and C-4 of the symmetric intermediates fumarate and succinate. Hence, the ^{13}C-label was transferred also into C-1 of oxaloacetate and its downstream products Asp, Thr and Lys (see also Fig. 7, red half circles). Remarkably, the position-specific incorporation of ^{13}C-carbon at C-1 of Glu and Pro, and C-4 of Asp, Thr and Lys reached values up to 50% when the bacteria were grown on glucose and as high as 40% when grown on lactate (Fig. 4A and B). These data demonstrated that the anaplerotic reaction catalysed by pyruvate carboxylase transferred the ^{13}C-label efficiently and quite specifically into C-4 of oxaloacetate and its related downstream products (Fig. 7), and, thereby, gave direct evidence of the heterotrophic CO_2 fixation. During growth on malate, the ^{13}C-label was found at the same positions, but the ^{13}C-excess of the respective M+1 isotopomers was significantly lower (<15%) (Fig. 4C). The amino acids derived from glycolytic precursors, especially Ser and Gly, were characterised by a ^{13}C incorporation at C-1 of 2.8, 3.6 or 4.5% (Ser) and 6.4, 8.8 or 7.7% (Gly), when *B. subtilis* W23 was grown on glucose, lactate or malate, respectively. This ^{13}C incorporation could again be explained by the equilibrium reactions of the TCA cycle: [4-^{13}C]oxaloacetate led to [4-^{13}C]-isotopomers of malate, fumarate and succinate. Since succinate and fumarate are symmetrical intermediates of the TCA cycle, they led in turn to an equal mixture of [1-^{13}C]- and [4-^{13}C]oxaloacetate (Fig. 7, red half circles). An active gluconeogenesis could then have transported the ^{13}C-label from the C-1 position of oxaloacetate into the C-1 position of PEP and upstream from there into [1-^{13}C]Ser and [1-^{13}C]Gly. However, *B. subtilis* W23 could also have used the reversible reaction of the Gly cleavage system (Kikuchi et al. 2008) to synthesise Gly, as shown in the following formula.

$$\text{Glycine} + H_4\,\text{folate} + NAD^+ \rightleftharpoons N^5, N^{10} - \text{methylene} - H_4\text{folate} + CO_2 + NH_4^+ + NADH + H^+$$

The reverse reaction of the glycine cleavage system could have afforded [1-^{13}C]Gly, which then serves as the precursor for Ser biosynthesis yielding [1-^{13}C]Ser without the requirement of an active pyruvate carboxylase (Kikuchi et al. 2008; Glycine, serine and threonine metabolism 2019). Alternatively, [1-^{13}C]Gly could be formed by cleavage of 2-aminoacetoacetate (obtained from Thr) whereby C-1 and C-2 of Thr are transformed into C-1 and C-2 of Gly, respectively. Thus, *via* this route the detected (low) label at C-1 of Thr is transferred to C-1 of Gly. Now, one could speculate that these alternative pathways should be active under all the experimental set-ups and, consequently, the same ^{13}C-excess of the respective M+1 isotopomers of Gly and Ser should have resulted in all three cases. This is not true (Fig. 4) and, therefore, the detected differences in ^{13}C incorporation indicate that a significant fraction of Ser and Gly was synthesised *via* [1-^{13}C]-PEP. However, we cannot exclude that different Gly biosynthesis pathways are used by *B. subtilis* W23 when growing on different organic substrates.

In summary, our experiments using $H^{13}CO_3^-$ as a tracer and *B. subtilis* W23 as a model organism, as well as our proof-of-principle experiment with a natural groundwater community, therefore provide solid evidence that EA-IRMS analysis of the biomass in conjunction with GC-MS analysis of protein- and cell wall-derived amino acids (i) reflect the core functional metabolic networks of the organism(s) under study and (ii) can identify the type of the main organic carbon substrate or at least the substrate family being used by the heterotrophic organism or organisms under study.

The general validity of this hypothesis is supported by the fact that almost all heterotrophs need to refill the TCA cycle by anaplerotic CO_2 fixation. For this purpose, heterotrophs use either pyruvate carboxylase that is highly conserved and found in a great variety of organisms, including prokaryotes, archaea, yeasts, fungi and higher organisms (e.g. mammals) or PEP carboxylase, which is also widely distributed in bacteria (Attwood 1995; Jitrapakdee and Wallace 1999; Sauer and Eikmanns 2005; Jitrapakdee et al. 2008). PEP carboxylase serves as another anaplerotic enzyme that catalyses the reaction from PEP to oxaloacetate *via* the addition of bicarbonate. Presumably, this results in the same labelling patterns when starting from

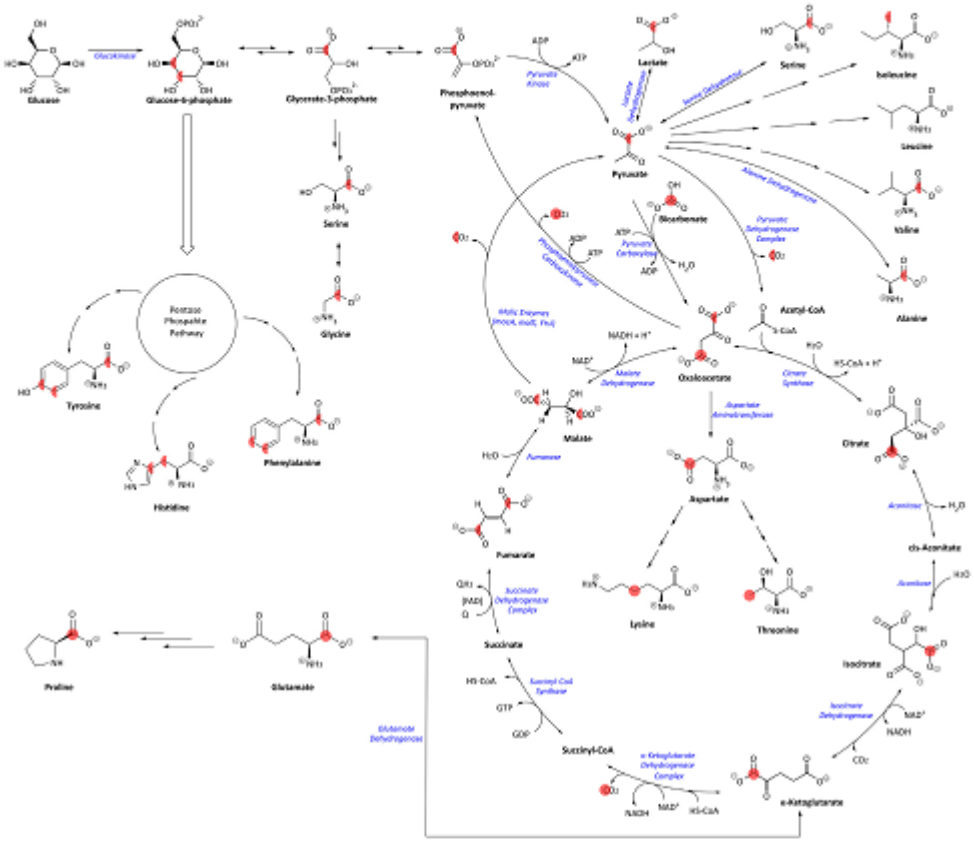

Figure 7. Metabolic network observed for B. subtilis W23 growing in M9 medium containing $H^{13}CO_3^-$ as a tracer. The full red circles mark the location of the ^{13}C-carbon atom detected in amino acids. On this basis, the labelling profiles of their respective precursors were reconstructed. The equilibrium between the reactions of the reductive branch of the TCA cycle could transfer the ^{13}C-label from oxaloacetate to malate, fumarate and succinate. The intrinsic symmetry of fumarate leads to the formation of a 0.5:0.5 mixture of [1-^{13}C]- and [4-^{13}C]malate, and [1-^{13}C]- and [4-^{13}C]oxaloacetate, respectively. This is indicated by the red half circles.

$H^{13}CO_3^-$ in comparison to organisms using the pyruvate carboxylase. Thus, labelling experiments using $H^{13}CO_3^-$ as a tracer bear high potential to generally assign the type of microbial DOC utilisation under various conditions.

SUPPLEMENTARY DATA

Supplementary data are available at FEMSEC online.

FUNDING

This work was funded by the Helmholtz Association and in part (to WE) by grants from the Hans-Fischer-Gesellschaft (Munich, Germany) and the Deutsche Forschungsgemeinschaft DFG (Bonn, Germany) (TRR235).

ACKNOWLEDGEMENTS

We thank Ellen Röhm (Geomicrobiology—University of Tübingen) for performing the HPLC measurements and Ramona Brejcha (Institute of Groundwater Ecology, Helmholtz Zentrum München) and Martina Daubmeier (Institute of Groundwater Ecology, Helmholtz Zentrum München) for supporting us in the acquisition of the elemental analyser-isotope ratio mass spectrometer analyses of the bacterial cell pellets.

Conflict of interest. None declared.

REFERENCES

Alonso-Saez L, Galand PE, Casamayor EO *et al.* High bicarbonate assimilation in the dark by Arctic bacteria. *ISME J* 2010;4:1581–90.

Attwood PV. The structure and the mechanism of action of pyruvate carboxylase. *Int J Biochem Cell Biol* 1995;27:231–49.

Bacher A, Chen F, Eisenreich W. Decoding biosynthetic pathways in plants by pulse-chase strategies using $^{13}CO_2$ as a universal tracer. *Metabolites* 2016;6:1–24.

Baltar F, Arístegui J, Sintes E et al. Significance of non-sinking particulate organic carbon and dark CO_2 fixation to heterotrophic carbon demand in the mesopelagic northeast Atlantic. *Geophys Res Lett* 2010;37:1–6.

Bassham JA, Calvin M. The way of CO_2 in plant photosynthesis. *Comp Biochem Physiol* 1962;4:187–204.

Berg IA. Ecological aspects of the distribution of different autotrophic CO_2 fixation pathways. *Appl Environ Microbiol* 2011;77:1925–36.

Born Timothy L, Blanchard JS. Structure/function studies on enzymes in the diaminopimelate pathway of bacterial cell wall biosynthesis. *Curr Opin Chem Biol* 1999;3:607–13.

Cazzulo JJ, Stoppani AO. Effects of adenosine phosphates and nicotinamide nucleotides on pyruvate carboxylase from baker's yeast. *Biochem J* 1969;112:755–62.

Cegelski L, Schaefer J. NMR determination of photorespiration in intact leaves using *in vivo* $^{13}CO_2$ labeling. *J Magn Reson* 2006;178:1–10.

Chubukov V, Uhr M, Le Chat L et al. Transcriptional regulation is insufficient to explain substrate-induced flux changes in *Bacillus subtilis*. *Mol Syst Biol* 2013;9:1–13.

DeLorenzo S, Brauer SL, Edgmont CA et al. Ubiquitous dissolved inorganic carbon assimilation by marine bacteria in the Pacific Northwest coastal ocean as determined by stable isotope probing. *PLoS One* 2012;7:1–15.

Diesterhaft MD, Freese E. Role of pyruvate carboxylase, phosphoenolpyruvate carboxykinase, and malic enzyme during growth and sporulation of *Bacillus subtilis*. *J Biol Chem* 1973;248:6062–70.

Dijkhuizen L, Harder W. Microbial metabolism of carbon dioxide. *Comprehensive Biotechnology* 1985;1:409–23.

Doronia NV, Trotsenko YA. Levels of carbon dioxide assimilation in bacteria with different pathways of C1 metabolism. *Mikrobiologiya* 1985;53:885–9.

Erb TJ. Carboxylases in natural and synthetic microbial pathways. *Appl Environ Microbiol* 2011;77:8466–77.

Eylert E, Schär J, Mertins S et al. Carbon metabolism of *Listeria monocytogenes* growing inside macrophages. *Mol Microbiol* 2008;69:1008–17.

Fuchs G. Alternative pathways of carbon dioxide fixation: insights into the early evolution of life? *Annu Rev Microbiol* 2011;65:631–58.

Giovannelli D, Sievert SM, Hügler M et al. Insight into the evolution of microbial metabolism from the deep-branching bacterium, *Thermovibrio ammonificans*. *Elife* 2017;6:1–31.

Giovannoni SJ, Stingl U. Molecular diversity and ecology of microbial plankton. *Nature* 2005;437:343–8.

Gleixner G. Soil organic matter dynamics: a biological perspective derived from the use of compound-specific isotopes studies. *Ecol Res* 2013;28:683–95.

Glycine, serine and threonine metabolism - Bacillus subtilis subsp. spizizenii W23 [Internet]. 2019. [cited 26.10.2019]. https://www.kegg.jp/kegg-bin/highlight_pathway?scale=1.0&map=bss00260&keyword=glycine, (accessed 15 May 2020).

Herndl GJ, Reinthaler T. Microbial control of the dark end of the biological pump. *Nat Geosci* 2013;6:718–24.

Hesselsoe M, Nielsen JL, Roslev P et al. Isotope labeling and microautoradiography of active heterotrophic bacteria on the basis of assimilation of $^{14}CO_2$. *Appl Environ Microbiol* 2005;71:646–55.

Heux S, Berges C, Millard P et al. Recent advances in high-throughput ^{13}C-fluxomics. *Curr Opin Biotechnol* 2017;43:104–9.

Huber C, Kraus F, Hanzlik M et al. Elements of metabolic evolution. *Chemistry* 2012;18:2063–80.

Ishihara H, Obata T, Sulpice R et al. Quantifying protein synthesis and degradation in Arabidopsis by dynamic $^{13}CO_2$ labeling and analysis of enrichment in individual amino acids in their free pools and in protein. *Plant Physiol* 2015;168:74–93.

Jitrapakdee S, St Maurice M, Rayment I et al. Structure, mechanism and regulation of pyruvate carboxylase. *Biochem J* 2008;413:369–87.

Jitrapakdee S, Wallace JC. Structure, function and regulation of pyruvate carboxylase. *Biochem J* 1999;340:1–16.

Johnson BT, Romanenko VI. Xenobiotic perturbation of microbial growth as measured by CO_2 uptake in aquatic heterotrophic bacteria. *J Great Lakes Res* 1984;10:245–50.

Kikuchi G, Motokawa Y, Yoshida T et al. Glycine cleavage system: reaction mechanism, physiological significance, and hyperglycinemia. *Proc Jpn Acad Ser B Phys Biol Sci* 2008;84:246–63.

Kleijn RJ, Buescher JM, Le Chat L et al. Metabolic fluxes during strong carbon catabolite repression by malate in *Bacillus subtilis*. *J Biol Chem*. 2010;285:1587–96.

Lee WN, Byerley LO, Bergner EA et al. Mass isotopomer analysis: theoretical and practical considerations. *Biol Mass Spectrom* 1991;20:451–8.

Lombard J, Moreira D. Early evolution of the biotin-dependent carboxylase family. *BMC Evol Biol* 2011;11:1–22.

Lysine biosynthesis - Reference pathway. 2020, . [cited 14.02.2020]. https://www.kegg.jp/kegg-bin/highlight_pathway?scale=1.0&map=map00300&keyword=Diaminopimelate, (accessed 15 May 2020).

Meyer FM, Stülke J. Malate metabolism in *Bacillus subtilis*: distinct roles for three classes of malate-oxidizing enzymes. *FEMS Microbiol Lett* 2013;339:17–22.

Middelburg JJ. Chemoautotrophy in the ocean. *Geophy Res Lett* 2011;38:1–4.

Miltner A, Kopinke F-D, Kindler R et al. Non-phototrophic CO_2 fixation by soil microorganisms. *Plant Soil* 2005;269:193–203.

Miltner A, Richnow H-H, Kopinke F-D et al. Assimilation of CO_2 by soil microorganisms and transformation into soil organic matter. *Org Geochem* 2004;35:1015–24.

Mirouze N, Bidnenko E, Noirot P et al. Genome-wide mapping of TnrA-binding sites provides new insights into the TnrA regulon in *Bacillus subtilis*. *Microbiologyopen* 2015;4:423–35.

Nielsen J. Systems biology of metabolism. *Annu Rev Biochem* 2017;86:245–75.

Owen OE, Kalhan SC, Hanson RW. The key role of anaplerosis and cataplerosis for citric acid cycle function. *J Biol Chem* 2002;277:30409–12.

Perez RC, Matin A. Carbon dioxide assimilation by *Thiobacillus novellus* under nutrient-limited mixotrophic conditions. *J Bacteriol* 1982;150:46–51.

Romanenko VI. Heterotrophic CO_2 assimilation by water bacterial flora. *Mikrobiologiia* 1964;33:679–83.

Roslev P, Larsen MB, Jørgensen D et al. Use of heterotrophic CO_2 assimilation as a measure of metabolic activity in planktonic and sessile bacteria. *J Microbiol Methods* 2004;59:381–93.

Römisch-Margl W, Schramek N, Radykewicz T et al. $^{13}CO_2$ as a universal metabolic tracer in isotopologue perturbation experiments. *Phytochemistry* 2007;68:2273–89.

Šantrůčková H, Bird MI, Elhottová D et al. Heterotrophic Fixation of CO_2 in Soil. *Microb Ecol* 2005;49:218–25.

Sauer U, Eikmanns BJ. The PEP-pyruvate-oxaloacetate node as the switch point for carbon flux distribution in bacteria. *FEMS Microbiol Rev* 2005;29:765–94.

Schilling O, Frick O, Herzberg C *et al.* Transcriptional and metabolic responses of *Bacillus subtilis* to the availability of organic acids: transcription regulation is important but not sufficient to account for metabolic adaptation. *Appl Environ Microbiol* 2007;73:499–507.

Schramek N, Wang H, Römisch-Margl W *et al.* Artemisinin biosynthesis in growing plants of *Artemisia annua*. A $^{13}CO_2$ study. *Phytochemistry* 2010;71:179–87.

Wegener G, Bausch M, Holler T *et al.* Assessing sub-seafloor microbial activity by combined stable isotope probing with deuterated water and ^{13}C-bicarbonate. *Environ Microbiol* 2012;14:1517–27.

Wood HG, Werkman CH. The utilisation of CO_2 in the dissimilation of glycerol by the propionic acid bacteria. *Biochem J* 1936;30:48–53.

Yakimov MM, La Cono V, Smedile F *et al.* Heterotrophic bicarbonate assimilation is the main process of *de novo* organic carbon synthesis in hadal zone of the Hellenic Trench, the deepest part of Mediterranean Sea. *Environ Microbiol Rep* 2014;6:709–22.

Zhu B, Stülke J. SubtiWiki in 2018: from genes and proteins to functional network annotation of the model organism *Bacillus subtilis*. *Nucleic Acids Res* 2018;46:743–8.